Sleep-control circuits in *Drosophila melanogaster.*



Laura Garmendia Sánchez

Supervisor: Professor Gero Miesenböck

Department of Physiology, Anatomy and Genetics

and

St John's College

University of Oxford

Thesis submitted in partial fulfilment of the requirements for the degree

of *Doctor of Philosophy in Physiology, Anatomy and Genetics.*

Michaelmas 2021

Abstract

Sleep is conserved across the animal kingdom, and it is essential for cognitive and physical wellbeing. Therefore, understanding the biological basis underlying sleep homeostasis is of critical importance. In *Drosophila melanogaster*, a small number of neurons with projections to the dorsal fan-shaped body (dFB) in the brain function as a homeostatic switch that controls sleep according to sleep need. During wake, these neurons are in an electrically silent (OFF) state and, as sleep pressure builds up, they switch to an electrically excitable (ON) state, promoting sleep. Dopamine signalling into the dFB neurons controls the switch from the ON to the OFF state, waking flies up. However, the relevant dopaminergic neurons that convey the arousal-promoting signals to the dFB are unknown, and so are the mechanisms and rules that govern their activity. In this study, I have identified and gained genetic access to a restricted subset of wake-promoting dopaminergic neurons with projections to the dFB. The accumulation of mitochondrial reactive oxygen species (ROS) increases the excitability of the dFB neurons and promotes sleep through the modulation of the plasma membrane Shaker channel β-subunit, Hyperkinetic. Here, I hypothesised that lipid peroxidation by-products link mitochondrial ROS to the modulation of Hyperkinetic. Accordingly, supplementing *Drosophila'*s diet with lipid peroxidation-resistant D-PUFAs resulted in a decrease in sleep. In addition, I evaluated the influence of ROS in tissues other than the dFB neurons in promoting sleep. Using an innovative inducible ROS-generating chemogenetic system based on the D-amino acid oxidase enzyme, I observed that inducing ROS in gut enterocytes (*MyO1A-GAL4* cells) increases sleep. Interestingly, I also found that dietary composition significantly altered sleep amount, further highlighting the gut as a potential target where diet, ROS, and sleep may intersect.

Acknowledgements

First and foremost, I would like to thank my supervisor, Gero Miesenböck, for giving me the opportunity to join his group and for his invaluable mentorship throughout this journey, which has made me grow immensely both professionally and personally. It has been a privilege to work alongside and learn from one of the brightest scientists in the world. In addition, I am extremely grateful to the current and former members of the Miesenböck group, whose scientific advice and support in the lab has been crucial: Anissa Kempf, Eleftheria Vrontou, Diogo Pimentel, Laura Chan, Katerina Christodoulou, Timothy Wong, Raffaele Sarnataro, Giacomo Bertuzzi, Alina Krebbers, Celina Hartmann, Susanne Szydlowski, Peter Hasenhuetl, Jan Kropf, Lea Ballenberger, Haram Park, Olof Rorsman, Patrick Liu and Lukas Groschner. I would certainly have not made it so far without your support!

I would also like to acknowledge my colleagues from the CNCB. In particular, Ruth Brain and Fiona Woods for their invaluable support, Tetsuya Noyima for sharing his expert knowledge in immunohistochemistry and confocal microscopy with me, as well as Mathew Herbert, Megan Neville and Ammerins De Haan for their advice on cloning and molecular biology. In addition, I would like to thank Korneel Hans for teaching me how to do yeast work, Misha Shchepinov for his collaboration on the D-PUFA project, and the Bernhard Spengler group for their collaboration on the mass spectrometry project.

I cannot begin to express my thanks to my family, my partner, and my friends, who have put up with me in my worst and best moments. A very special thank you to my friend Raquel Cuella for her emotional support and for proofreading my thesis.

Finally, I would like to thank La Caixa Foundation and *Ayuntamiento de Sallent de Gállego* for their financial support.

Declaration

I confirm that this thesis has been composed by myself and has not been submitted for any degree in this University or elsewhere. The results here presented were obtained by myself.

Abbreviations

AD	Activation domain
CDF	Chemically defined food
CTCF	Corrected total cell fluorescence
D-ALA	D-Alanine
DAAO	D-amino acid oxidase
DAT	Dopamine transporter
Dat	Dopamine N-acetyltransferase
DBD	DNA-binding domain
dFB	Dorsal fan-shaped body
GFP	Green fluorescence protein
L-ALA	L-Alanine
MB	Mushroom body
NADPH	Nicotinamide adenine dinucleotide phosphate
NGS	Normal goat serum
PAL	Protocerebral anterior lateral
PAM	Protocerebral anterior medial
PBS	Phosphate-buffered saline
PI	Pars intercerebrallis
PPL1	Protocerebral posterior lateral cluster 1
PPL2	Protocerebral posterior lateral cluster 2

PPM1	Protocerebral posterior medial cluster
PPM2	Protocerebral posterior medial cluster
PPM3	Protocerebral posterior medial cluster
PUFA	Polyunsaturated fatty acid
ROS	Reactive oxygen species
vFB	Ventral fan-shaped body
VUM	ventral unpaired medial
YFP	Yellow fluorescence protein
PCR	Polymerase chain reaction

Table of Contents

Chapter 1: Introduction……..……...1

1.1 The importance of sleep……1

1.2 The two-process model of sleep control……2

1.3 Drosophila melanogaster as a model for sleep research……..3

1.3.1 The fruit fly as a genetic powerhouse……..3

1.3.2 Sleep homeostasis in Drosophila……5

1.3.3 The dFB sleep circuitry: Drosophila's sleep homeostat……6

1.3.3.1 From sleep to wake: the dopaminergic input to the dFB and the ON-to-OFF switch……8

1.3.3.2 From wake to sleep: mitochondrial oxidative stress and the OFF-to-ON switch……9

Chapter 2: Results I - Identifying and gaining restricted access to Drosophila's dopamine wake-promoting inputs to the dFB……..16

2.1 INTRODUCTION……16

2.1.1 Dopamine's function in the regulation of sleep across species……16

2.1.2 Drosophila's dopamine wake-promoting neurons……18

2.1.3 Research aims……20

2.2 RESULTS……...21

2.2.1 Confirmation of the wake-promoting phenotype of R12D12-GAL4 and R91D10-GAL4……...22

2.2.2 Confocal imaging confirms anatomical overlap between the dFB neurons and the R12D12-GAL4 and R91D10-GAL4 lines……25
2.2.3 Detection of monoaminergic neurons in the R12D12-GAL4 and R91D10-GAL4 lines……..28
2.2.4 Generating and selecting split-GAL4 lines to gain genetic access to putative dopaminergic inputs to the dFB……..33
2.2.5 Anatomical and functional characterisation of candidate split-GAL4 lines……36
(1) Dopaminergic expression in split-GAL4 candidate lines……...36
(2) Anatomical relation between split-GAL4 candidate lines and dFB neurons……39
(3) Behavioural phenotype of split-GAL4 candidate lines..……..46

Chapter 3: Results II – Linking oxidative stress, lipid peroxidation and sleep homeostasis in Drosophila……49
3.1 INTRODUCTION……49
3.1.1 Finding the cause for sleep: the free radical flux theory……49
3.1.2 Linking oxidative stress, lipid peroxidation and sleep homeostasis in Drosophila……..51
3.1.3 Research aims……54
3.2 RESULTS……55
3.2.1 Development of an inducible chemogenetic system for mapping sleep-relevant sites of ROS production in Drosophila……..55
(1) Generation of DAAO-based chemogenetic tools for ROS induction in Drosophila……55

(2) Validation of Drosophila ROS-inducing chemogenetic tools in vitro…….59

(3) Behaviourally testing the DAAO-based chemogenetic system in the dFB neurons in vivo…… ..……..62

(4) Using the DAAO-based chemogenetic system to increase ROS in the gut……67

3.2.2 Testing the effect of lipid peroxidation resistant deuterated PUFAs on sleep in Drosophila……71

(1) Measuring the effect of supplementing different dietary media with non-deuterated PUFAs (H-PUFAs) on sleep……73

(2) Testing the effect of supplementing Drosophila food media with D-PUFAs on sleep……76

(3) Using a chemically defined food (CDF) media to supplement D-PUFAs into Drosophila diet and measure the effects of this manipulation on sleep……81

Chapter 4. Discussion and Future Directions……85

4.1 Drosophila's dFB sleep neurons: a recap……85

4.2 Wake-promoting inputs to the dFB……86

4.2.1 Refined access to Drosophila's wake-promoting dopamine neurons: inputs to the dFB……...86

4.2.2 Non-dopaminergic wake promoting circuits in Drosophila……...88

4.2.3 Future directions……89

4.3 ROS, lipid peroxidation and sleep……..91

4.3.1 ROS in the gut may promote sleep……..……...…91

4.3.2 Chemogenetically inducing ROS in the dFB neurons

does not increase sleep: what could have caused this?.....93

4.3.3 Diet composition affects sleep amount……..……..93

4.3.4 D-PUFAs may link lipid peroxidation to sleep in Drosophila…….……..95

4.3.5 Future directions…….……97

Chapter 5: Materials and Methods……99

5.1 Fly husbandry methods……99

5.2 Molecular biology methods for the generation of transgenic flies……..…101

5.2.1 Generation of split-GAL4 constructs with traditional

and Gateway cloning……..…101

5.2.2 Generation of DAAO constructs using traditional

restriction site-based cloning……103

5.3 Imaging methods……...…105

5.3.1 Immunohistochemistry and confocal imaging……..105

5.3.2 In vitro chemogenetic tests, confocal imaging,

and quantification of fluorescence……107

5.4 Diet manipulation methods……107

5.4.1 In vivo chemogenetics……107

5.4.2 Deuterated PUFA feeding experiments……..……108

5.4.2.1 PUFA aliquots and storage……108

5.4.2.2 PUFA-containing media……...108

5.4.2.3 Yeast culture……..109

5.5 Behavioural analyses methods……110

5.5.1 Sleep assays……110

5.5.2 Sleep deprivation methods……110

5.6 Statistical Analyses……..111

Chapter 6: Bibliography……..112

List of Figures

Figure 1.1 The two-process model of sleep regulation (from Borbély, 1982)……2

Figure 1.2 Genetic tools for spatial refinement of transgene expression in Drosophila……4

Figure 1.3 The dFB sleep switch……..8

Figure 1.4. Sleep and wake mechanisms in Drosophila: my research questions..…14

Figure 2.1 Dopaminergic neurons in the fly brain……19

Figure 2.2 Thermogenetic neuronal activation reveals a wake-promoting phenotype in the R12D12-GAL4 and R91D10-GAL4 lines……24

Figure 2.3 Anatomical overlap between the R23E10 neurons and the wake-promoting candidate lines R12D12-GAL4 and R91D10-GAL4……27

Figure 2.4. Monoaminergic expression in R12D12-GAL4……..30

Figure 2.5. Monoaminergic expression in the R91D10-GAL4 line……32

Figure 2.6. Anatomy of split-GAL4 hemidriver combinations……35

Figure 2.7. Dopaminergic expression of split-GAL4 lines confirmed immunohistochemically……38

Figure 2.8. Anatomical overlap between the R23E10 neurons and the split-GAL4 candidate lines……42

Figure 2.9. Characterising the identity of TH-C-AD; Ddc-R60F07-DBD cell bodies immunohistochemically……44

Figure 2.10. Thermogenetic activation of split-GAL4 candidate lines reveals that dopaminergic R91D10p65;TH-DBD and TH-C-AD; Ddc-R60F07-DBD neurons are wake-promoting, but not R12D12p65;TH-DBD neurons…….47

Figure 3.1 The HyPer-DAAO-based chemogenetic system……..58

Figure 3.2. Development and validation of a DAAO-based ROS-inducing chemogenetic system……..61

Figure 3.3 Behaviourally testing DAAO-based chemogenetic tools in the R23E10 neurons in vivo……..65

Figure 3.4. Sleep is increased by driving chemogenetic activation of a DAAO-based ROS-inducing system in in the Myo1A-GAL4 gut line. …….69

Figure 3.5. D-PUFAs have a protective effect on lipid peroxidation…….72

Figure 3.6. Supplementing two Drosophila media with non-deuterated PUFAs (H-PUFAs) does not affect sleep…….75

Figure 3.7. Dietarily supplementing 2mM D-PUFA through a sucrose-agar or a standard brown molasses-based Drosophila media does not reduce baseline or rebound sleep…….78

Figure 3.8. Increasing dietarily supplemented D-PUFA to 10mM and a longer exposure time does not significantly decrease sleep……..80

Figure 3.9. Using chemically defined food (CDF) media and longer culture time to selectively feed Drosophila with 2mM of D-PUFA……..83

List of Tables

Table 5.1.1 GAL4 and LexA driver stocks……...….99

Table 5.1.2 split-GAL4 driver stocks……..…..100

Table 5.1.3 UAS and LexAop responder stocks…….……..100

Table 5.1.4 Mutant stocks…….……101

Table 5.2.1.1 Primers for initial amplification of enhancer sequences
for traditional cloning……..……103

Table 5.2.1.2 Primers for initial amplification of enhancer sequences
for gateway cloning……..……103

Table 5.2.2.1 Primers for amplification of DAAO sequences……..……105

Table 5.3.1.1 Primary antibodies…….……106

Table 5.3.1.2 Secondary antibodies…….……...106

Table 5.4.2.1.1 PUFAs used in this study……..……108

Chapter 1: Introduction

1.1 The importance of sleep.

Sleep is a fundamental behaviour: Although its main function remains a subject of debate, it is indisputable that sleep is critical for the wellbeing of species across the animal kingdom. From flies to humans, sleep influences key physiological processes, including synaptic plasticity, memory consolidation and cognitive performance (Donlea, 2019; Diekelmann and Born, 2010; Tononi and Cirelli, 2014), immune function (Irwinn and Opp, 2017; Toda et al., 2019), and metabolism (Sharma and Kavuru, 2010). Furthermore, experiments with rats and flies suggest that sustained sleep deprivation can eventually lead to death (Bergmann and Rechtschaffen, 2002; Shaw et al., 2002). Despite the detrimental consequences of sleep deprivation, about one third of today's population suffers from at least mild insomnia and sleep disturbances are also commonly seen in an array of health conditions, ranging from mood disorders to obesity and metabolic syndrome (Roth, 2007; Benca et al., 1997; Beccuti and Pannain, 2011; Koren et al., 2016). In order to tackle this problem, it is crucial to first understand the biological basis underlying the regulation and function of sleep.

1.2 The two-process model of sleep control.

According to Borbély's influential model of sleep regulation, sleep is under the control of two interacting processes: a circadian process (Process C) and a homeostatic

process (Process S) (Fig. 1.1). The circadian process regulates the timing of sleep across the day-night cycle, while the length and depth of sleep depend on the time spent awake prior to sleep and are thus regulated homeostatically (Borbély, 1982). Accordingly, lack of sleep generates an increase in sleep need, leading to deeper and longer periods of sleep known as rebound sleep, the main landmark of a homeostatic response. While the molecular mechanisms underpinning the circadian control of sleep have been characterised in detail (Patke et al., 2020), comparatively little is known about the mechanisms that control sleep homeostasis.

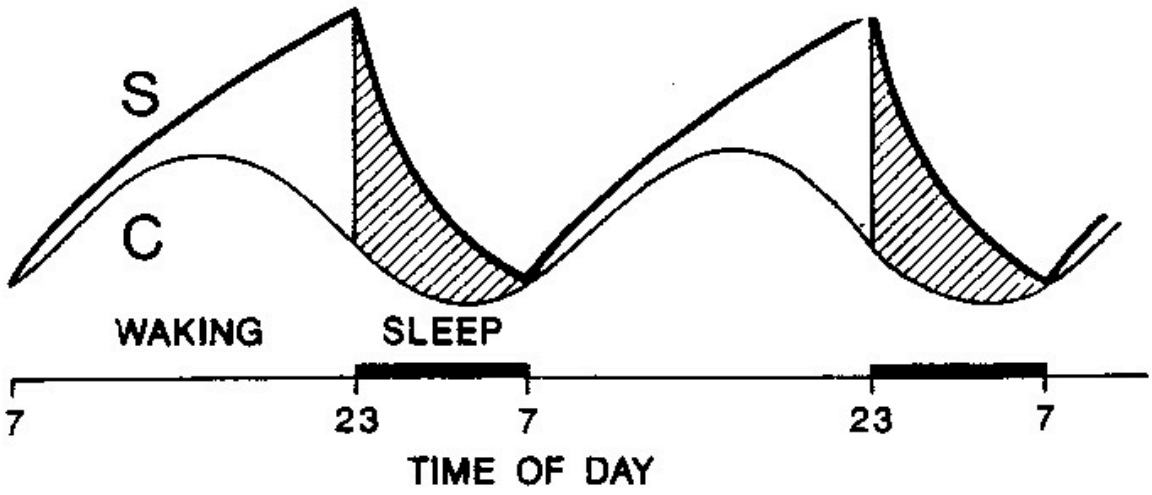


Figure 1.1 The two-process model of sleep regulation (from Borbély, 1982). A graphic illustration of the two-process model of sleep regulation by Alexander Borbély. The horizontal axis represents time across the 24-hour cycle. The circadian process (Process C) is seen as a sine wave that fluctuates between wake and sleep as a function of the light and dark cycle with periods of 24h. The homeostatic process (Process S) increases with wake time and decreases rapidly once a threshold is reached and sleep is triggered. The interaction of these two processes determines the time and duration of sleep.

1.3 Drosophila melanogaster as a model for sleep research.

1.3.1 The fruit fly as a genetic powerhouse.

Drosophila melanogaster has a relatively simple nervous system with only about 100,000 neurons (Kohl and Jefferis, 2011); nonetheless, it exhibits many complex behaviours, including sleep/wake cycles under circadian and homeostatic control (Shaw et al., 2000; Hendricks et al., 2000). Drosophila's strength as a model system also stems from the ability to easily conduct powerful forward genetic screens that make it possible to link distinct genetic mutations to specific behavioural phenotypes (Bellen et al., 2010). Indeed, several genes crucial for sleep regulation have been discovered through this approach. For example, *Shaker*, which encodes a voltage-gated potassium channel, was the first gene identified through a forward genetic screen for a short-sleeping fruit fly mutant (Cirelli et al., 2005). Other sleep-related genes identified though this approach include the short-sleeping mutant *Hyperkinetic* (Bushey et al., 2007), which encodes a subunit of the Shaker channel, the dopamine transporter gene *DAT* (Kume et al., 2005) and and the Rho GTPase-activating protein crossveinless-c (Donlea 2014).

The range of powerful *Drosophila* genetic tools includes binary expression systems like GAL4/UAS (Brand and Perrimon 1992; Duffy 2002) and LexA/LexAOP (Lai and Lee, 2006), as well as libraries of thousands of driver lines. These allow temporal and spatial specificity of transgene expression, offering genetic access to many distinct groups of neurons in the fly brain. Intersectional tools like split-GAL4 allow further refinement of these lines (Fig. 1.2).

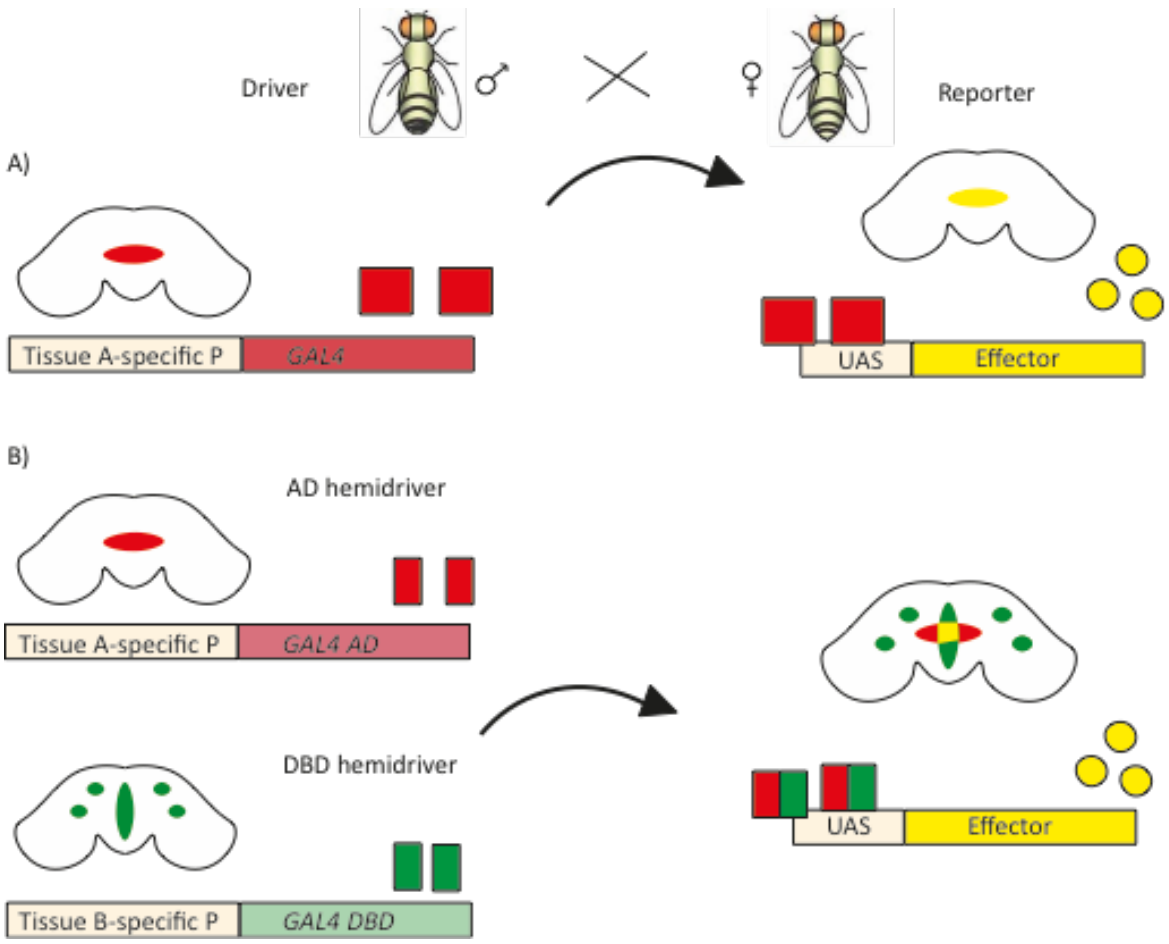


Figure 1.2 Genetic tools for spatial refinement of transgene expression in *Drosophila*. A) The GAL4/UAS binary expression system. Tissue-specific expression of a transgene can be achieved by mating of 'driver' and 'reporter' lines. The 'driver' line expresses the GAL4 protein under the control of a tissue-specific promoter. The 'reporter' line contains an effector under the control of the UAS sequence. Transcription of the effector transgene is driven by GAL4 binding to the UAS sequence (Brand and Perrimon, 1993). B) Improved spatial refinement of transgene expression with the split-GAL4 tool. In these transgenic fly lines, one line expresses the transcription activation domain (AD) of GAL4 under a promoter of interest (Tissue A-specific promoter, in red) while a second line expresses a DNA binding domain (DBD) GAL4 hemidriver under a different promoter (Tissue B-specific promoter, in green). Only in cells where the two hemidrivers are co-expressed (in yellow) a functional GAL4 is reconstituted to drive expression of the effector transgene (Luan et al., 2006; Pfeiffer et al., 2010).

In sum, this impressive genetic toolkit, together with the fly's simple nervous system and short generation time (Jennings, 2011), make *Drosophila* a powerful model system to decode the neuronal, genetic, and molecular mechanisms that control sleep.

1.3.2 Sleep homeostasis in Drosophila.

In 2000, two independent studies demonstrated that *Drosophila melanogaster* is a viable model system to study sleep (Hendricks et al., 2000; Shaw et al., 2000). These seminal studies characterised sleep in flies as periods of inactivity equal or longer than five minutes, which fulfil the behavioural criteria that define sleep. Such criteria include a sleep-specific posture, an increased arousal threshold, rapid reversibility, and homeostatic and circadian control. Both Hendricks and Shaw found that flies rest for almost half of the day and that inactivity occurs primarily during the night. In vivo electrophysiological recordings of *Drosophila* brains also uncovered electrical signatures that correlate with sleep and arousal states in flies (Nitz et al., 2002; van Swinderen et al., 2004) Furthermore, fly sleep has been shown to share similarities with mammalian sleep: mirroring mammalian sleep, sleep duration in flies decreases with age, it is modulated by known mammalian sleep-regulating drugs, and it affects the expression genes which are similarly regulated in rodents (Shaw et al., 2000; Hendricks et al., 2000; Hendricks et al., 2003). Taken together, this work established *Drosophila* as a powerful model system to study sleep.

Since then, significant effort has been focused on using *Drosophila* as a tool to decipher the molecular and cellular mechanisms underlying the homeostatic regulation of sleep. Many of these studies corroborated the similarities between fly and mammalian sleep (Allada et al., 2017; Yap et al., 2017). A number of structures have been linked to sleep regulation in the fly brain, including the mushroom body

(Pitman et al., 2016), the pars intercerebralis (Foltenyi et al 2007), the dorsal fan-shaped body (Donlea et al., 2011) and, more recently, the ellipsoid body (Liu et al., 2016). It has been difficult, however, to elucidate the relationships among these structures within the sleep-regulating circuitry, and their function in regulating homeostatic sleep: Which neuronal clusters sense information about sleep need and integrate it to generate sleep drive? Which ones act as effectors to modulate sleep accordingly? And, what are the molecular mechanisms used to perform such functions?

1.3.3 The dFB sleep circuitry - Drosophila's sleep homeostat.

A significant step towards answering the abovementioned questions was the discovery of the so-called dorsal fan-shaped body (dFB) sleep-promoting neurons: A cluster of about a dozen neurons in each hemisphere of the fly brain that project to the dorsal fan-shaped (dFB) body and function as the effector arm of *Drosophila*'s sleep homeostat. Donlea et al. (2011) showed that thermogenetic activation of these neurons in *Drosophila* can induce sleep on demand. Accordingly, Na+ channel (NaChBac)-mediated chronic hyperactivation of dFB neurons increases daytime sleep to levels usually seen at night (Ni et al., 2019). On the other hand, reductions in the excitability of these neurons promote wake and obstruct sleep homeostasis: targeted ablation of the Rho-GTPase-activating protein crossveinless-c in the dFB inhibits the excitability of these neurons, which causes insomnia and prevents rebound sleep (Donlea et al., 2014); similarly, dopaminergic input to the dFB neurons blocks their excitability and inhibits sleep (Liu et al., 2012; Pimentel et al., 2016). Therefore, these studies suggest that the activity and function of the dFB neurons is necessary for sleep and sleep rebound in the fly.

Furthermore, Pimentel et al. (2016) showed that dFB neurons adjust their electrical output to sleep need: just like a switch, they transition from an electrically silent (OFF) state during wake to an electrically excitable (ON) state as sleep need increases, eventually triggering sleep (Fig. 1.3). Behind these changes in membrane excitability lies the antagonistic regulation of two potassium conductances. During waking, the two-pore domain ("leak") potassium channel Sandman imposes electrical silence, while increased A-type currents through the voltage-gated Shaker potassium channel support tonic firing during sleep (Donlea et al., 2014; Pimentel et al., 2016).

Another important set of neurons in the fly's sleep homeostat system is the R2/R5 ring neurons of the ellipsoid body (EB), which function upstream of the dFB sleep-promoting neurons to generate sleep pressure (Liu et al., 2016). However, R2/R5 neurons lack an obvious anatomical connection with the dFB sleep-promoting neurons and how information from the EB and from other units of the sleep homeostat reaches the dFB sleep-promoting neurons remains largely unknown.

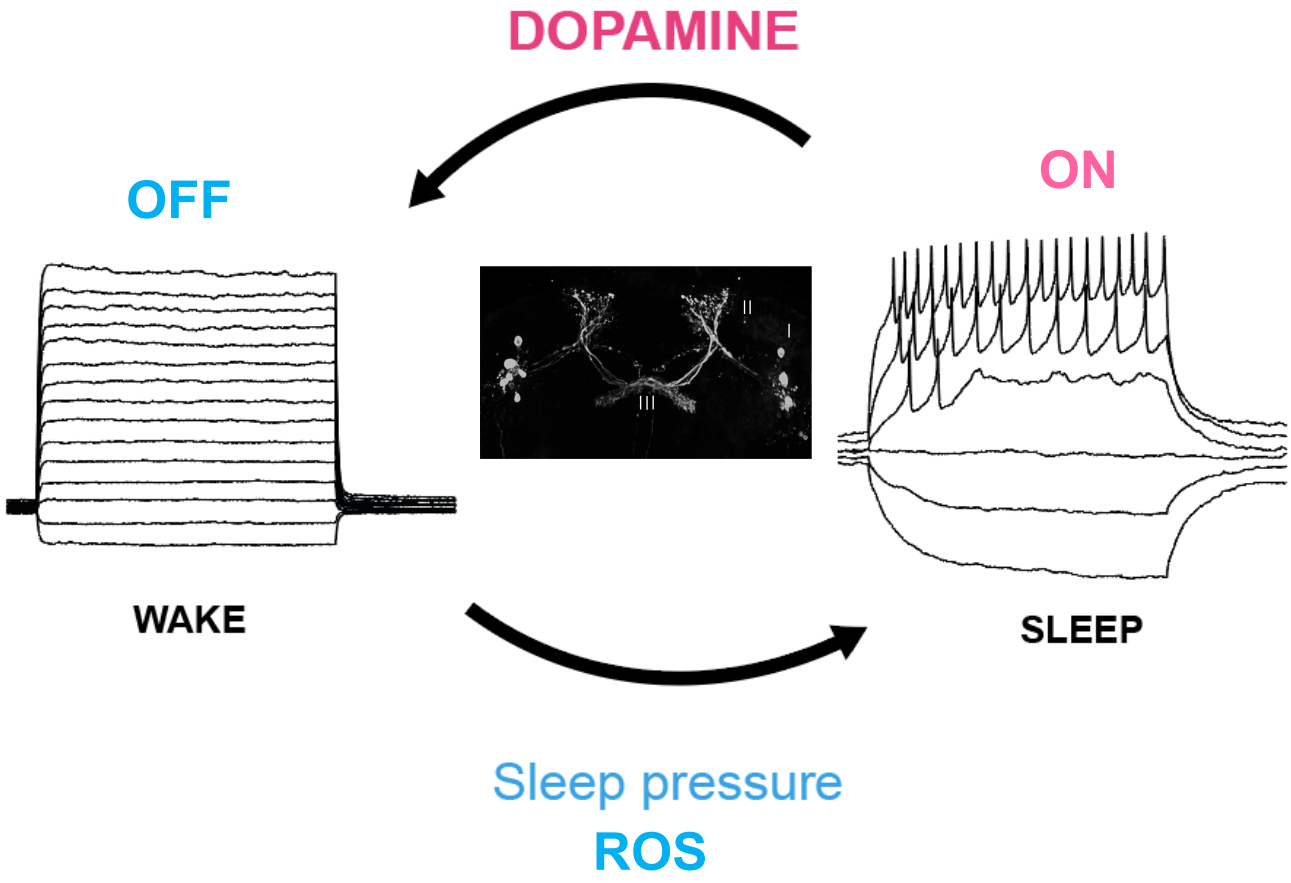


Figure 1.3 The dFB sleep switch. In flies, sleep state is coupled with the electrical activity of dFB neurons. When flies are awake and sleep pressure is low (left), dFB neurons are electrically silent (OFF); as sleep pressure increases, reflected in an increase in mitochondrial reactive oxygen species (ROS), dFB neurons will switch into an electrically active (ON) state and flies will sleep. The switch from sleep (ON) to wake (OFF) state is mediated by dopaminergic signalling. The image in the centre of the diagram represents the dFB neurons. dFB cell bodies are located laterally in each hemisphere of the brain (I). These cell bodies send projections connecting to the dorsal dendritic tufts (II) and the axonal fan-shaped arch in the central complex of the fly brain (Pimentel et al., 2016).

1.3.3.1 From sleep to wake – the dopaminergic input to the dFB and the ON-to-OFF switch.

Indeed, dopamine is the only direct wake-promoting input to the dFB neurons identified to date. Dopamine acutely hyperpolarises the dFB neurons, effectively switching them from an electrically active (ON) into an electrically silent (OFF) state and, consequently, waking sleeping flies up (Pimentel et al., 2016) (Fig. 1.3). Given dopamine's crucial role in regulating sleep, understanding how the wake-promoting dopaminergic neurons are regulated becomes the next logical step. What are the rules governing the activity of dopamine neurons? Which are the intrinsic molecular mechanisms that mediate their wake-promoting function? How and when are they activated? By which signals and neurons? Does their excitability vary with sleep pressure?

Despite the established role of dopamine in suppressing sleep circuits and promoting wakefulness, it is still unclear which are the relevant dopaminergic neurons (or neuron) that convey the arousal-promoting signals to the dFB. Since the identities of the relevant neurons are unknown, the mechanisms that regulate the activity and function of wake-promoting dopamine neurons themselves have never been investigated. To answer all these questions, gaining restricted genetic access to the relevant dopaminergic inputs driving the sleep-to-wake switch will represent a crucial conceptual advance.

In addition to dopamine, other neurotransmitters and neuropeptides have been shown to promote wakefulness in *Drosophila*; these include octopamine, the fly homologue of noradrenaline, and neuropeptide F, the homologue of mammalian neuropeptide Y (Crocker and Shegal, 2008; Crocker et al., 2010; Chung et al., 2017). Like dopamine,

these signals have also been linked to sleep homeostasis in vertebrates, further proving a degree of conservation across species of the mechanisms that control sleep (Szentirmai and Krueger, 2006; Hilakivi et al., 1998; Murillo-Rodríguez et al., 2007; Zimmerman et al., 2008**)**. The relationship between these signals and the dFB neurons has not been investigated to date. However, it is sensible to hypothesise that, like the multiple wake-promoting nuclei in the ascending arousal system of mammals, different neuronal clusters may provide arousing stimuli to the dFB in flies.

Taken together, identifying and understanding the function of the presynaptic partners to the dFB neurons will provide a full picture on the cycle of sleep regulation. With this purpose in mind, I gained genetic access and investigated the anatomical and functional connection of putative dopaminergic pre-synaptic partners to the dFB neurons. Results from this work are detailed in **Chapter 2** of this thesis.

1.3.3.2 From wake to sleep – mitochondrial oxidative stress and the OFF-to-ON switch.

Reactive oxygen species (ROS) are by-products of certain reduction-oxidation reactions, processes involving a transfer of electrons to highly reactive elements such as oxygen (Halliwell and Gutteridge, 2015). Within the cell, ROS are unstable molecules generated primarily as by-products of the mitochondrial electron transport chain or by oxidoreductase enzymes. In excess, ROS can cause oxidative stress and damage lipids, proteins, and DNA, even leading to cell death (Ryter et al., 2007). However, increasing evidence indicates that ROS also play a key role in the regulation of diverse intracellular physiological functions, for example, by reversibly modulating enzymatic activity (Finkel. 2011).

In the 1990's, Reimund's controversial 'free radical flux theory of sleep' proposed that ROS accumulate in neurons during wake and that, in this way, the fundamental function of sleep would be to clear accumulated ROS, acting as an antioxidant for the brain (Reimund, 1994). Since then, several studies have suggested a link between sleep and ROS, since sleep deprivation can produce signs of oxidative stress in the brain and peripheral organs, both in mammals and in the fruit fly (see review by Villafuente et al., 2015 and Chapter III). Furthermore, a small number of early studies pointed to the idea of ROS causing sleep, since the administration of ROS-producing substances was found to increase sleep in rodents (Komoda et al., 1990, Honda et al., 1994; Ikeda et al., 2005).

In line with this, Kempf et al. (2019) found that ROS is centrally involved in controlling homeostatic sleep in *Drosophila* through the modulation of dFB neuronal activity: Sleep loss leads to the accumulation of ROS in the mitochondria of dFB neurons, and this elevation in ROS increases the excitability of dFB neurons, thereby promoting sleep. This increase in neuronal activity is triggered by the oxidation of the nicotinamide adenine dinucleotide phosphate (NADPH) cofactor bound to Hyperkinetic (Gulbis and McKinnon, 1999); the oxidation of the cofactor into its NADP+ form alters the kinetics of the Shaker channel which, by slowing the inactivation of the A-type current, increases the frequency of action potentials, thus promoting sleep.

However, a question that arises now is the following: how does elevated ROS in the mitochondria translate into the modulation of Hyperkinetic at the plasma membrane? One may hypothesise that ROS produced in the mitochondria could reach Hyperkinetic's oxidoreductase domain through diffusion. However, since mitochondrial ROS are short-lived, this is unlikely (Halliwell and Gutteridge, 2015).

Furthermore, longer-lived lipid peroxidation products such as aldehydes are established redox substrates of Hyperkinetic: Structural studies have shown that Kvβ subunits are members of the aldo-keto reductase superfamily, a group of proteins that reduce carbonyl substrates (Long et al., 2005; Weng et al., 2006; Barski et al., 2009); Functional studies have further confirmed that Kvβ subunits use aldehydes as a substrate to catalyse the oxidation of the NADPH+ co-factor (Tipparaju et al., 2008). Therefore, a more plausible hypothesis is that short-lived mitochondrial ROS, such as O2− and H_2O_2, react locally to trigger the release of longer-lived lipid peroxidation by-products, which Hyperkinetic would then reduce in a coupled red-ox reaction that oxidises NADPH into NADP+.

Another question arising from this is whether the ROS-mediated modulation of sleep homeostasis is a process limited to the dFB neurons or whether it occurs globally across a range of different tissues in the fruit fly. A recent study by Vaccaro et al. (2020) shows that sleep deprivation increases ROS in the gut of flies. Therefore, could ROS in non-neuronal tissues, such as the gut, promote sleep?

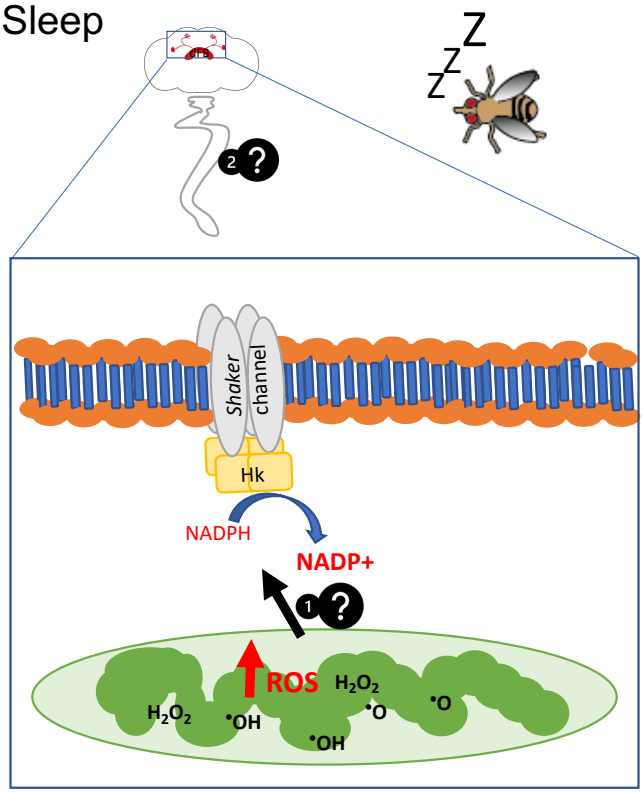
Altogether, this is consistent with the hypothesis that reactive oxygen species (ROS) generated in the mitochondria of certain tissues during wake lead to the peroxidation of membrane lipids, thus generating longer-lived medium-chain aldehydes which serve as substrates for the aldo-keto reductase activity of the sleep-modulating Hyperkinetic. In the present thesis, I addressed two aspects of this model:

1. To identify sleep-relevant sites of ROS production, I developed a chemogenetic system to induce ROS in non-neuronal tissues such as the gut, and I assessed the effect of these manipulations on sleep.

2. Using reinforced dietary polyunsaturated fatty acids resistant to oxidative stress, I attempted to prevent lipid peroxidation and investigated the impact of this manipulation on sleep.

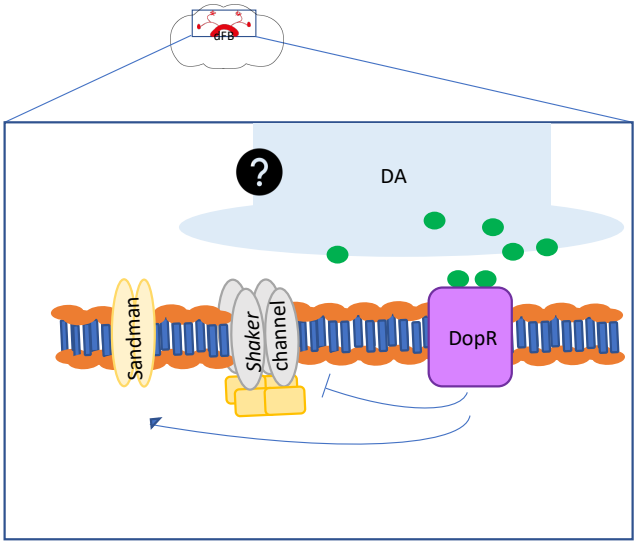
Results from this work are discussed in **Chapter 3.**

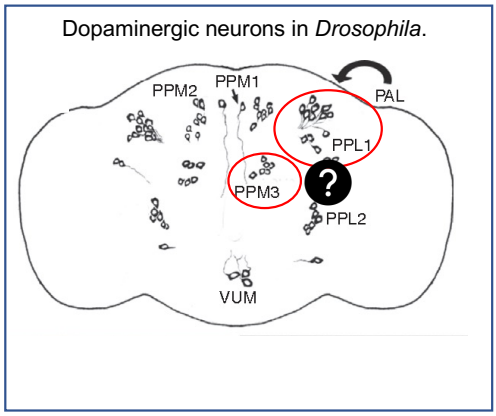
Sleep



1. **How does the increase of ROS in the mitochondria modulate Hk at the plasma membrane?**
2. **Does ROS also modulate sleep in cells and tissues other than the dFB, such as the gut?**

Wake





Where does the wake-promoting dopaminergic input to the dFB come from?

Figure 1.4. Sleep and wake mechanisms in Drosophila: my research questions. Top: the accumulation of mitochondrial ROS in the dFB neurons promote sleep through the modulation of Hyperkinetic (Hk) subunit at the plasma membrane. My research investigates two questions arising from this: (1) How does this translate into the modulation of a channel at the plasma membrane? (2) Does ROS promote sleep through other cells/tissues, such as the gut? Bottom: Dopamine silences dFB neurons through the D1-like dopamine receptor DopR, which inhibits A-type K+ Shaker currents and increases “leak” channel Sandman’s K+ currents (Pimentel et al., 2016). Drosophila’s brain contains 125 dopamine neurons (right image). PPL1 and PPM3 neurons have been implicated in promoting wake through the fan-shaped body. The relevant wake-promoting dopamine inputs within these clusters have not been identified. My research investigates the following key question: which are the relevant dopaminergic inputs that regulate sleep through the dFB?

Chapter 2: Results I - Identifying and gaining restricted access to *Drosophila's* dopamine wake-promoting inputs to the dFB.

2.1 INTRODUCTION

2.1.1 Dopamine's function in the regulation of sleep across species.

Dopamine is a catecholamine neuromodulator with a key function regulating a range of behaviours, including motor control, motivation, and arousal (Klein et al., 2019). Several lines of evidence point to dopamine's key function in the regulation of sleep across species, including in humans. For example, drugs that increase dopamine levels in the brain, such as modafinil and amphetamines, also promote wake (Wisor, 2013; Goodwin et al., 2009). In addition, there is evidence suggesting that sleep deprivation decreases dopamine receptor D2R expression in regions of the human brain (Volkow et al., 2012), and sleep disturbances are commonly seen in patients suffering from diseases that alter the dopaminergic system, such as in Parkinson's disease (Thorpy and Adler, 2005; Mehta et al., 2008).

In mammals, direct evidence for the wake-promoting role of dopamine comes primarily from rodent knockout and pharmacological studies with dopamine receptor agonists and antagonists. For instance, knocking out the dopamine transporter DAT in mice, which elevates dopamine levels in the brain, decreases sleep (Wisor et al., 2001). Similarly, Isaac and Berridge (2003) showed that centrally administering agonists to stimulate dopamine receptors in the brain promote wake in rodents. However, our

understanding of the sleep-relevant dopaminergic circuitry in mammals remains limited. In 2006, Lu et al. suggested that dopaminergic neurons from the ventral periaqueductal grey are involved in promoting wake, since ablating them significantly increased sleep. Yet, how these neurons interact with other players in the mammalian sleep circuitry is not known. More recently, Eban-Rothschild (2016) showed that dopaminergic ventral tegmental area (VTA) neurons play a key role in the maintenance of the awake state, with different projections of dopamine VTA neurons differentially modulating wake. Therefore, although several lines of evidence demonstrate dopamine's key wake-promoting function in mammals, the complexity of the mammalian brain makes it extremely challenging to fully understand the dopaminergic sleep-regulating circuitry.

Since sleep was discovered in *Drosophila*, several studies have demonstrated dopamine's key wake-promoting function in this model. Early evidence by Shaw et al. (2000) suggested that the enzyme dopamine N-acetyltransferase (*Dat*), an enzyme involved in the catabolism of monoamines, regulates wake in fruit flies. In 2005, Kume et al. found that the short sleep phenotype of *fumin* flies was caused by a mutation in the dopamine transporter (DAT), which removes dopamine from the synaptic cleft transporting it back to the pre-synaptic terminal of dopaminergic neurons. Furthermore, the short sleep phenotype and altered response to sleep deprivation of mutants such as *insomniac* and *Cullin-3* was also found to depend on dopaminergic signalling (Pfeiffenberger and Allada, 2012). Altogether, these studies proved dopamine's crucial role as an arousing signal in *Drosophila'*s sleep homeostasis.

In this context, given its much simpler nervous system and genetic tractability, *Drosophila* becomes an attractive model to dissect the sleep-relevant dopaminergic

circuits in the fly and identify the mechanisms used by dopaminergic neurons to modulate sleep and wake.

2.1.2 Drosophila's dopamine wake-promoting neurons.

The adult fly brain contains an estimated 125 dopaminergic neurons per hemisphere organised in anatomically defined clusters (White et al., 2010) (Fig. 2.1). Dopamine is a key wake-promoting neurotransmitter in the fly, but it is unclear which dopamine neurons are driving this phenotype.

Pimentel et al. (2016) demonstrated that dopamine wakes *Drosophila* up by modulating the membrane excitability of the sleep-promoting dFB neurons: it acts on two different time scales through the antagonistic modulation of two potassium channels, leading to acute and transient hyperpolarisation within tens of milliseconds, sufficient to wake flies up, or to a lasting suppression of excitability in the dFB neurons within minutes, thereby preventing sleep (Pimentel et al., 2016). It is thought that PPL1 and/or PPM3 dopaminergic neurons suppress sleep through D1-like receptor-mediated signalling in the fan-shaped body (Ueno et al., 2012; Liu et al., 2012, Pimentel et al., 2016). The Ueno et al. (2012) study suggested that the wake-promoting dopaminergic input to the fan-shaped body comes from the PPM3 cluster. In contrast, Liu et al. (2012) proposed that a single wake-promoting dopaminergic neuron from the PPL1 cluster projects to the fan-shaped body. This way, it is still unclear which dopaminergic clusters send wake-promoting inputs to the dFB. Neither of these studies were able to genetically isolate the targeted wake-promoting dopamine neurons, which is an essential step to carry out research on the mechanisms that regulate the function of these neurons. Furthermore, neither of them

proved that their candidate dopamine neurons can drive the ON-to-OFF switch in the dFB, the ultimate proof that they are functional inputs to the dFB.

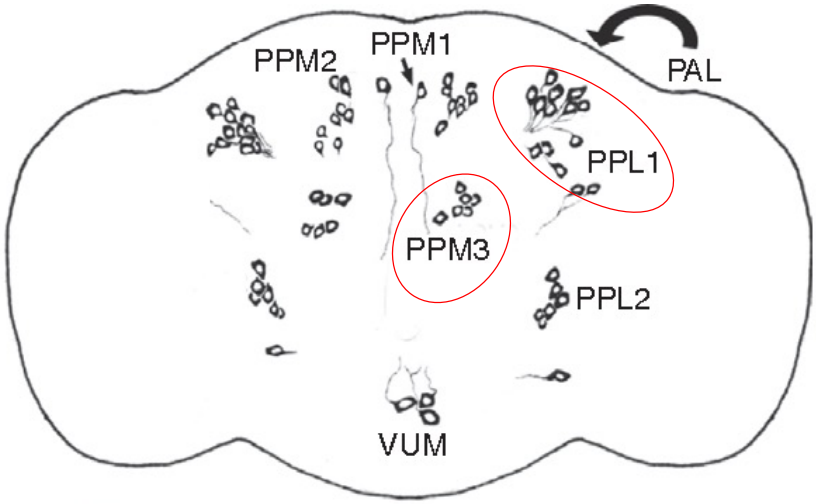


Figure 2.1 Dopaminergic neurons in the fly brain. Diagram representing the main dopaminergic neuronal clusters in the *Drosophila melanogaster* brain. PPM1= protocerebral posterior medial cluster 1; PPM2= protocerebral posterior medial cluster 2; PPM3= protocerebral posterior medial cluster 3; PPL1= protocerebral posterior lateral cluster 1; PPL2= protocerebral posterior lateral cluster 2; VUM= ventral unpaired medial; PAL= protocerebral anterior lateral; PAM = protocerebral anterior medial. Figure adapted from Whitworth, 2011.

2.1.3 Research aims:

Despite the established role of dopamine in suppressing sleep circuits and promoting wakefulness, it is still unclear which neurons from the PPL1 and/or PPM3 neuronal clusters convey the arousal-promoting dopamine signals to the dFB. Because the identities of the relevant neurons are unknown, the mechanisms that regulate the activity and function of wake-promoting dopamine neurons themselves have never been investigated. To answer these questions, it is first crucial to identify the relevant dopaminergic inputs to the dFB sleep circuit. This way, the aim of this project was to gain genetic access to the relevant wake-promoting dopaminergic inputs to the dFB, as well as to characterise them functionally and anatomically.

2.2 RESULTS

In order to gain genetic access to dFB neuronal inputs, I started by selecting a group of GAL4 lines previously identified through a MATLAB anatomical co-localisation screen (Miesenböck, unpublished). This in-silico screen used the *R84C10-GAL4* line as an anatomical reference for the dFB neurons, which is anatomically identical to the *R23E10-GAL4* neurons. Regions of interest (ROIs) were drawn in the dendritic tufts of the neurons and the dorsal fan-shaped body of the registered R84C10-GAL4 stack and a list of lines with the strongest overlap in the ROIs was compiled. From a set of 3,495 registered GAL4 lines in the Janelia Farm GAL4 collection (Jennet et al., 2012), 26 neuronal GAL4 lines with putative anatomical overlapping projections to the dendritic tuft and axonal arch of the sleep-promoting dFB neurons were identified; an initial behavioural thermogenetic screen revealed 2 sleep- and 9 wake-promoting lines. Whether these phenotypes derived from the direct interaction with the dFB remained unknown.

As a first step towards the identification and characterisation of wake-promoting partners to the dFB neurons, I initially selected two candidate lines from the in-silico screen: *R12D12-GAL4* and *R91D10-GAL4.* *R12D12-GAL4* expresses under the control of an enhancer for *dunce*, a gene encoding the cAMP phosphodiesterase catalytic subunit, with an established function in memory and learning (Dudai et al., 1976), courtship (Tully and Gold, 1993) and circadian rhythms (Levine et al., 1994). *R91D10-GAL4* expresses under the control of an enhancer for *drp12,* a gene encoding a plasma membrane immunoglobulin-like domain (Nakamura et al., 2002) linked to synaptic organisation (Carrillo et al., 2015).

The rationale for this prioritisation was the following:

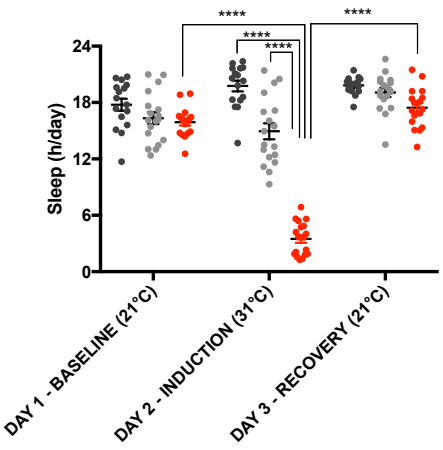
1. As confirmed through thermogenetic activation experiments, both lines have a very strong wake promoting phenotype (see subsection 2.2.1).
2. As confirmed using confocal imaging, both lines showed an overlap with the dendritic tuft and axonal arch of the dFB neurons (see subsection 2.2.2).
3. Out of all preliminary wake-promoting candidate lines from the bioinformatics screen, only *R91D10-GAL4* and *R12D12-GAL4* capture dopaminergic neurons (see subsection 2.2.3).

2.2.1 Confirmation of the wake-promoting phenotype of R12D12-GAL4 and R91D10-GAL4

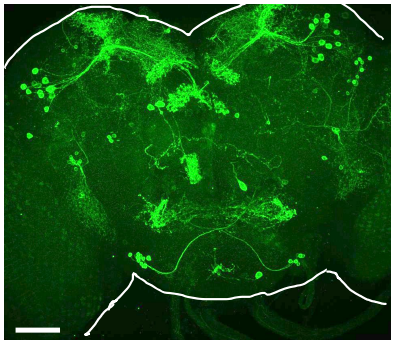
The initial behavioural characterisation of the candidate lines identified through bioinformatics was performed using thermogenetic activation. This method allows sustained temporal control of neuronal activity over long periods of time by using flies expressing the heat-sensitive transient receptor potential A1 channel from a *UAS*-driven transgene (*UAS-dTrpA1*) under GAL4 control. A limitation of this method is that the *UAS-dTrpA1* transgene alone (as a genetic control) can influence sleep when thermoactivation is induced through increased temperature, most likely due to leaky expression of the transgene (Fig 2.2). Therefore, in order to confirm the phenotype of the *R12D12-* and *R91D10-GAL4* lines and ensure that it was not an artifact of the preliminary experiments, I combined the GAL4 lines with a different *UAS-dTrpA1*, adapted the protocol to avoid leaky expression of the transgene and performed two more independent experimental repeats. Although I observed that the *UAS-dTrpA1*

transgene alone still had an effect on sleep, the experiments confirmed that the wake-promoting phenotype of of the GAL4 lines was real (Fig. 2.2).

A)

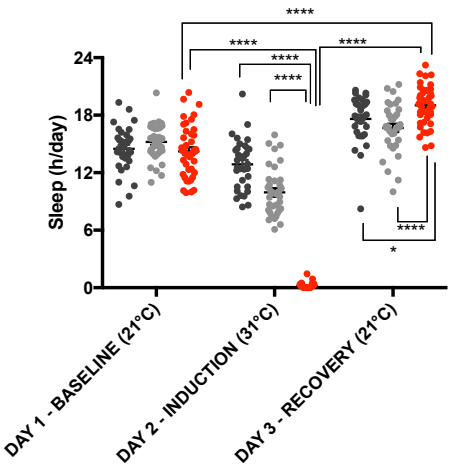


R12D12-GAL4> mCD8::GFP

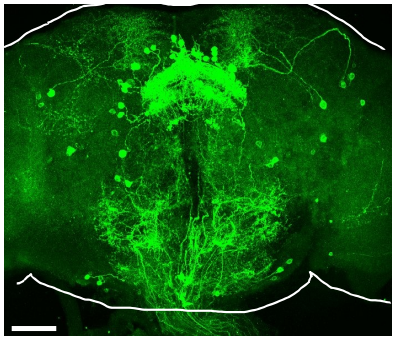


- *R12D12-GAL4/ +*
- *UAS-dTrpA1/+*
- *R12D12-GAL4 > UAS-dTrpA1*

B)



R91D10-GAL4> mCD8::GFP



- *R91D10-GAL4/+*
- *UAS-dTrpA1/+*
- *R91D10-GAL4 > UASdTrpA1*

Figure 2.2 **Thermogenetic neuronal activation reveals a wake-promoting phenotype in the *R12D12-GAL4* and *R91D10-GAL4* lines.** A) On the left: Thermogenetic activation eliminates sleep in *R12D12-GAL4>UAS*-dTrpA1 flies, compared to the UAS (*UAS-dTrpA1/+)* and GAL4 (*R12D12-GAL4*/+) controls. A two-way ANOVA analysis revealed a significant interaction of thermogenetic condition/day x genotype ($F(4, 98) = 83.46$; $P<0.0001$). Further analysis with a Tukey's multiple comparisons test revealed a significant decrease in sleep in *R12D12-GAL4>UAS-dTrpA1* compared to the UAS and GAL4 controls during thermogenetic-induced neuronal activation (DAY 2-INDUCTION at 31°C) ($P<0.0001$). On the right: maximum intensity projection showing the expression of the *R12D12-GAL4* line, labelled here by *UAS-mCD8::GFP*. Scale bar= 50μm. B) Thermogenetic activation eliminates sleep in *R91D10-GAL4> UAS-dTrpA1* flies, compared to the UAS (*UAS-dTrpA1/+*) and GAL4 (*R91D10-GAL4*/+) controls. A two-way ANOVA analysis revealed a significant interaction of thermogenetic condition/day x genotype ($F(4, 218) = 235.4$, $P<0.0001$). Further analysis with a Tukey's multiple comparisons test revealed a significant decrease in sleep in *R91D10-GAL4> UAS-dTrpA1* compared to the UAS and GAL4 controls during thermogenic-induced neuronal activation (DAY 2-INDUCTION at 31° C) ($P<0.0001$). On the right: maximum intensity projection showing the expression of the *R91D10-GAL4* line, labelled here by UAS-mCD8::GFP. Scale bar= 50μm. For behavioural data in A) and B): sample size varies in each group (genotype), with n= 16-42. Data is shown as mean ± SEM. Individual values are plotted as dots in the graphs. p-values: *=p<0.05; ****=p<0.0001.

2.2.2 Confocal imaging confirms anatomical overlap between the dFB neurons and the R12D12-GAL4 and R91D10-GAL4 lines.

Because the presumptive anatomical overlap of the candidate GAL4-lines with the sleep-promoting dFB neurons was based on data from a bioinformatics analysis, the next essential step was to validate this in vivo. To this end, I generated flies expressing the *UAS-mCD8::GFP* reporter under GAL4 control together with *R23E10-LexA* driving expression of *LexAop-mCherry* in the dFB neurons (Fig. 2.3 A)). Adult brains were

stained with anti-rabbit GFP and anti-rat mCherry antibodies to amplify their fluorescence signals and subsequently imaged in a confocal microscope. This revealed a strong co-localisation of the *R12D12-GAL4* neuronal projections with the distal dendritic branch of the dFB sleep-promoting neurons as well as overlapping expression in the medial branch of the dendritic tuft and the dFB axonal arch (Fig. 2.3 B). I also observed overlap of the *R91D10-GAL4* projections in the dendritic tuft of the dFB neurons, primarily in the medial branch, and strong presence of neurites in close proximity to the dFB axonal arch (Fig 2.3 C). My observations are in line with the results from the bioinformatics screen.

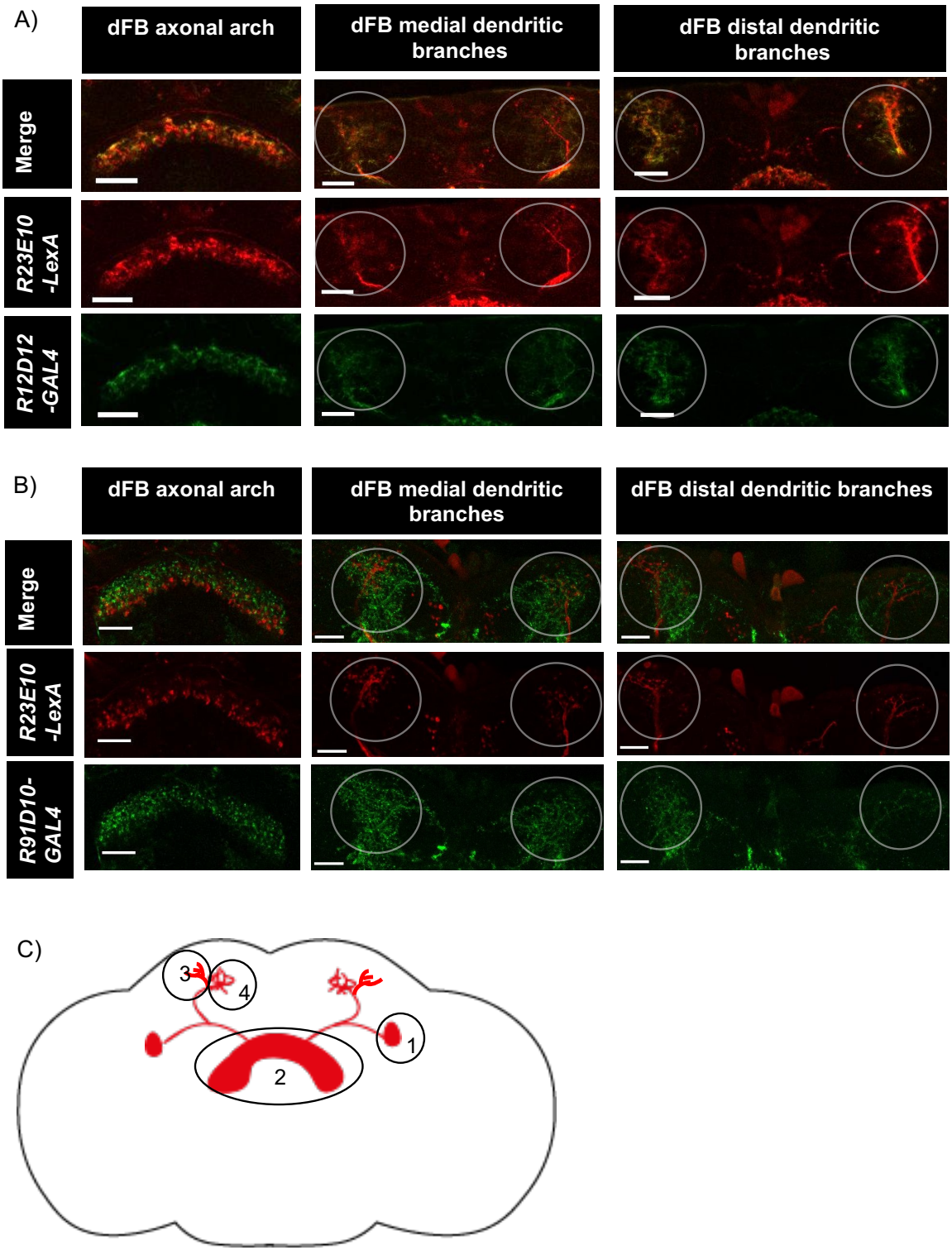


Figure 2.3 **Anatomical overlap between the R23E10 (dFB) neurons and the wake-promoting candidate lines *R12D12-GAL4 and R91D10-GAL4.*.** A) Maximum intensity projection of a confocal z-

stack section showing the anatomical overlap between the *R12D12-GAL4* (labelled with *UAS-mCD8::GFP*, in green) with the distal (right) and medial (centre) dendritic branches and the axonal projections (left) of the dFB sleep neurons (dFB axonal arch), labelled here by the *R23E10-GAL4* line (labelled by LexAop-mCherry, in red). n=7. Scale bar=20μm. B) Maximum intensity projection of a confocal z-stack showing the anatomical overlap between the *R91D10-GAL4* (labelled with *UAS-mCD8::GFP*, in green) with the distal (right) and medial (centre) dendritic branches and the axonic projections (right) of the dFB neurons, labelled by *R23E10-GAL4* (labelled by *LexAop-mCherry*, in red). n=5. Scale bar=20μm. C) Illustration depicting the anatomical structure of the dFB neurons. (1) represents the dFB cell bodies, (2) represents the axonic projections, (3) the distal dendritic tuft and (4) the medial dendritic tuft of the dFB sleep neurons.

2.2.3 Detection of monoaminergic neurons in the R12D12-GAL4 and R91D10-GAL4 lines.

As a first step to define the neurotransmitter identity of the wake-promoting neurons captured by the *R12D12-GAL4 and R91D10-GAL4* lines, I performed immunocytochemistry experiments to label dopaminergic (anti-TH antibody), octopaminergic (anti-Tdc2 antibody) and serotonergic (anti-5HT antibody) neurons in adult *Drosophila* brains expressing *UAS-mCD8::GFP* under GAL4 control. Considering the key function of dopamine in regulating dFB neuronal activity (Pimentel et al., 2016) as well as, more generally, the essential role of monoamines in sleep regulation in flies (Nall and Sehgal, 2014), the initial characterisation of monoaminergic expression in the wake-promoting GAL4 lines was the most logical step. These experiments revealed that the *R12D12-GAL4* line contains neurons from the PPL1 cluster of dopaminergic neurons (Fig. 2.4 A) i) as well as serotoninergic expression (Fig 2.4. B)). No octopaminergic expression was detected in the *R12D12-GAL4* line

(Fig. 2.4 C)). A single dopaminergic cell from the PPL1 cluster of each hemisphere was detected in the *R91D10-GAL4* line (Fig. 2.5 A). This line also contains broad serotoninergic expression (Fig. 2.5 B)), but no octopaminergic expression was detected in the *R91D10-GAL4* line (Fig. 2.5 C)).

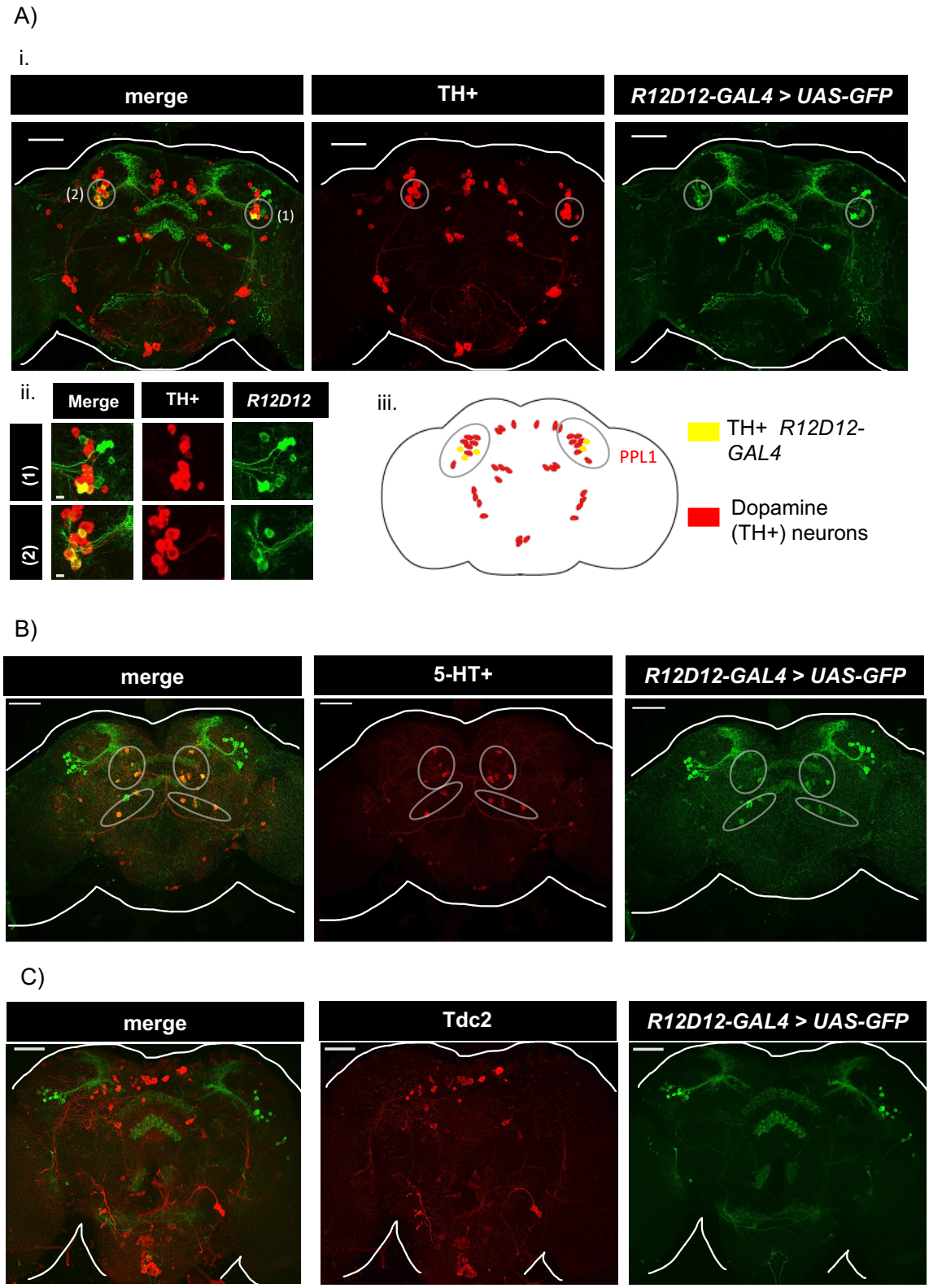


Figure 2.4. Monoaminergic expression in *R12D12-GAL4*. A) i) Maximum intensity projection of a confocal z-stack section showing co-localisation (in yellow) between neurons in the *R12D12-GAL4* line

(anti-GFP, in green) and dopaminergic neurons (anti-TH, in red)) in an adult fly brain. (1) and (2) show co-localisation in the PPL1 clusters of the right and left hemispheres, respectively. Scale bar= 50μm. n= 5. ii) Overlap between cell *R12D12-GAL4* and PPL1 TH+ neurons. Scale bar= 10um. iii) Illustration showing the dopaminergic neuronal clusters in the *Drosophila* brain (in red) and the PPL1 TH+ neurons contained by the *R12D12-GAL4* line (in yellow). B) Maximum intensity projection of a confocal z-stack showing the expression of the *R12D12-GAL4* line (anti-GFP, in green) and serotonergic neurons (anti-5-HT, in red) in an adult fly brain. n=5. Scale bar= 50μm. Circles point to the areas of co-localization between 5-HT+ and *R12D12-GAL4* cell bodies. C) Maximum intensity projection of a confocal z-stack showing the expression of the *R12D12-GAL4* line (anti-GFP, in green) and octopaminergic neurons (anti-Tdc2, in red) in an adult fly brain. n=5. Scale bar= 50μm.

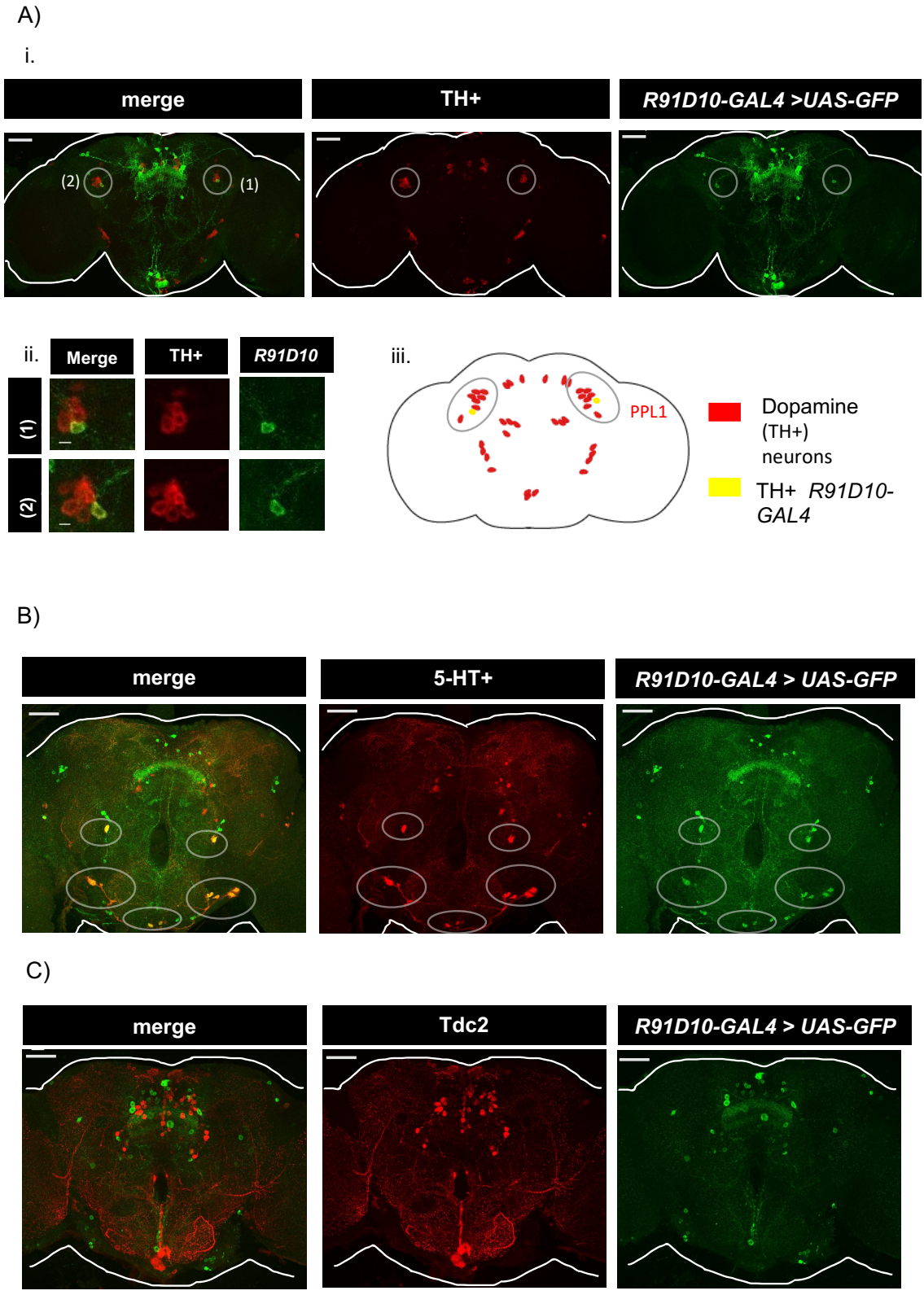


Figure 2.5. Monoaminergic expression in the *R91D10-GAL4* line. A) i) Maximum intensity projection of a confocal z-stack section showing co-localisation (in yellow) between neurons in the *R91D10-GAL4*

line (anti-GFP, in green) and dopaminergic neurons (anti-TH, in red)) in an adult fly brain. (1) and (2) show co-localisation in the PPL1 clusters of the right and left hemispheres, respectively. Scale bar= 50µm. n= 5. ii) Overlap between cell *R91D10-GAL4* line and PPL1 TH+ neurons. Scale bar= 10um. iii) Illustration showing the dopaminergic neurons in the *Drosophila* brain (in red) and the PPL1 TH+ neurons within the *R91D10-GAL4* line (in yellow). B) Maximum intensity projection of a confocal z-stack showing the expression of the *R91D10-GAL4* line (anti-GFP, in green) and serotonergic neurons (anti-5-HT, in red) in an adult fly brain. n=12. Scale bar= 50µm. Circles point to the areas of co-localization between 5-HT+ and *R91D10-GAL4* cell bodies. C) Maximum intensity projection of a confocal z-stack showing the expression of the *R91D10-GAL4* line (anti-GFP, in green) and octopaminergic neurons (anti-Tdc2, in red) in an adult fly brain. n=12. Scale bar= 50µm.

2.2.4 Generating and selecting split-GAL4 lines to gain genetic access to putative dopaminergic inputs to the dFB.

The wake-promoting *R12D12-GAL4* and *R91D10-GAL4* lines show expression in several neurons, but only a few of these cells are dopaminergic. To gain improved genetic access to the few dopamine neurons within the two selected GAL4 lines, I generated split-GAL4 hemidriver lines with the aim of intersecting the anatomically identified GAL4 lines with the expression domain of dopaminergic neurons. In these transgenic fly lines, one line expresses the transcription activation domain (AD) of GAL4 under a promoter of interest, while a second line expresses a DNA binding domain (DBD) GAL4 hemidriver under a different promoter. Only in cells where the two hemidrivers are co-expressed is a functional GAL4 reconstituted to drive expression of the effector transgene (Luan et al., 2006) (see Fig. 1.2 in Chapter 1 for a more detailed explanation).

Based on the promoter sequences of the *R12D12-GAL4* and *R91D10-GAL4* lines, I generated a total of 6 hemidriver lines: based on each promoter, I generated a line with the VP16 AD, a line with the p65 AD and another line with the DBD. In parallel, split-GAL4 hemidriver versions based on the promoter sequences of *R12D12-GAL4* and *R91D10-GAL4* were made publicly available by the Janelia split-GAL4 collection. Because of their stronger expression, the Janelia-made hemidrivers were used henceforth. TH hemidrivers expressing either a p65AD or a DBD under the control of the TH promoter (i.e., in dopaminergic neurons) were also obtained from the Janelia split-GAL4 collection.

While at least ~30 neuronal cell bodies were counted in the original *R12D12-GAL4* and the *R91D10-GAL4* (see Fig 2.2), the initial characterisation of the intersection between the *R12D12-p65* or the *R91D10-p65* hemidrivers with the *TH-DBD* hemidriver expressed in only 2-3 neurons in each hemisphere (Fig 2.6 A)). Similarly, the intersection between the *R91D10-p65* with the *TH-DBD* hemidriver expressed only 3 neurons in each hemisphere, one more dorsal-medially-located and the other two more anterior-laterally-located (Fig. 2.6 B)).

In addition to the *R12D12p-65;TH-DBD* and *R91D10-p65;TH-DBD* split-GAL4 lines, I obtained a third candidate line from the Mark Wu group as an additional strategy to gain restricted genetic access to the dopaminergic inputs to the dFB (Xie et al., 2018). In 2018, Xie et al. developed a group of 40 split-GAL4 hemidriver combinations to facilitate the study of restricted dopaminergic circuits. Out of these lines, the study reported that 3 contained a single PPL1 dopaminergic neuron with projections to the dFB. Although I found that the expression pattern of these lines was broader than

anticipated, I selected one of them, *TH-C-AD; Ddc-R60F07-DBD*, since its expression was restricted enough be considered a promising candidate for isolating the sleep-relevant dopaminergic neurons (Fig 2.6). This line contained around 6-7 cell bodies per hemisphere and projections in the dFB, but also in other areas including the ventral fan-shaped body (vFB) and MB (Fig 2.6 C)).

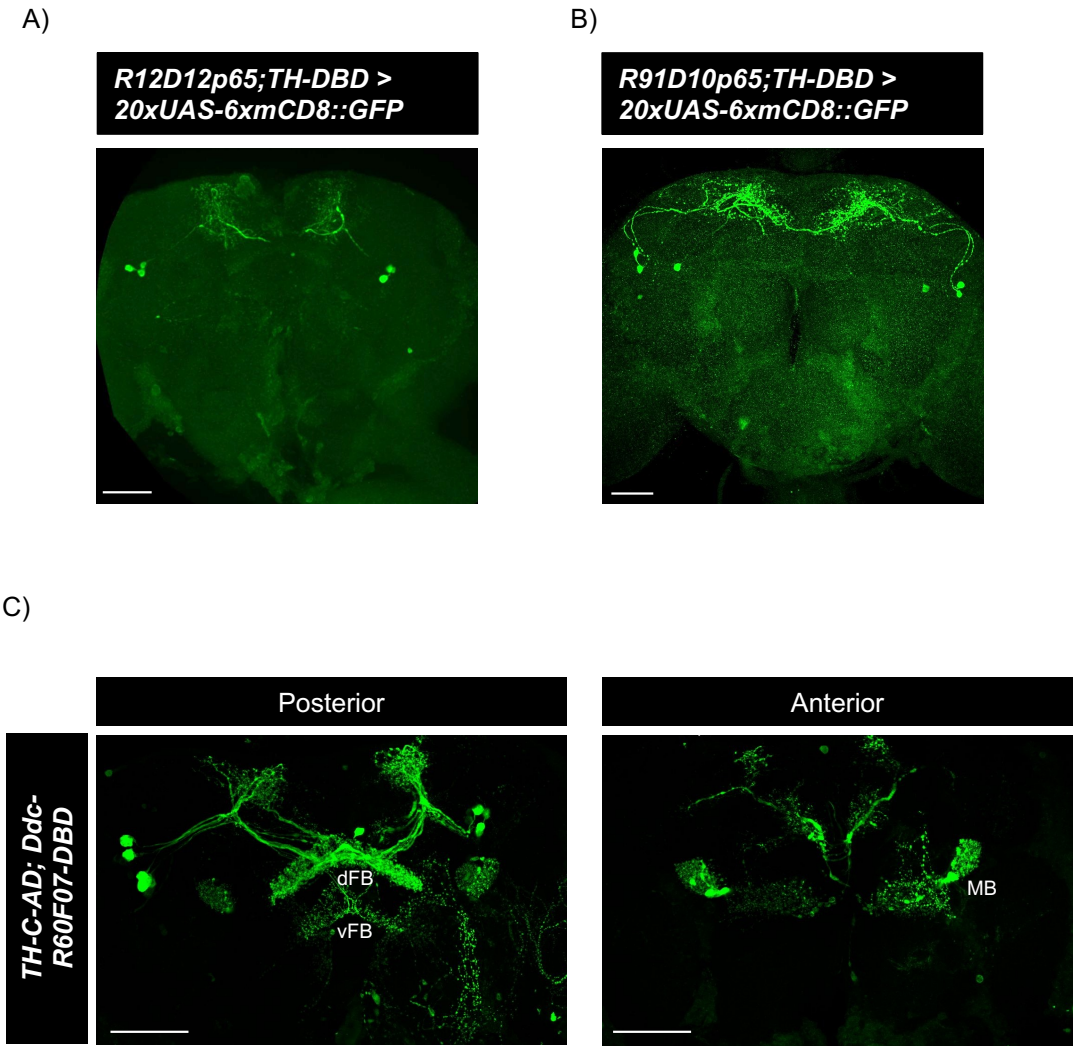


Figure 2.6. Anatomy of split-GAL4 hemidriver combinations. A) Maximum intensity projection of a confocal z-stack showing the anatomical expression of the *R12D12p65;TH-DBD* line (labelled with

UAS-20xUAS6xmCD8::GFP). B) Maximum intensity projection of a confocal z-stack showing the anatomical expression of the *R91D10p65;TH-DBD* line (labelled with *UAS-20xUAS6xmCD8::GFP*). C) Maximum intensity projection of a confocal z-stack showing the anatomical expression of the *R12D12p65;TH-DBD* line (labelled with *UAS-20xUAS6xmCD8::GFP* and stained with anti-GFP). dFB= dorsal fan-shaped body; vFB= ventral fan-shaped body; MB= mushroom bodies. Scale bar = 50μm.

2.2.5 Anatomical and functional characterisation of candidate split-GAL4 lines.

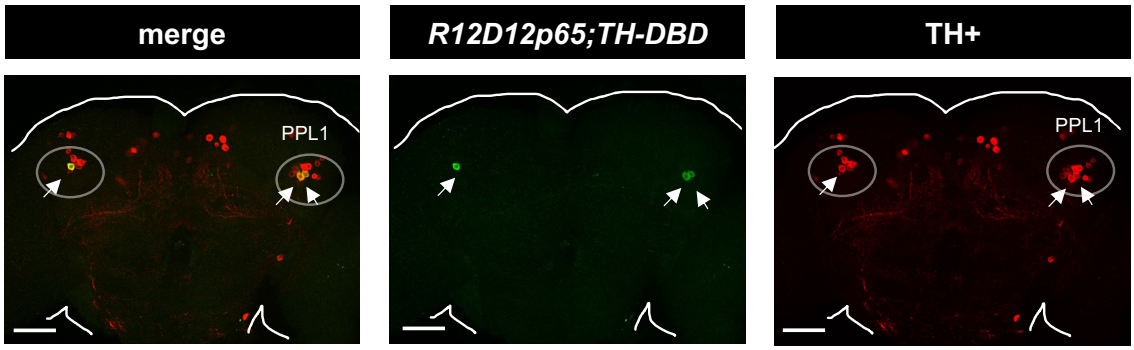
After selecting the three split-GAL4 candidate lines, the next key steps were to (1) confirm that the neurons they express are dopaminergic, (2) confirm that their projections anatomically overlap with the dFB sleep neurons, (3) test whether they have a wake-promoting phenotype and (4) (only if step 1, 2 and 3 hold) physiologically prove the connection between the putative dopamine neurons and the dFB.

(1) Dopaminergic expression in split-GAL4 candidate lines:

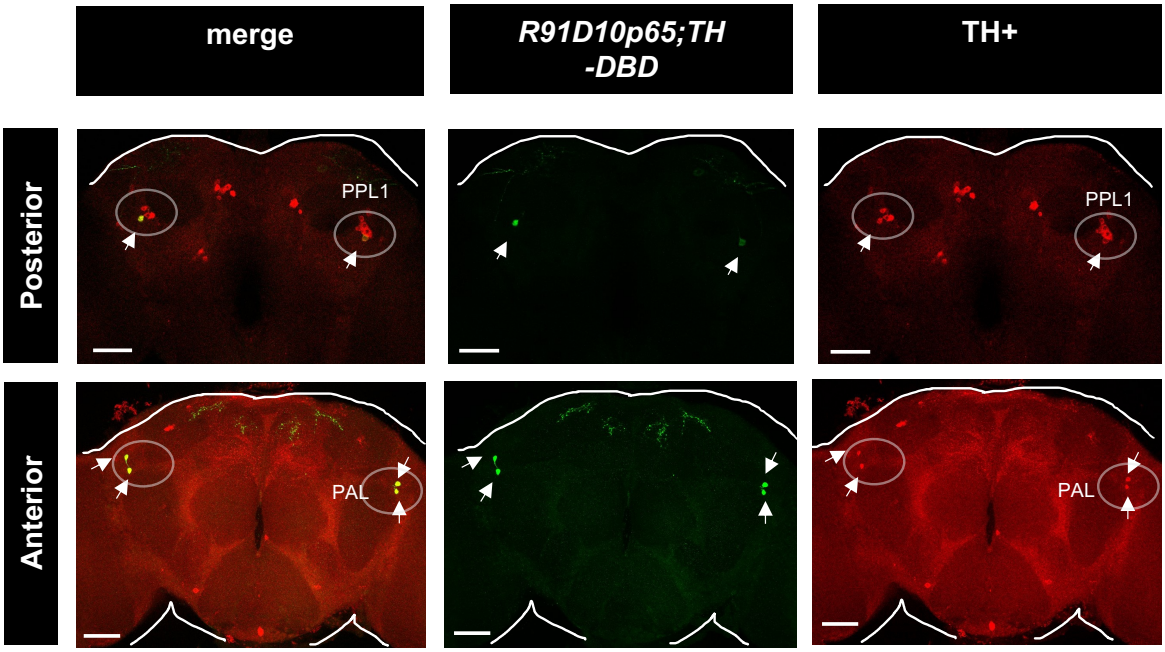
In theory, the three split-GAL4 candidates should express only dopaminergic neurons, given that all three lines contain at least a hemidriver derived from the TH promoter. Nevertheless, this is not always the case in practice and, therefore, it was important to verify it experimentally. With this goal in mind, I performed immunohistochemistry experiments by labelling dopaminergic neurons (anti-TH antibody) in adult *Drosophila* brains expressing *20xUAS-6xmCD8::GFP* under GAL4 control. This confirmed that all neurons labelled by the *R12D12p-65;TH-DBD* and *R91D10-p65;TH-DBD* are dopaminergic (Fig 2.7 A) and B)). The *R12D12p-65;TH-DBD* expresses in 2-3 PPL1 dopaminergic neurons per hemisphere (Fig 2.7 A)), while *R91D10-p65;TH-DBD* contains only 1 PPL1 dopaminergic neurons and 2 PAL dopamine neurons in each hemisphere (Fig 2.7 B)). I also found that *TH-C-AD; Ddc-R60F07-DBD* expresses in

2 dopaminergic neurons from the PPL1 cluster and one from the PPM2 in each hemisphere, plus at least 3-4 non-dopaminergic neurons (non-TH+) per hemisphere (Fig 2.7 (C)).

A)


merge
R12D12p65;TH-DBD
TH+
PPL1
PPL1

B)


merge
R91D10p65;TH -DBD
TH+
Posterior
Anterior
PPL1
PPL1
PAL
PAL

C)

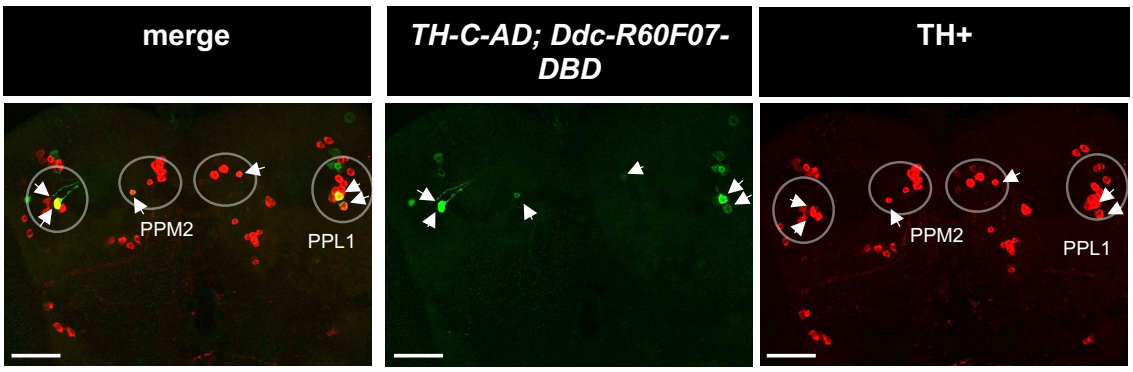

merge
TH-C-AD; Ddc-R60F07-DBD
TH+
PPM2
PPL1
PPM2
PPL1

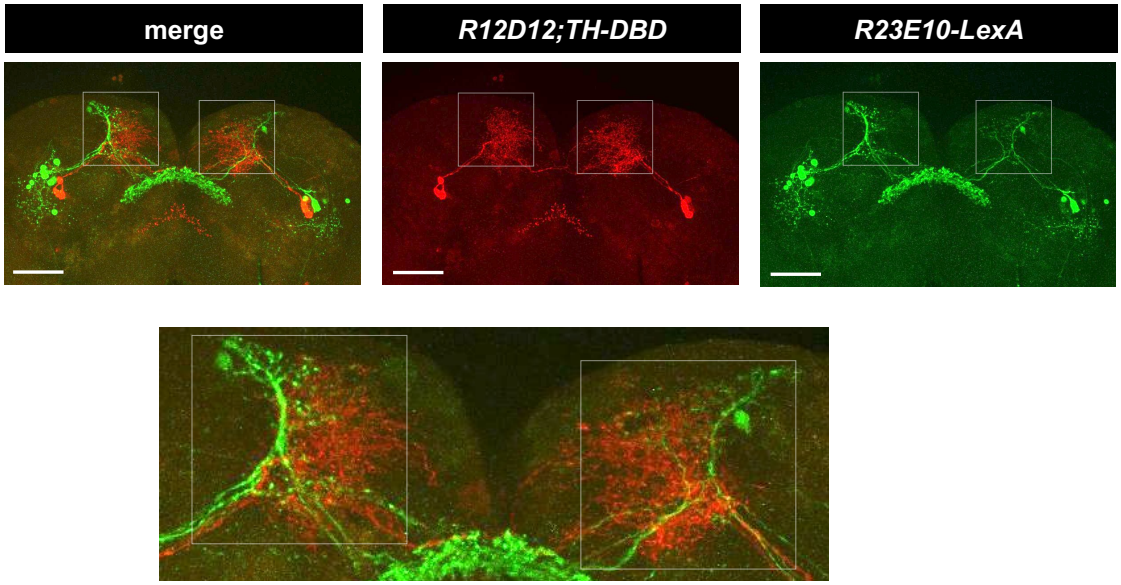
Figure 2.7. Dopaminergic expression of split-GAL4 lines confirmed immunohistochemically. A) Maximum intensity projection of a confocal z-stack section showing co-localisation (in yellow) between the *R12D12p65;TH-DBD* (labelled with *UAS-20xUAS6xmCD8::GFP* and stained with anti-GFP, in green) and dopamine TH+ neurons (labelled with anti-TH, in red). Circled areas show PPL1 dopaminergic clusters in the right and left hemispheres. Arrows point to TH+ *R12D12p65;TH-DBD* cell bodies (yellow). n=4; Scale bar=50μm. B) Maximum intensity projection of a confocal z-stack showing co-localisation (in yellow) between the *R91D10p65;TH-DBD* (labelled with *UAS-20xUAS6xmCD8::GFP* and stained with anti-GFP, in green) and dopamine TH+ neurons (labelled with anti-TH, in red). Top row images show posterior view of the brain and circled areas point to PPL1 dopaminergic clusters. Bottom row images show anterior view of the brain and circled areas surround PAL dopaminergic clusters. Arrows point to TH+ *R91D10p65;TH-DBD* cell bodies (yellow). n=4; Scale bar=50μm. C) Maximum intensity projection of a confocal z-stack showing co-localisation (in yellow) between the *TH-C-AD; Ddc-R60F07-DBD* (labelled with *UAS-20xUAS6xmCD8::GFP* and stained with anti-GFP, in green) and dopamine TH+ neurons (labelled with anti-TH, in red). Circles located laterally surround PPL1 dopaminergic clusters and circles located more medially surround PPM2 dopaminergic clusters in the right and left hemispheres. Arrows point to *TH-C-AD; Ddc-R60F07-DBD* cell bodies (yellow). n=4; Scale bar=50μm.

(2) Anatomical relation between split-GAL4 candidate lines and dFB neurons:

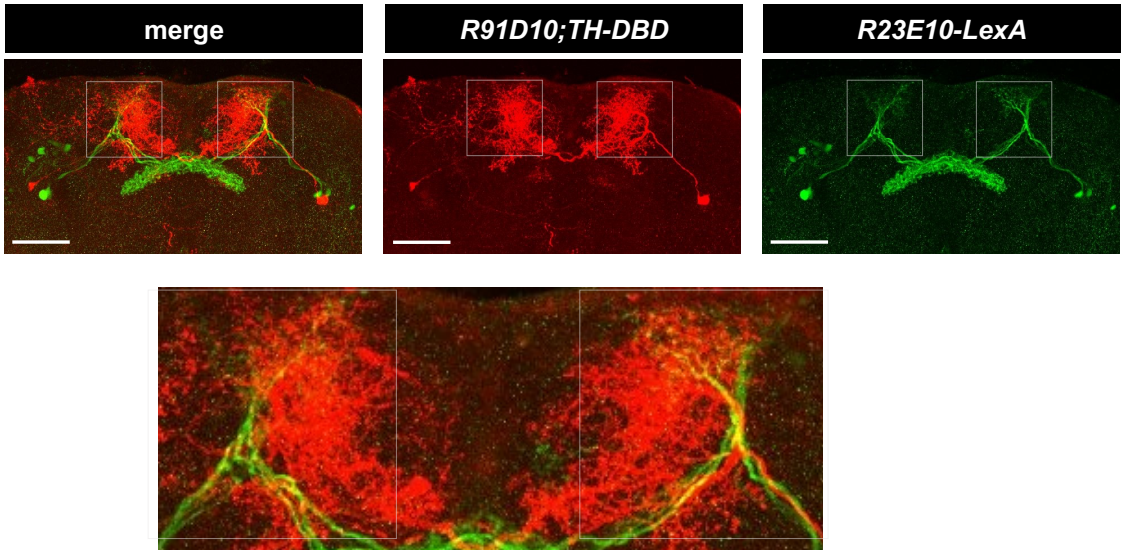
In order to understand the anatomical relationship between the split-GAL4 lines and the dFB sleep neurons I performed immunohistochemistry experiments where fly brains expressing *UAS-myr-RFP* under the control of a split-GAL4 line (labelled by anti-RFP, in red), and *LexAoP-mCD8::GFP* under the control of *R23E10-LexA* (labelled by anti-GFP, in green), were simultaneously immunostained. I found that the *R12D12;TH-DBD* PPL1 cluster dopamine neurons send projections towards the dendritic branch of the dFB neurons, primarily surrounding the dFB medial dendritic

tufts (Fig 2.8 A)). Similarly, each of the two PPL1 *R91D10p65;TH-DBD* dopamine neurons project towards the dFB dendritic trees, surrounding some of the dFB neuronal projections all the way up along its dendritic branch as well around the dFB projection that connects with the axonic arch (Fig 2.8 B)). Anatomic overlap is observed primarily with the dFB dendritic tufts, and to a lesser extent, with dFB axons in the fan-shaped body (Fig 2.8 B)). Surprisingly, I found that two neurons from the *TH-C-AD; Ddc-R60F07-DBD* completely overlapped with two dFB neurons labelled by *R23E10-LexA*, suggesting that these two neurons within the *TH-C-AD; Ddc-R60F07-DBD* are indeed *R23E10-LexA* neurons (Fig 2.8 C)). This finding was unusual given that *TH-C-AD; Ddc-R60F07-DBD* has a strong wake-promoting phenotype and *R23E1-0LexA* labels the dFB neurons, which are sleep-promoting. Because *TH-C-AD; Ddc-R60F07-DBD* expresses in dopaminergic and non-dopaminergic neurons, I decided to investigate the neurotransmitter identity of its dFB-overlapping neurons more closely and rule out the possibility that the *R23E10-LexA* neurons within this line are also dopaminergic. To do this, I simultaneously immunostained TH+ neurons (anti-TH, blue) in fly brains expressing *20xUAS-6xGFP* under *TH-C-AD; Ddc-R60F07-DBD* control (labelled by anti-GFP, green) and *LexAop-mCherry* in *R23E10-LexA* neurons (labelled by anti-mCherry, red) (Fig 2.9). This confirmed that the two *R23E10-LexA*-overlapping *TH-C-AD; Ddc-R60F07-DBD* neurons in each hemisphere are not dopaminergic neurons (Fig 2.9 A)). Therefore, in adult flies between 3-10 days of age, *TH-C-AD; Ddc-R60F07-DBD* contains two *R23E10-LexA* neurons per hemisphere, 3 dopaminergic neurons per hemisphere (two in the PPL1 cluster and 1 in the PPM2 cluster) and 3 other neurons of unidentified identity per hemisphere (Fig 2.9 B)).

A)


merge
R12D12;TH-DBD
R23E10-LexA

B)


merge
R91D10;TH-DBD
R23E10-LexA

C)

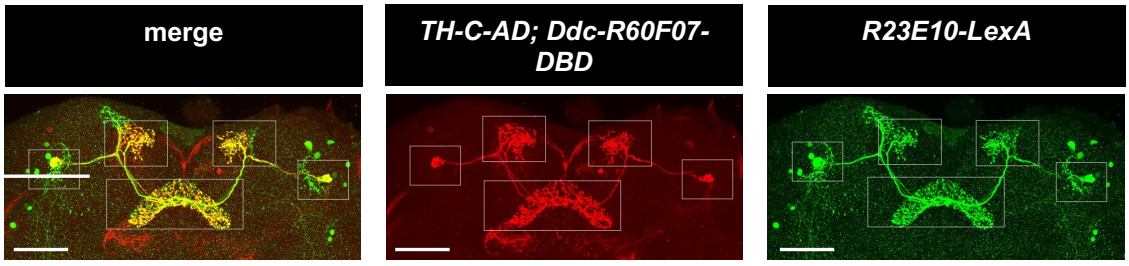
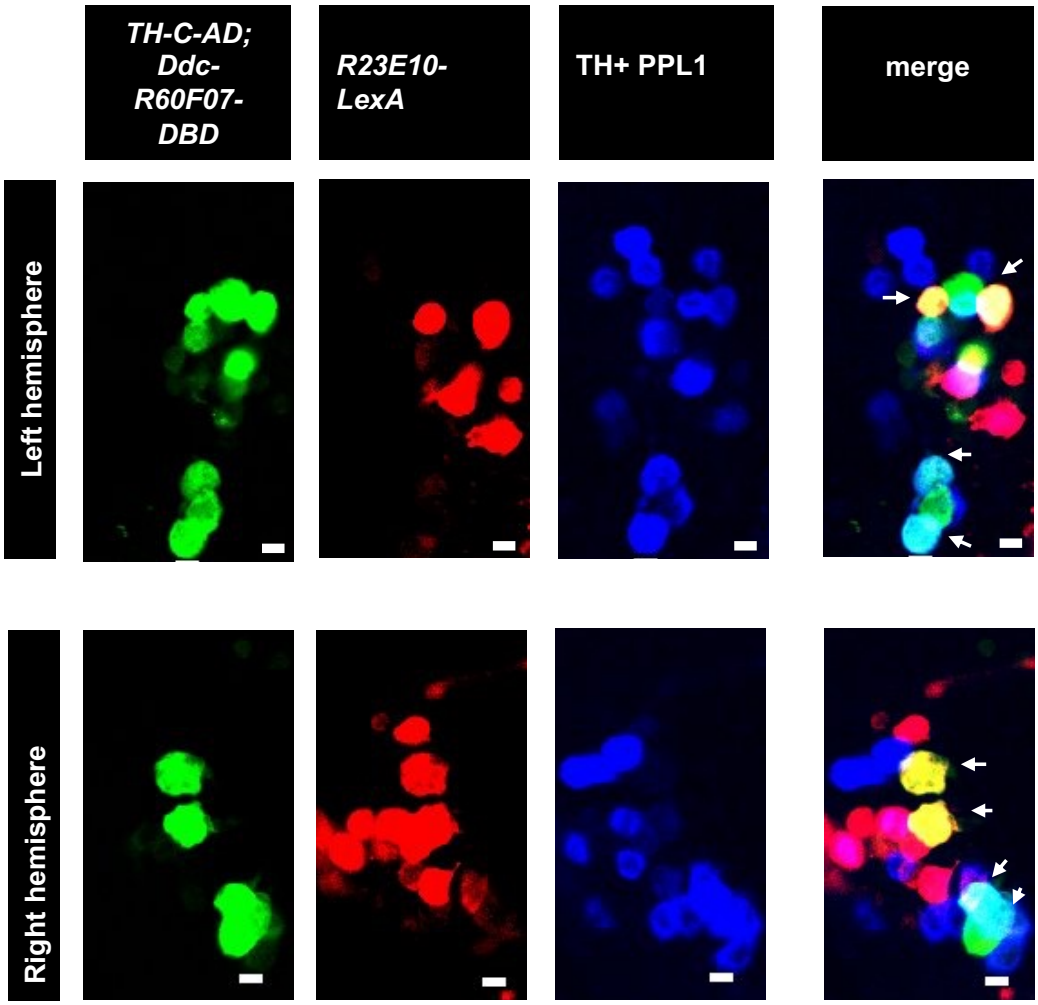
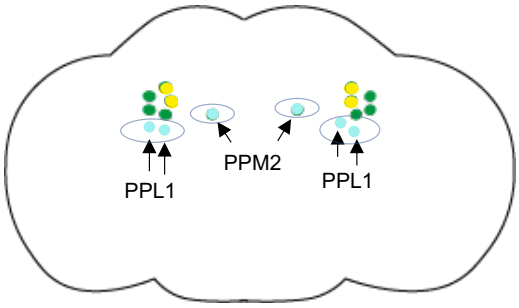

merge
TH-C-AD; Ddc-R60F07-DBD
R23E10-LexA

Figure 2.8. Anatomical overlap between the R23E10 (dFB) neurons and the split-GAL4 candidate lines. A) Maximum intensity projection of a confocal z-stack section showing the anatomical overlap between the *R12D12p65;TH-DBD* line**,** labelled here with *UAS-myr-RFP* (in red), and the *R23E10-LexA* (dFB) neurons, labelled by the *LexAop-GFP* (in green). Scale bar= 50μm. On the bottom, amplified image showing close anatomical intermingling between *R12D12p65;TH-DBD* and the dFB dendrites. n=5. B) Maximum intensity projection of a confocal z-stack showing the anatomical overlap between the *R91D10p65;TH-DBD* line*,* labelled here with *UAS-myr-RFP* (in red), and the *R23E10-LexA* neurons, labelled by the *LexAop-GFP* (in green). Scale bar= 50μm. n=4. On the bottom, amplified image showing close anatomical co-localisation between *R91D10p65;TH-DBD* and the dFB dendrites. C) Maximum intensity projection of a confocal z-stack showing the anatomical overlap between *TH-C-AD; Ddc-R60F07-DBD*, labelled here with *UAS-myr-RFP* (in red), and the *R23E10-LexA* neurons, labelled by the *LexAop-GFP* (in green). Scale bar= 50μm. n=4. Areas in yellow denote co-localisation.

A)



B)



Dopamine (TH+) cell bodies

TH-C-AD; Ddc-R60F07-DBD cell bodies

R23E10-LexA cell bodies

\+ = *Dopaminergic (TH+) TH-C-AD; Ddc-R60F07-DBD neurons*

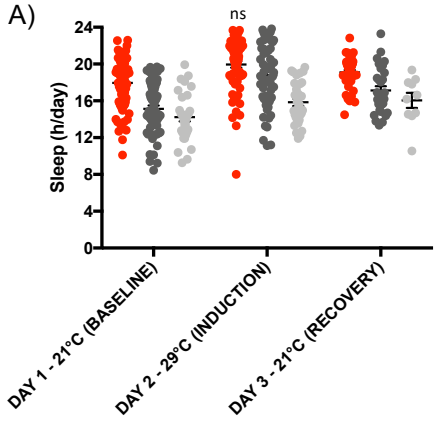
\+ = *TH-C-AD; Ddc-R60F07-DBD* and *R23E10-LexA* overlap

Figure 2.9. Characterising the identity of *TH-C-AD; Ddc-R60F07-DBD* cell bodies immunohistochemically. A) Maximum intensity projection of a confocal z-stack section showing the *TH-C-AD; Ddc-R60F07-DBD* cell bodies and any overlap with TH+ PPL1 neurons or *R23E10-LexA* (dFB) neurons. *TH-C-AD; Ddc-R60F07-DBD* expressed *20xUAS6xmCD8::GFP* and were stained with anti-GFP antibody (green). *R24E10-LexA* expressed *LexAo-pmCherry* and was stained with anti-mCherry antibody (red). Dopaminergic (TH+) neurons were stained with an anti-TH antibody (dark blue). Top images are from the left cerebral hemisphere while bottom images are from the right cerebral hemisphere. Two *TH-C-AD; Ddc-R60F07-DBD* cell bodies overlap with *R23E10-LexA* (yellow). Two separate *TH-C-AD; Ddc-R60F07-DBD* overlap with TH+ neurons (light blue). n=4. Scale bar= 5μm. B) Diagram illustrating the composition of the *TH-C-AD; Ddc-R60F07-DBD* line. Its 6 dopaminergic neurons are depicted in light blue (2 from each PPL1 cluster and 1 from each PPM2 dopaminergic cluster). Its *R23E10-LexA*-overalapping neurons are in yellow (2 in each hemisphere). The remaining 6 neurons depicted in green (3 in each hemisphere) are of unknown identity.

(3) Behavioural phenotype of split-GAL4 candidate lines:

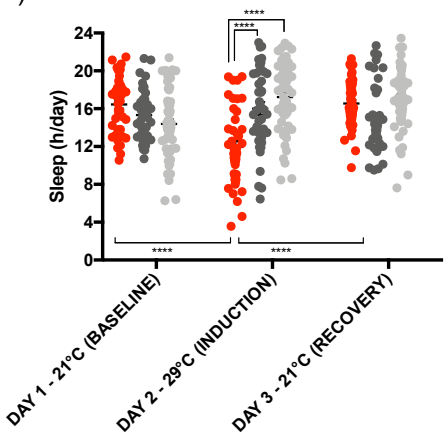
Dopaminergic signalling into the dFB neurons leads to a decrease in total daily sleep time (Pimentel et al., 2016). Although I see close intermingling between the split-GAL4 candidate lines and the dFB, I needed to verify whether they had a wake-promoting phenotype. To test this, I thermogenetically activated each of the split-GAL4 lines. I found that activating the *R12D12p65;TH-DBD* did not produce any significant changes in sleep phenotype, indicating that this line did not contain any sleep-relevant dopaminergic neurons (Fig. 2.10 A)). In contrast, activating *R91D10p65;TH-DBD* led to a significant decrease in sleep, which shows that *R91D10p65;TH-DBD* dopamine neurons are wake-promoting (Fig 2.10 B)). *TH-C-AD; Ddc-R60F07-DBD* showed a significant sleep decrease upon its activation. However, because *TH-C-AD; Ddc-R60F07-DBD* also expresses in some non-dopaminergic neurons, I investigated whether this wake-promoting phenotype was driven by its dopaminergic neurons or its non-dopaminergic neurons. To test this, I activated *TH-C-AD; Ddc-R60F07-DBD* thermogenetically while simultaneously knocking-down its dopaminergic transmission (by using an RNAi targeting TH, the rate-limiting enzyme in the synthesis of dopamine). I found that knocking-down dopaminergic transmission blocked the wake-promoting effect of thermogenetically activating the *TH-C-AD; Ddc-R60F07-DBD,* thus suggesting that the dopaminergic neurons within this split-GAL4 line have a wake-promoting function. To confirm this, it would be ideal to repeat the experiment with an additional control group to control for a possible dilution effect of the GAL4 protein (Fig. 2.10 C)).

A)



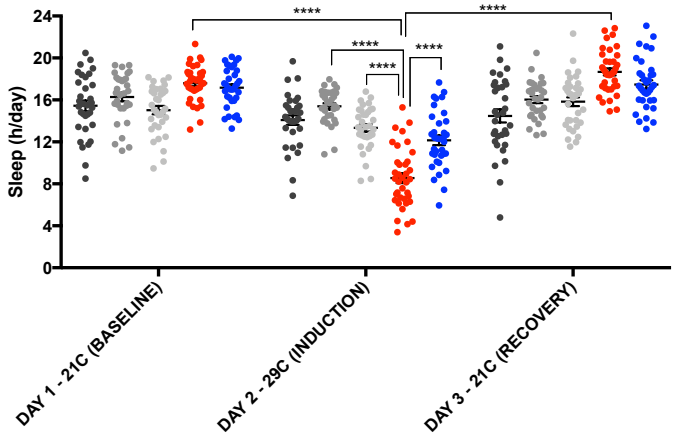
- *R12D12p65;TH-DBD > UASTrpA*
- *R12D12p65/+;TH-DBD/+*
- *UAS-dTrpA/+*

B)



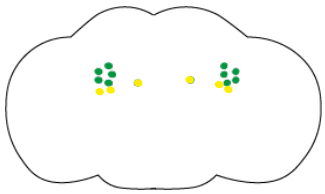
- *R91D10p65;TH-DBD > UASTrpA*
- *R91D10p65/+;TH-DBD/+*
- *UASTrpA/+*

C) i.



- *UAS-dTrpA1/+ ; UAS-THmiR/+*
- *TH-C-AD/+; Ddc-R60F07-DBD/+*
- *UAS-dTrpA1/+*
- *TH-C-AD; Ddc-R60F07-DBD > UAS-dTrpA1*
- *TH-C-AD; Ddc-R60F07-DBD > UAS-dTrpA1; UAS-THmiR*

ii.



Non-dopaminergic *TH-C-AD; Ddc-R60F07-DBD*

Dopaminergic *TH-C-AD; Ddc-R60F07-DBD neurons*

Figure 2.10. Thermogenetic activation of split-GAL4 candidate lines reveals that dopaminergic *R91D10p65;TH-DBD* and *TH-C-AD; Ddc-R60F07-DBD* neurons are wake-promoting, but not *R12D12p65;TH-DBD* neurons. A) Activating *R12D12p65;TH-DBD* thermogenetically does not affect total sleep time. Two-way ANOVA analysis shows there is no significant interaction of thermogenetic condition/day (temperature) x genotype ($F(4, 399) = 2.199$; $P=0.0684$). B) Thermogenetic activation of *R91D10p65;TH-DBD (R91D10p65;TH-DBD>UASdTrpA* during INDUCTION day at 31°C) significantly reduces sleep compared to genetic controls (*R91D10p65;TH-DBD*/+ and *UASdTrpA/+)* during INDUCTION day as well as compared to temperature controls (*R91D10p65;TH-DBD>UASdTrpA* sleep duration in BASELINE and RECOVERY days), as revealed by a two-way ANOVA analysis followed by Tukey's multiple comparison test. The two-way ANOVA analysis revealed a significant interaction between thermogenetic condition/day (temperature) x genotype ($F(4, 405)) = 16.89$; $P<0.0001$). C) i) Thermogenetic activation of *TH-C-AD; Ddc-R60F07-DBD* (*TH-C-AD; Ddc-R60F07-DBD >UASdTrpA* during INDUCTION day at 31°C) leads to a significant decrease in total daily sleep duration compared to genetic controls (*TH-C-AD; Ddc-R60F07-DBD* /+ and *UASdTrpA/+)* and to temperature controls (*TH-C-AD; Ddc-R60F07-DBD >UASdTrpA* sleep duration in BASELINE and RECOVERY days), as revealed by a two-way ANOVA analysis followed by Tukey's multiple comparison test. The two-way ANOVA analysis revealed a significant interaction between thermogenetic condition/day (temperature) x genotype ($F(8,498)) = 29.45$; $P<0.0001$). Furthermore, RNAi-mediated knockdown of dopaminergic transmission in *TH-C-AD; Ddc-R60F07-DBD* (*TH-C-AD; Ddc-R60F07-DBD>UASdTrpA;THmiR,* in blue) blocks *TH-C-AD; Ddc-R60F07-DBD>UAS-dTrpA's* wake-promoting phenotype (in red), indicating that dopaminergic neurons within *TH-C-AD; Ddc-R60F07-DBD* drive its wake-promoting phenotype. ii) Diagram illustrating the composition of the *TH-C-AD; Ddc-R60F07-DBD* line with its 6 dopaminergic neurons in yellow and non-dopaminergic neurons in green. As seen in i) dopaminergic neurons drive the line's wake-promoting phenotype. For behavioural data in A), B) and C): sample size varies in each group (genotype), with n= 16-48. Data is shown as mean ± SEM. Individual values are plotted as dots in the graphs. In A) and C) data was pooled from two independent experimental repeats. In B) data was pooled from three independent experimental repeats. **** = $P<0.0001$. ns= non-significant.

Chapter 3: Results II – Linking oxidative stress, lipid peroxidation and sleep homeostasis in *Drosophila*.

3.1 INTRODUCTION

3.1.1 Finding the cause for sleep: the free radical flux theory.

In the early 20th century, Henri Piéron's 'hypnotoxin theory of sleep' presented a physiological explanation for the cause of sleep. He observed that, when cerebrospinal fluid from sleep-deprived dogs was injected into well-rested dogs, this induced somnolence in the recipient animals. In this way, Piéron's theory proposed that, during wake, a certain "toxin" would accumulate which, after reaching a certain threshold, could induce sleep (Piéron et al., 1913). But what is the nature of this sleep-inducing, "hypnotoxin", substance? This question has remained a mystery for decades.

The brain is one of the most energetically demanding organs of the body – it is estimated that, only during rest, 20% of the body's energy is used by the brain (Raichle and Gusnard, 2002). One of the unavoidable consequences of this is the high generation of reactive oxygen species (ROS) in neurons – these unstable molecules derived from molecular oxygen are generated primarily as by-products of the mitochondrial electron transport chain or by oxidoreductase enzymes and, if not properly neutralised, will cause damage to lipids, proteins and DNA, and even lead to cell death (Halliwell and Gutteridge, 2015; Ryter et al., 2007). Based on this idea, in 1994, Reimund's controversial 'free radical flux theory of sleep' proposed that reactive

oxygen species (ROS) accumulate in neurons during wake and that, in this way, the fundamental function of sleep would be to clear accumulated ROS, acting as an antioxidant for the brain (Reimund, 1994).

Because findings were initially contradictory, with time, the popularity of this hypothesis decreased. However, several studies have now shown that sleep deprivation is associated with an increase in oxidative stress in various regions of the rat and mouse brains, regardless of the sleep deprivation method used (Villafuerte et al., 2015). For example, after sleep deprivation, increased lipid peroxidation has been reported in areas such as the hippocampus and prefrontal cortex (Lima et al., 2014; Vollert et al., 2011). In addition, numerous studies have shown that sleep deprivation alters antioxidant expression across regions in the rat and mouse brain (Ramanathan et al., 2002;). This way, considerable evidence points to the connection between sleep deprivation and an increase in oxidative stress.

But is this a bi-directional relationship where oxidative stress can induce sleep? In the 1990's, a small number of studies pointed for the first time to the idea of ROS being involved in regulating sleep. The marker of oxidative stress oxidised glutathione (GSSG) was first identified amongst the active components of the "sleep-promoting substance" isolated from the brainstem extract of sleep deprived rats; later, it was found to increase sleep when administered in rats and rabbits (Komoda et al., 1990, Honda et al., 1994; Kimura et al., 1998). In addition, administering t-butyl hydroperoxide at low concentrations, an organic compound which generates ROS, was found to increase sleep; local application of the same compound in the preoptic/anterior hypothalamus induced the release of the sleep-promoting

neuromodulators adenosine and nitric oxide (Ikeda et al., 2005). Altogether, these findings introduced the idea that sleep may originate in response to increased ROS as a way to protect the brain from oxidative damage.

3.1.2 Linking oxidative stress, lipid peroxidation and sleep homeostasis in Drosophila.

More recently, the use of *Drosophila* as a model organism to study sleep not only has reinforced these ideas, but importantly, it has made it possible to begin characterising in detail the mechanisms that link ROS to sleep. Amita Sehgal's group provided the first evidence of a connexion between oxidative stress and the function of sleep in *Drosophila*. They found that chronically treating flies with a low dose of the oxidative stress-producing agent paraquat induced a breakdown of sleep-wake cycles reminiscent of that observed with aging. This supported the idea that the accumulation of oxidative damage with age contributes to the deterioration in sleep quality (Koh et al., 2006). More recently, another group has discovered that sensitivity to paraquat-induced acute oxidative stress is a shared phenotype amongst a diverse group of short-sleeping mutant flies; all types of short-sleeping flies died faster than control flies when exposed to oxidative stress, while they were not differentially affected by starvation or by pathogenic infections (Hill et al., 2018). In addition, they found that increasing sleep time had a protective effect against oxidative stress in flies and that overexpressing antioxidant genes to reduce ROS in the fly brain led to a decrease in sleep (Hill et al., 2018). Thus, this work supported the hypothesis that protecting against oxidative stress is a core function of sleep, as well as suggesting that ROS could play a role in regulating sleep.

Recent work by my group not only demonstrates a role for ROS in regulating sleep homeostasis in the fruit fly, but it provides for the first time a characterisation of the mechanisms whereby ROS controls sleep by modulating the biophysical state of *Drosophila*'s dFB sleep neurons. Kempf et al. (2019) showed that sleep loss elevates mitochondrial ROS in dFB neurons. This increase in ROS, in turn, modulates the activity of dFB neurons by oxidising the NADPH cofactor bound to the Kvβ subunit, Hyperkinetic, which alters the kinetics of the *Shaker* channel, eventually leading to increased firing of the dFB neurons and, in consequence, inducing sleep (Kempf et al., 2019). This way, in the dFB neurons of the fly, energy metabolism, oxidative stress and sleep become mechanistically connected.

However, a question that arises from this finding is the following: if ROS accumulates in the mitochondria, how does this translate into the modulation of an ion channel at the plasma membrane? Mitochondrial ROS, such as as O_2^- and H_2O_2, are short-lived species and, therefore, it is unlikely that they reach the plasma membrane to react directly with Hyperkinetic. An alternative hypothesis is that the Shaker channel is internalised by the mitochondria, where it could be directly oxidised before being translocated back to the plasma membrane. However, numerous functional and structural studies have shown that longer-lived lipid peroxidation products such as aldehydes are redox substrates of Hyperkinetic (Long et al., 2005; Weng et al., 2006; Barski et al., 2009; Tipparaju et al., 2008). Therefore, a more plausible explanation is that mitochondrial ROS react locally on the lipid bilayer causing lipid peroxidation and triggering the release of longer-lived lipid peroxidation by-products; the longer-lived

by-products of lipid peroxidation would then react with Hyperkinetic at the plasma membrane.

A second question is whether this phenomenon is restricted to the dFB neurons or if it occurs in tissues other than the dFB. It is even conceivable that the phenomenon linking oxidative stress and sleep occurs outside the brain, in non-neuronal tissues. Studies with rodents have demonstrated the effects that sleep deprivation can have in non-neuronal physiological systems (Everson et al., 2004; Everson et al., 2000). These include the molecular consequences of sleep deprivation on peripheral tissues such as the lung and heart, as well as possible differences on oxidative stress (Anafi et al., 2013; Lungato et al., 2013; Chang et al., 2008; Chang et al., 2006; Everson et al., 2005; de Oliveira et al., 2002). In this way, some have hypothesised that oxidative stress in organs other than the brain may underlie the physiological effects experienced in peripheral systems after sleep deprivation. More recently, Vaccaro et al. (2020) showed direct evidence of the effects that sleep deprivation has on peripheral tissue oxidative stress. They found that sleep deprivation increased ROS in the fly and mouse gut, which triggered oxidative stress and was the cause of premature death in flies. But, could the accumulation of ROS in the gut, or other peripheral tissues, cause an increase in sleep? Since it is not known whether a bidirectional relationship exists between ROS and sleep in peripheral tissues, this question remains open.

3.1.3 Research aims:

Previous work by the Miesenböck group established a clear connection between ROS and sleep in the dFB neurons of the fly: Sleep deprivation increases mitochondrial ROS, and the elevation of ROS in the mitochondria increases sleep through the modulation of Hyperkinetic at the plasma membrane. Whether this phenomenon occurs in tissues other than the dFB is unknown. In addition, it remains unclear how this increase in ROS translates into the modulation of a channel at the plasma membrane. I hypothesised that ROS generated in the mitochondria of certain tissues during wake lead to the peroxidation of membrane lipids, whose breakdown produces medium-chain aldehydes. These aldehydes serve as substrates for the aldo-keto reductase activity of Hyperkinetic, eventually modulating sleep. In this chapter, I outline my research on the following tenets of this working model:

1. To determine the causal effect of ROS on sleep across tissues, I developed a chemogenetic system to induce ROS in non-neuronal tissues such as the gut, and I assessed the effect of these manipulations on sleep.

2. I aimed to prevent lipid peroxidation through dietary supplementation of reinforced deuterated polyunsaturated fatty acids (D-PUFAs) and investigated the impact of this manipulation on sleep.

3.2 RESULTS

3.2.1 Development of an inducible chemogenetic system for mapping sleep-relevant sites of ROS production in Drosophila.

(1) Generation of DAAO-based chemogenetic tools for ROS induction in Drosophila.

To generate ROS across *Drosophila*'s tissues, ideally, one would use an inducible system that can reliably generate ROS at the adult *Drosophila* stage, in a time-controlled fashion and in any genetically defined cellular population in the fruit fly. The light-inducible miniSOG was successfully used to generate ROS in the dFB neurons and induce sleep (Kempf et al., 2019; Shu et al., 2011). However, since miniSOG generates superoxide, the most unstable ROS, it is technically challenging to use: due to the instability of miniSOG-generated superoxide, Kempf et al. (2019) used membrane-targeted expression of miniSOG near the Hyperkinetic subunit in order to effectively induce sleep. The photosensitive nature of miniSOG also makes it potentially technically difficult for use in non-neuronal tissues. Therefore, with the goal of effectively inducing ROS in tissues like the gut, I devised and developed a hydrogen peroxide (H_2O_2)-inducible chemogenetic system based on the D-amino acid oxidase (DAAO) enzyme-encoding gene from yeast *Rhodotorula gracilis (R.gracillis)*. This DAAO-based chemogenetic tool should be less technically challenging to use and a much more powerful tool for ROS induction for the following reasons: (1) H_2O_2 is more stable than superoxide; (2) since it is a chemogenetic system, it should be possible to

control the amount of ROS generated in a concentration-dependent manner based on the substrate dose-response relationship.

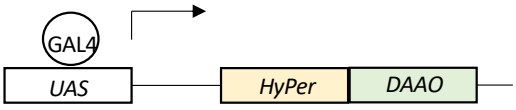
The specific choice of the DAAO from *R.gracillis* as compared to other versions of the protein is based on the following reasons. First, D-amino acid oxidases are enzymes which oxidise D-amino acids to the corresponding α-keto acids, generating in this process the ROS hydrogen peroxide (H_2O_2) and ammonia (Alonso et al., 1998; Pollegioni et al., 2007). Unlike the DAAO from other species, *R.gracillis* DAAO has absolute stereospecificity towards D-amino acids, with no activity towards L-amino acids (Pollegioni et al., 1992). Compared to other DAAOs, it also has a high turnover number (i.e., the maximum number of substrate molecules transformed per unit time by a single enzyme molecule when the enzyme is the rate-limiting factor), making it more suitable as an inducible chemogenetic system (Pollegioni et al., 2007).

I therefore adapted to *Drosophila melanogaster* the *R.gracillis* DAAO-based ROS-inducing chemogenetic tools designed by Matlashov et al. (2014) for use in eukaryotic cells and by Steinhorn et al. (2018) for use in the rat. Based on this I generated the following transgenic fly lines, either under UAS control or LexAop control: *UAS-HyPer-DAAO, UAS-SypHer2-DAAO, UAS-DAAO, LexAop-HyPer-DAAO, LexAop-SypHer2-DAAO and LexAop-DAAO.* In its most basic forms, *UAS-DAAO* and *LexAop-DAAO* were built with the sole purpose of generating ROS in a tissue-specific manner on demand. HyPer is a genetically encoded ratiometric H_2O_2-sensitive fluorescent biosensor (Belousov et al., 2006), and therefore, I linked it with the DAAO chemogenetic system (generating the *UAS-HyPer-DAAO and LexAop-HyPer-DAAO* transgenes) with the additional objective of verifying and quantifying intracellular

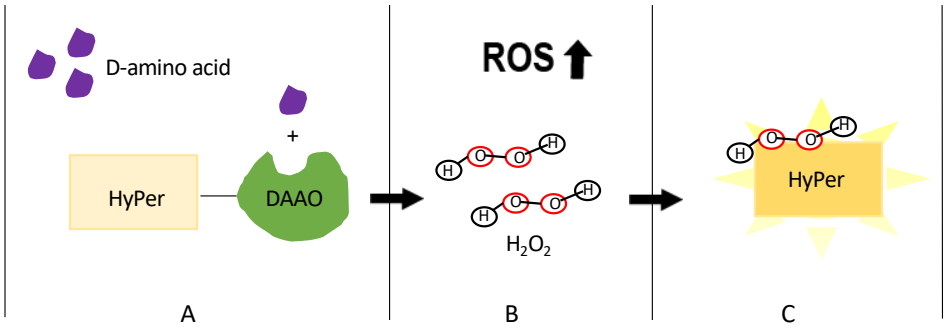
DAAO-generated increases in ROS levels upon chemogenetic induction (Fig 3.1.). In addition, I also linked the DAAO-based chemogenetic system with the H_2O_2-insensitive probe SypHer2 (in the UAS-*SypHer2-DAAO and LexAop-SypHer2-DAAO* transgenes), generated by mutating one of HyPer's H_2O_2-sensitive cysteine residues into serine (Matlashov et al., 2014), which serves as a control to ensure that any observed changes in HyPer cell fluorescence are real changes in ROS levels, rather than a product of changes in pH (see explanation in Fig 3.1).

I verified the presence of the DAAO-based transgenes in the transgenic flies' genomic DNA through PCR-based genotyping. Furthermore, because *HyPer* and *SyPher2* encode circularly permutated yellow fluorescence proteins (cpYFP) and there are anti-GFP antibodies reactive to YFP, I verified the expression of *HyPer-DAAO*- and *SyPher2-DAAO*-containing constructs in transgenic flies through immunohistochemistry: expression of these constructs was driven in the R23E10 neurons of the fly brain, which were dissected, immunostained and imaged in a confocal microscope. As seen in Fig 3.2 A, the *HyPer-DAAO*- and *SyPher2-DAAO* systems achieved highly specific and robust expression in the R23E10 neurons.

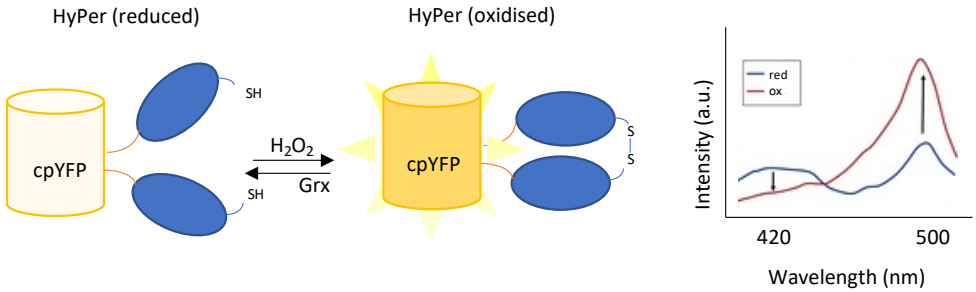
i.



ii.



iii.



iv.

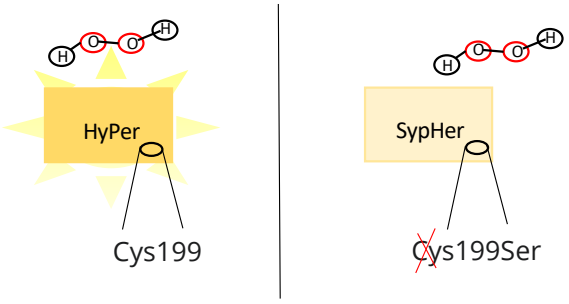


Figure 3.1 The *HyPer-DAAO*-based chemogenetic system. i. Illustration of the genetic construct *UAS-HyPer-DAAO*. Binding of the GAL4 protein (expressed in a tissue-specific fashion) to the UAS will

lead to the expression of the HyPer-linked DAAO enzyme. ii. A. D-amino acids binds to the DAAO enzyme, which the oxidation of the D-amino acid. B. This process leads to the generation of ROS (in particular, H_2O_2). C. This increase in H_2O_2 is detected by the HyPer sensor and translated into an increase in emitted fluorescence, therefore making it possible to quantify the DAAO-induced changes in intracellular ROS levels. iii. Left image: The HyPer sensor is a circularly permutated yellow fluorescent protein (cpYFP) linked to the highly H_2O_2-sensitive bacterial transcription factor OxyR ratiometric sensor (left image). Upon oxidation by H_2O_2, OxyR forms an intramolecular disulphide bond that elicits conformational rearrangements which are then transmitted into the chromophore centre of a fluorescent moiety of cpYFP, causing fluorescence alterations that can be detected. Oxidised OxyR in HyPer can be reduced back through enzymatic reactions by endogenous glutaredoxins (gtx). Right image (graph): the cpYFP protein has two excitation peaks, one at 420nm and another at 500 nm, and a single emission peak at 516 nm. When H_2O_2, oxidises the OxyR domain, the intensity of fluorescence excited at 420nm decreases, while the intensity of fluorescence excited at 500nm increases. Adapted from Smolyarova et al., (2021). iv. The HyPer sensor on the left, with Cys199, and the SypHer sensor on the right, which lacks the peroxidatic cysteine Cys199 due to the Cys199Ser mutation. This makes it insensitive to H_2O_2 while maintaining HyPer's pH sensitivity in the physiological pH range 6-8. SypHer is used as control to HyPer to ensure that any changes observed in fluorescence are true increases in H_2O_2 and not due to changes in pH.

(2) Validation of Drosophila ROS-inducing chemogenetic tools ex vivo.

As an initial step to verify the validity of these tools, they were expressed in the dFB sleep neurons, labelled by *R23E10-GAL4*, and I tested their chemogenetic ROS-inducing function *ex vivo*.

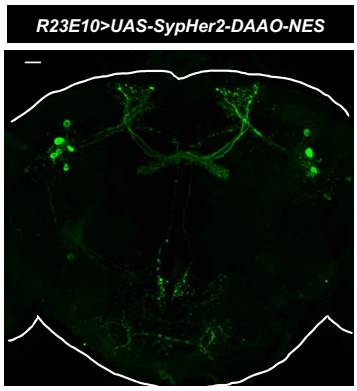
From the available neutral D-amino acids that DAAO degrades, I chose D-Alanine (D-ALA) as the substrate for the DAAO chemogenetic tool because – (1) it is amongst the preferred substrates of microbial DAAO and, compared to other tested substrates, it has the highest catalytic efficiency (Vmax/Km ratio) in yeast DAAO (Pollegioni, 1992)

and (2) Matlashov et al. (2014) and Steinhorn et al. (2018) successfully used D-Ala as a substrate for their DAAO-based chemogenetic tools to generate ROS in eukaryotic cells and in the heart of rats, respectively. In addition, it is important to note that, unlike other D-amino acids, D-ALA has no known physiological function in *Drosophila* (Tomita et al., 2015).

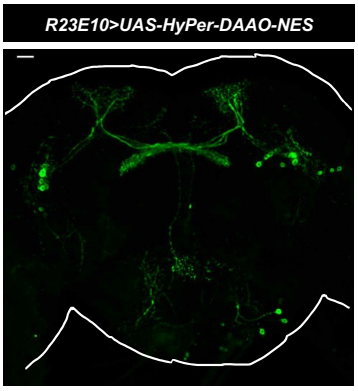
I incubated dissected brains in a solution containing either D-ALA, L-ALA or a control solution with no amino acid and took confocal images of the brains immediately after incubation in order to measure fluorescence levels and quantify changes in ROS expression. I found that incubating *HyPer-DAAO*-expressing brains in a 10mM D-ALA solution for approximately 1 hour produced a significant increase ($p<0.0001$) in fluorescence in the dFB neurons compared to those incubated in a 10mM L-ALA solution or a control solution with no amino acid for the same time (Fig 3.2 B)). Similarly, when *SyPher2-DAAO*-expressing brains were incubated in a 10mM D-ALA solution for 1 hour, this produced no significant increase in fluorescence (Fig 3.2 B)).

A)

i.

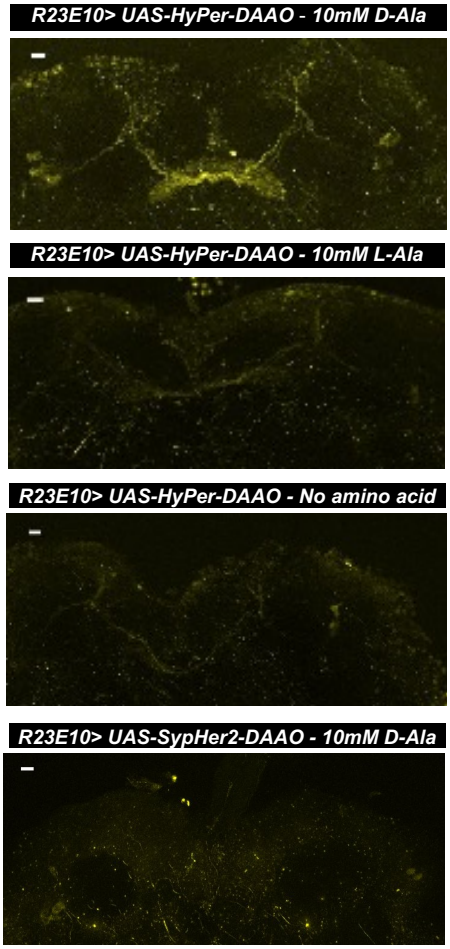


ii.

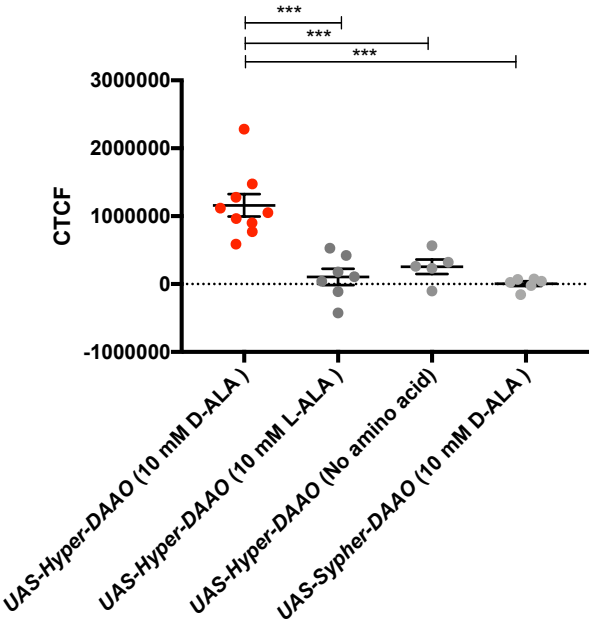


B)

i.



ii.



iii.

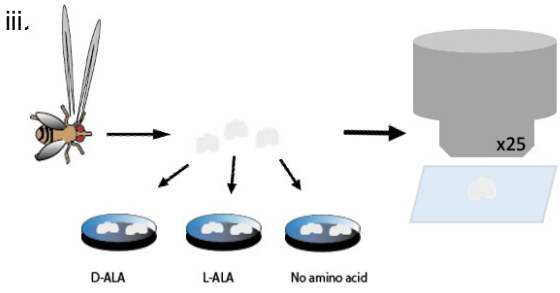


Figure 3.2. **Development and validation of a DAAO-based ROS-inducing chemogenetic system.** A) Maximum intensity projection confocal images of anti-rabbit-GFP-stained brains expressing the ROS-inducing chemogenetic constructs in the *R23E10-GAL4* neurons*.* Scale bar=20μm. B) Chemogenetic-driven increase in ROS in *R23E10-GAL4* neurons *ex vivo*. i. Representative maximum intensity projection images of confocal z-stacks of R23E10 neurons of the fly brain. Scale bar=10μm. ii. Quantification of the corrected total cell fluorescence (CTCF) in the *R23E10-GAL4* neurons. Individual values (CTFC from each image) are plotted in the graph as dots. Data is shown as mean ± SEM. For statistical analysis, one-way ANOVA followed by Tukey's multiple comparison test was used. *** indicates a p-value <0.001. Sample size: *UAS-HyPer-DAAO* (10mM D-ALA): n=9; *UAS-HyPer-DAAO* (10mM L-ALA): n=7; *UAS-HyPer-DAAO* (No amino acid): n=5; *UAS-SypHer2-DAAO* (10mM D-ALA): n=8. iii. Graphic representation of experimental procedure used to validate the DAAO-based ROS-inducing chemogenetic tools: fly brains are dissected, incubated in a D-ALA, L-ALA or a no-amino acid control solution for 1 hour and immediately imaged under a confocal microscope.

(3) Behaviourally testing the DAAO-based chemogenetic system in the dFB neurons in vivo.

To use the ROS-generating chemogenetic system to screen for sleep-relevant sites of ROS induction across any tissue of the fly, it was essential to first determine the appropriate conditions to effectively use it *in vivo*. Given that Kempf et al. (2019) previously showed that inducing ROS in the dFB (*R23E10-GAL4*) neurons increases sleep, one would expect that if the right conditions were met to chemogenetically induce ROS in the dFB neurons with the DAAO system, this should also increase sleep. Accordingly, I decided to first test the DAAO system in the R23E10 neurons to determine the most appropriate conditions to use the system *in vivo*. I hypothesised that, by finding the minimum DAAO substrate dose that induces sleep (when chemogenetically inducing ROS in the R23E10 neurons) and the maximum dose that

does not cause toxicity, I would be able to determine the appropriate range of substrate concentrations and conditions to use the system across tissues.

In this way, immediately after eclosion, female flies expressing *HyPer-DAAO* in the R23E10 neurons, as well as their parental controls, were transferred to a sucrose food medium with a specific concentration of either D-ALA, L-ALA or a control sucrose medium with no amino acid. After 3 full days, they were transferred to individual glass tubes containing the equivalent fresh food medium and loaded into the *Drosophila Activity Monitoring* (DAM) System to quantify their sleep.

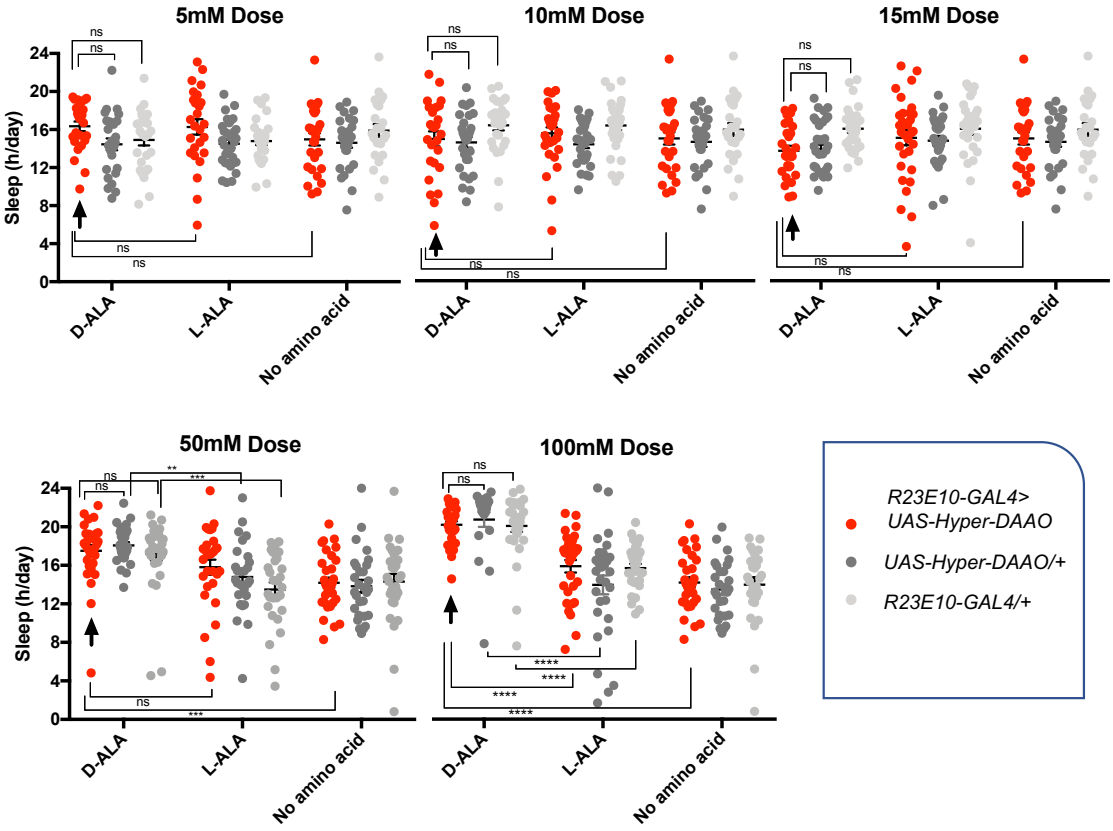
As an initial step, I tested D-ALA substrate concentrations ranging from 5mM to 15mM and found no significant effect on sleep (two-way (Fig. 3.3. A)). Given that 10mM were used by Matlashov et al. (2014) to effectively generate ROS in cells and Steinhorn et al. (2018) used 1M to chemogenetically induce ROS in the heart of rats I decided to feed flies with higher concentrations of D-ALA. Using a 500mM concentration of D-ALA was highly toxic in flies, since they died only after 3-4 days (data not shown). I next tested 100mM and 50mM D-ALA concentrations and found that this led to a significant increase in inactivity regardless of the genotype (i.e. both in the experimental and the genetic control groups) (Fig. 3.3. A)).

Around the same time, a study by Dai et al., (2019) had characterised for the first time the expression of the *Drosophila melanogaster* endogenous DAAO, which is encoded by two genes and expressed both in the brain and gut of *Drosophila*. Dai et al., (2019) also suggested an involvement of the endogenous fly DAAO on modulating sleep time indirectly through the regulation of D-Serine (D-Ser) levels, an amino acid which can modulate sleep through its NMDA receptor activity (Dai et al., 2019; Tomita et al., 2015). Therefore, I hypothesised that the unspecific behavioural phenotype triggered

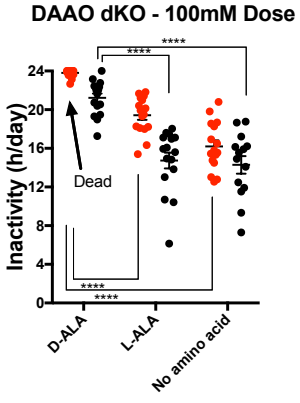
by 50mM and 100mM of D-ALA feeding could be linked to excess D-ALA acting on the endogenous fly DAAO, as this might lead to increased levels of D-Ser if DAAO is saturated by oxidising D-ALA molecules. Because of this, I wanted to test whether it may be suitable to use my yeast DAAO-based chemogenetic tool in a fly with a *DAAO* Knock-out (KO) background. With this objective in mind, I acquired the *DAAO* double KO flies (DAAO dKO) generated by Dai et al. (2019) and tested whether the lack of endogenous fly DAAO blocked the unspecific phenotype caused by feeding flies with a 100mM D-ALA. However, this did not prevent the D-ALA feeding toxic effect, as most *DAAO* dKO flies exposed to D-ALA died after 4 days (Fig. 3.3 B)). Therefore, I abandoned the idea of using the DAAO-based chemogenetic system in a fly *DAAO* dKO background.

Another possibility was that the hydrogen peroxide sensor HyPer could be contributing to not seeing the expected increase in sleep when feeding flies expressing the chemogenetic system in the R23E10 neurons with non-toxic concentrations of D-ALA: in the process of detecting the DAAO-generated H_2O_2, HyPer may be temporarily sequestering some of this H_2O_2, which could make it more difficult to reach the right concentrations of intracellular ROS levels in the R23E10 neurons to trigger the expected increase in sleep. Thus, I decided to test whether by using the *UAS-DAAO* tool in lieu of *UAS-HyPer-DAAO* I could effectively increase sleep by chemogenetically generating ROS in the dFB neurons. However, I found that feeding flies with a 15mM or a 30mM D-ALA concentration did not produce a significant increase in sleep in flies expressing the DAAO chemogenetic tool in R23E10 neurons as compared to genetic and treatment controls (Fig 3.3. C)).

A)


5mM Dose
10mM Dose
15mM Dose
50mM Dose
100mM Dose
Sleep (h/day)
D-ALA
L-ALA
No amino acid
R23E10-GAL4>
UAS-Hyper-DAAO
UAS-Hyper-DAAO/+
R23E10-GAL4/+

B)


DAAO dKO - 100mM Dose
Inactivity (h/day)
Dead
D-ALA
L-ALA
No amino acid
DAAO dKO
Cs

C)

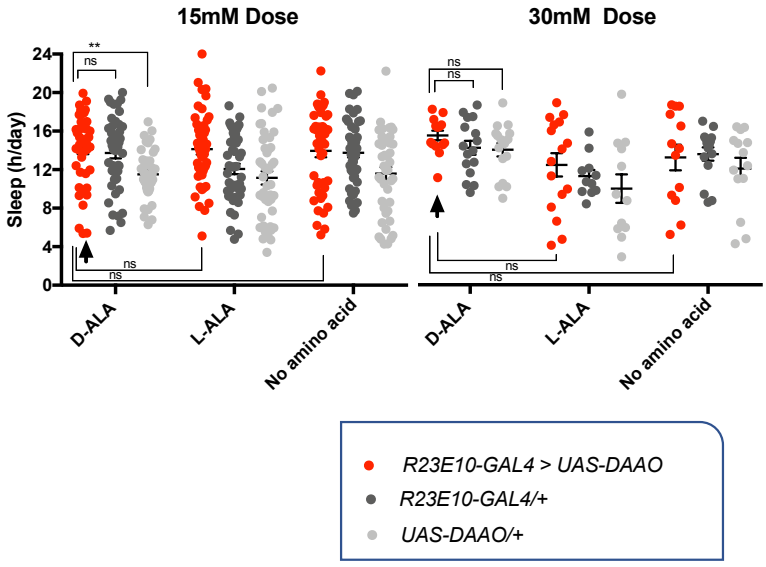

15mM Dose
30mM Dose
Sleep (h/day)
D-ALA
L-ALA
No amino acid
R23E10-GAL4 > UAS-DAAO
R23E10-GAL4/+
UAS-DAAO/+

Figure 3.3 **Behaviourally testing DAAO-based chemogenetic tools in the R23E10 neurons in vivo.** A) Behavioural effect of feeding flies expressing *UAS-Hyper-DAAO* in the R23E10 neurons with 5mM, 10mM, 15mM, 50mM and 100mM concentrations of the DAAO substrate D-ALA. Black arrows point to the experimental group: *R23E10-GAL4>UAS-hyper DAAO* (in red) with the D-ALA substrate. Genotypic parental controls *R23E10-GAL4/+* and *UAS-HyPer-DAAO/+* are represented in dark grey and light grey, respectively. In each graph, data was pooled from two independent experimental repeats. For statistical analysis, two-way ANOVA was carried out (interaction effect was non-significant in all cases: 5mM – $F(4, 236)=1.372$, $p=0.244$; 10mM – $F(4, 244) = 0.2184$, $p= 0.928$; 15mM – $F(4, 248) = 0.4829$, $p=0.7483$; 50mM – $F(4, 254) = 1.197$, $p=0.3127$; 100mM – $F(4, 251)= 1.084$, $p=0.3648$)), followed by Tukey's multiple comparison test. p-values: ns= non-significant; **= $p<0.01$; *** = $p<0.001$; ****=$p<0.0001$. B) Testing the effect of 100mM D-ALA feeding on *DAAO* dKO flies. Black arrow points to experimental group, *DAAO* dKO flies (red) under D-ALA treatment. These died after 4 days on treatment. Cs (Cantonese) flies (in black) were used as a control for comparison. For statistical analysis, two-way ANOVA was carried out, followed by Tukey's multiple comparison test. p-values: ****=$p<0.0001$. C) Behavioural effect of feeding flies expressing *UAS-DAAO* in the R23E10 neurons with 15mM and 30mM concentrations of the DAAO substrate D-ALA. Black arrows point to the experimental group: *R23E10-GAL4>UAS-DAAO* (in red) with the D-ALA substrate. Genotypic parental controls *R23E10-GAL4/+* and *UAS-DAAO/+* are represented in dark grey and light grey, respectively. Data was pooled from two independent experimental repeats in the 15mM graph and one repeat in the 30mM graph. For statistical analysis, two-way ANOVA was carried out (interaction effect was non-significant at both doses: 15mM – $F (4, 392) = 0.8541$, $p=0.4916$; 30mM – $F(4, 118) = 0.3216$, $p=0.8630$), followed by Tukey's multiple comparison test was used. p-values: ns= non-significant; **= $p<0.01$. For all graphs in A), B) and C): individual values from each fly are plotted in the graph as dots. Data is shown as mean ± SEM.

(4) Using the DAAO-based chemogenetic system to increase ROS in the gut.

My ultimate objective in this project was to eventually use the DAAO chemogenetic tool to identify sleep-relevant non-neural tissues of ROS production in the fly body. Vaccaro et al. (2020) had recently shown that sleep deprivation increases ROS in the gut of flies. Therefore, it was a top priority to test the DAAO chemogenetic system in the gut. Could I use DAAO to increase ROS in the gut? And would this cause a sleep phenotype?

With this purpose in mind, I performed a series of experiments where I used *Myo1A-GAL4*, a widely used enterocyte-marker GAL4 line in fly intestinal studies (Jiang et al., 2011; Buchon et al., 2010), to express *UAS-HyPer-DAAO* or *UAS-DAAO* in the gut (Fig. 3.4). I found that a 15mM D-ALA dose chemogenetically activated *UAS-HyPer-DAAO* in the *Myo1A-GAL4* cells and led to a significant increase in total sleep (Fig 3.4. B)). Similarly, using a 15mM dose, I effectively activated *UAS-DAAO* in *Myo1A-GAL4* cells, which also produced a significant increase in total sleep time (Fig 3.4 C)). Using a 30mM dose also led to a significant increase in sleep in the *UAS-DAAO>Myo1A-GAL4* group as compared to genetic and treatment controls (Fig 3.4 C)). However, with a 30mM D-ALA dose, although not as prominent as in the *UAS-DAAO>Myo1A-GAL4* group, a significant increase in sleep was observed in the *UAS-DAAO/+* and *Myo1A-GAL4/+* controls on 30mM D-ALA compared to its respective treatment controls (on L-Ala and no amino acid). This suggests that at a 30mM dose, some of the non-specific/toxic effects of high D-ALA doses can be observed and, therefore, 15mM is the optimal dose to activate the chemogenetic system without triggering off-target effects.

To ensure that the observed increase in sleep was not caused by any motor alterations, I further analysed the activity of flies during wake bouts across the three experiments. I found that chemogenetically inducing ROS in *Myo1A-GAL4* did not cause a significant difference in motor activity (bin crosses/min during wake) (Fig 3.4 B) and C)). However, upon closer examination of the *Myo1A-GAL4* line, I found that, while *Myo1A-GAL4* labels most strongly the midgut cells, it also has some leaky expression in the brain (Fig 3.4 A)). Therefore, one cannot rule out the possibility that the observed sleep-promoting effect, or part of it, was triggered by ROS increases in the brain and further experiments with other gut-specific GAL4 lines are required.

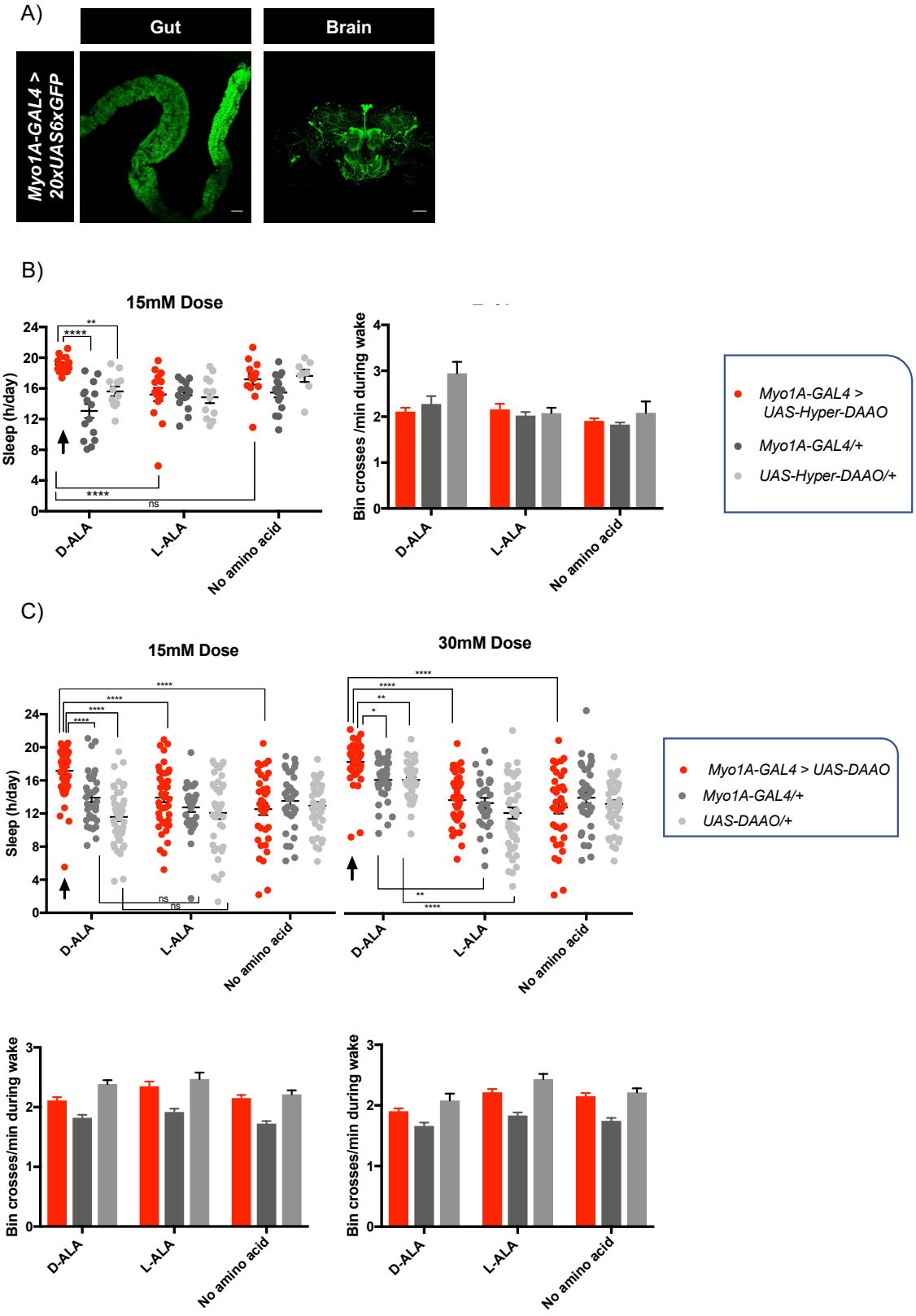

A)
Gut
Brain
Myo1A-GAL4 > 20xUAS6xGFP
B)
15mM Dose
Sleep (h/day)
Bin crosses /min during wake
D-ALA
L-ALA
No amino acid
Myo1A-GAL4 > UAS-Hyper-DAAO
Myo1A-GAL4/+
UAS-Hyper-DAAO/+
C)
15mM Dose
30mM Dose
Sleep (h/day)
Bin crosses/min during wake
D-ALA
L-ALA
No amino acid
Myo1A-GAL4 > UAS-DAAO
Myo1A-GAL4/+
UAS-DAAO/+

Figure 3.4. Sleep is increased by driving chemogenetic activation of a DAAO-based ROS-inducing system in in the Myo1A-GAL4 gut line. A) Maximum intensity projections of *Myo1A-GAL4>20xUAS6xmCD8::GFP*. Scale bar=50μm. B) Chemogenetically activating *UAS-HyPer-DAAO in Myo1A-GAL4* with a 15mM D-ALA dose. On the left, total daily sleep graph. On the right, a graph showing motor activity during wake, measured as bin crosses/min during wake. For statistical analysis, two-way ANOVA was carried out, followed by Tukey's multiple comparison test. In total sleep, two-way ANOVA revealed a significant interaction effect ($F(4, 113) = 6.258$, $p=0.0001$). Two-way ANOVA analysis of bin crosses/min data showed no significant interaction effect ($F(4, 113) = 2.218$, $p=0.0715$). Data in B) is from a single experimental repeat. P-values: ns= non-significant; **= $p<0.01$; ****=$p<0.0001$. C) Chemogenetically activating *UAS-DAAO* in *Myo1A-GAL4* with a 15mM (left graphs) and 30mM (right graphs) D-ALA dose. On top, total daily sleep graphs. On bottom, graphs showing motor activity during wake, measured as bin crosses/min during wake. For statistical analysis, two-way ANOVA was carried out, followed by Tukey's multiple comparison test. At 15mM, two-way ANOVA revealed a significant interaction effect in total sleep in *Myo1A-GAL4>UAS-DAAO* ($F(4, 347)= 8.455$, $p<0.0001$), while there was no significant interaction effect in activity during wake ($F(4,347)=0.7014$, $p=5914$). At 30mM, two-way ANOVA revealed a significant interaction effect in total sleep in *Myo1A-GAL4>UAS-DAAO* ($F(4, 334)= 2.844$, $p<0.0242$), while there was no significant interaction effect in activity during wake ($F(4,334)=0.7297$, $p=0.5722$). P-values: ns= non-significant; *= $p=0.0126$ **= $p<0.01$; ****=$p<0.0001$. For total sleep graphs in B) and C): individual values from each fly are plotted in the graph as dots. Data is shown as mean ± SEM. For activity during wake, data displayed as mean (bar) + SEM.

3.2.2. Testing the effect of lipid peroxidation resistant deuterated PUFAs on sleep in Drosophila.

How can mitochondrial ROS reach a channel at the plasma membrane to modulate sleep? This is another key missing piece in our understanding of ROS-mediated sleep control. In this light, our working model proposes that ROS generated in the mitochondria of certain tissues during wake lead to the peroxidation of membrane lipids, whose breakdown produces medium-chain aldehydes, which then serve as substrates for the aldo-keto reductase activity of Hyperkinetic, eventually modulating sleep. If this hypothesis is correct, one would expect that preventing lipid peroxidation would reduce sleep.

To directly prevent lipid peroxidation, I decided to use the novel lipid peroxidation-resistant deuterated polyunsaturated fatty acid (D-PUFAs) drugs developed by Mikhail S. Shchepinov at Retrotope Inc (Hill et al., 2011; see Shchepinov, 2020 for review). Retrotope Inc has developed deuterated versions of a range of PUFAs, where the hydrogens at bis-allylic positions have been replaced by the heavier isotope deuterium, making them more resistant to oxidative attack and slowing down lipid peroxidation (Shchepinov, 2020). Fig. 3.5). Integration of a small amount of D-PUFAs into the lipid membranes of yeast and mammalian cells (20% in the total pool of membrane PUFAs) is sufficient to profoundly inhibit the chain reaction of non-deuterated PUFAs and protect membranes against the damaging effects of lipid peroxidation (Firsov et al., 2019. Andreyev et al., 2015; Hill et al., 2012). Therefore, if we can integrate enough D-PUFAs into *Drosophila*'s lipid membranes through dietary

supplementation, this should reduce lipid peroxidation and, if our working model is correct, it should also reduce sleep.

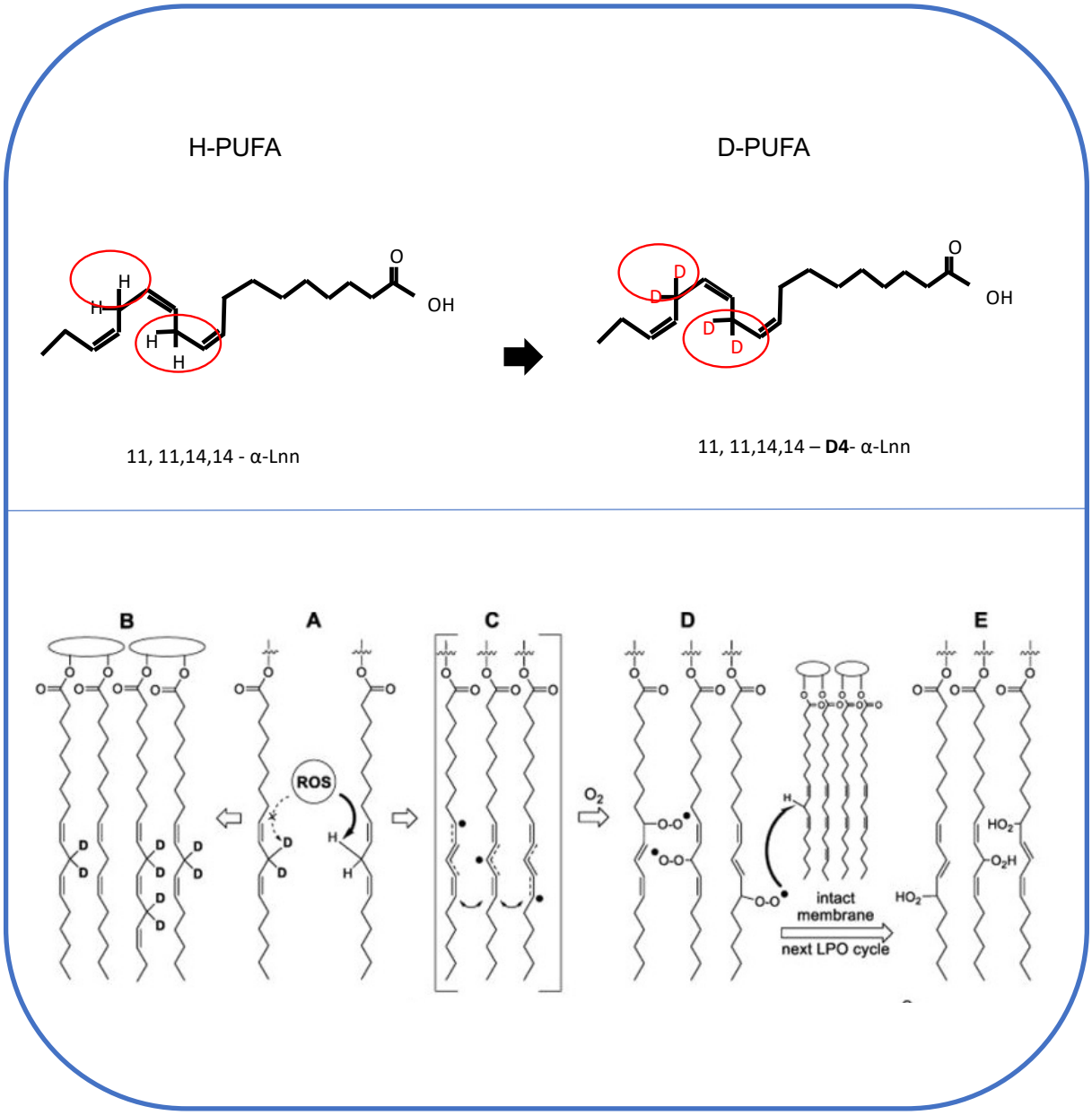


Figure 3.5. D-PUFAs have a protective effect on lipid peroxidation.

Top diagram: deuterated polyunsaturated fatty acids (D-PUFAs). On the left, linolenic acid, a standard PUFA (referred to as H-PUFA, given its hydrogen atoms) with 4 hydrogen atoms at bis-allylic locations.

On the right, the deuterated version of linolenic acid, where its 4 hydrogen atoms at bis-allylic locations have been replaced by deuterium (Shchepinov, 2020). Bottom diagram: protective effect of D-PUFAs on lipid peroxidation (LPO). PUFAs at the plasma membrane are highly susceptible to lipid peroxidation, since electrons can easily be abstracted by hydroxyl radicals from their bis-allylic-located (between double bonds) hydrogen atoms (A); this creates an unstable lipid radical (C), which can react with oxygen, forming a fatty acid peroxyl radical (D) and reacting with another PUFA to form a new lipid radical and exponentially propagate lipid peroxidation across membrane PUFAs (E). On the other hand, if PUFAs are deuterated (D-PUFA), this inhibits the rate-limiting step of ROS-driven abstraction off a bis-allylic site (B), therefore protecting lipid membranes from lipid peroxidation (adapted from Raefsky et al., 2018).

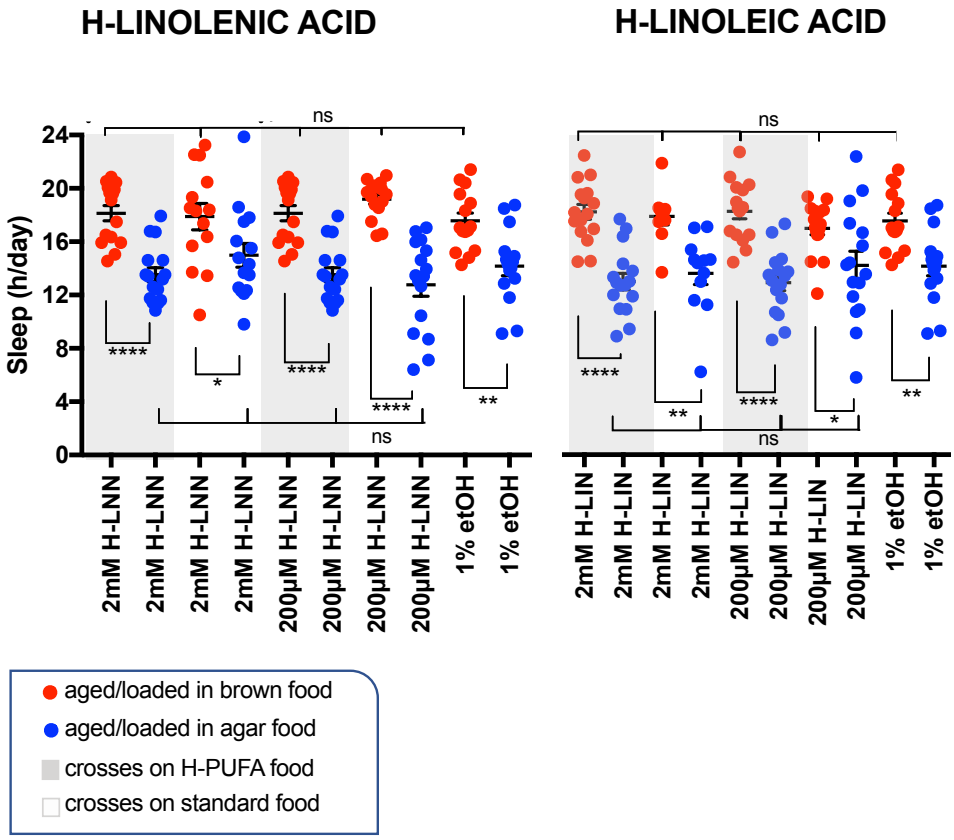
(1) Measuring the effect of supplementing different dietary media with non-deuterated PUFAs (H-PUFAs) on sleep.

In *Drosophila's* lipid membranes, alpha-linoleic acid (C18:2) and alpha-linolenic acid (C18:3) are the most abundant PUFAs and there are no long-chain fatty acids with chains longer than 20 carbons (Shen et al., 2010). Because of that, I used D2-Linoleic acid (D-LIN) and D4-Linolenic acid (D-LNN) D-PUFA drugs in my experiments with the aim of preventing lipid peroxidation in *Drosophila*. However, before supplementing D-LIN and D-LNN into *Drosophila's* diet, I performed a series of control experiments to find whether supplementing *Drosophila's* diet with different concentrations of non-deuterated PUFAs (H-PUFAs) would cause any sleep phenotypes, either if supplemented from the egg and larval stage (setting up crosses on food supplemented with PUFAs) or if supplemented on food only after eclosion up until when sleep recordings were performed, and using two different base *Drosophila* dietary media: (1) a standard molasses-based *Drosophila* medium and (2) a 5% sucrose-agar medium.

Furthermore, because yeast *Saccharomyces Cerevisiae* are a natural key source of nutrition throughout *Drosophila's* lifecycle (Quan, 2018; Hoang et al., 2015) and given that they readily incorporate PUFAs into their lipid membranes (Hill et al., 2011), I also sprinkled after-eclosion *Drosophila* media with PUFA-treated yeast to potentially facilitate ingestion and incorporation of PUFA's into *Drosophila's* lipid membranes. These experiments showed that, while the base food medium has a significant effect on baseline sleep (flies sleep significantly more on the standard brown medium than on the sucrose-agar medium), supplementing either media with either 200μm or 2mM of PUFA + yeast (treated with the corresponding PUFA) did not produce any significant changes in sleep amount (Fig 3.6).

A)

i.


H-LINOLENIC ACID
H-LINOLEIC ACID
Sleep (h/day)
24
20
16
12
8
4
0
ns
****
*
****
****
ns
**
2mM H-LNN
2mM H-LNN
2mM H-LNN
2mM H-LNN
200µM H-LNN
200µM H-LNN
200µM H-LNN
200µM H-LNN
1% etOH
1% etOH
ns
****
**
****
*
ns
**
2mM H-LIN
2mM H-LIN
2mM H-LIN
2mM H-LIN
200µM H-LIN
200µM H-LIN
200µM H-LIN
200µM H-LIN
1% etOH
1% etOH
aged/loaded in brown food
aged/loaded in agar food
crosses on H-PUFA food
crosses on standard food

ii.

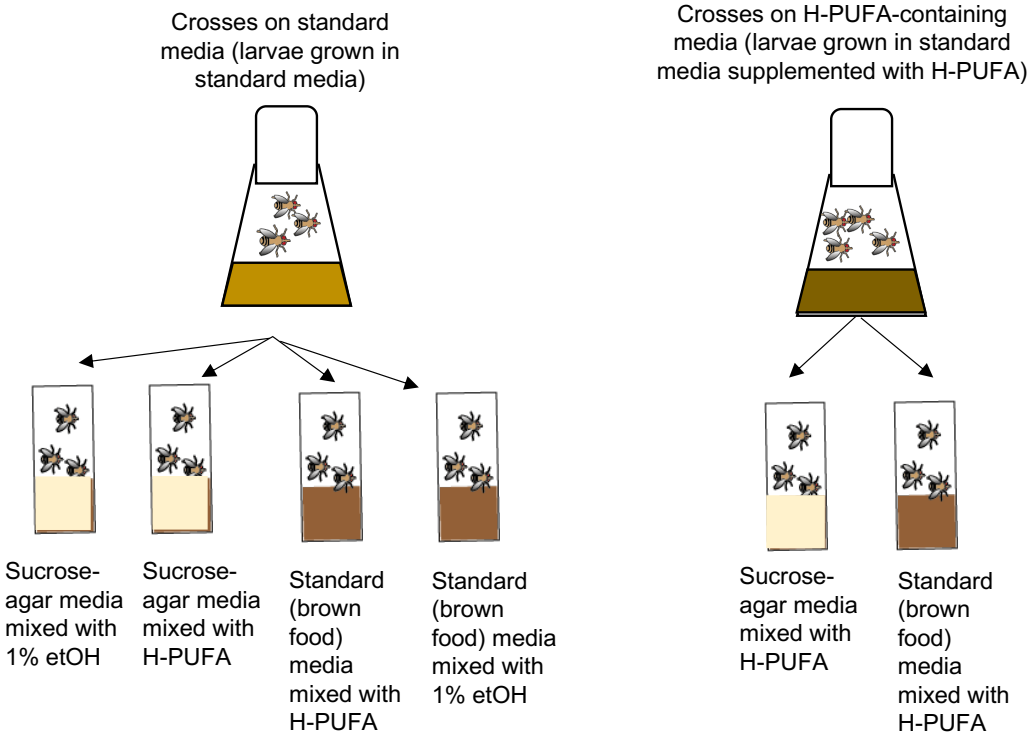

Crosses on standard media (larvae grown in standard media)
Crosses on H-PUFA-containing media (larvae grown in standard media supplemented with H-PUFA)
Sucrose-agar media mixed with 1% etOH
Sucrose-agar media mixed with H-PUFA
Standard (brown food) media mixed with H-PUFA
Standard (brown food) media mixed with 1% etOH
Sucrose-agar media mixed with H-PUFA
Standard (brown food) media mixed with H-PUFA

Figure 3.6. Supplementing two Drosophila media with non-deuterated PUFAs (H-PUFAs) does not affect sleep. i) Effect of diet on sleep time. The following factors were considered: media, either a standard molasses-based brown food or a sucrose agar food; concentration of supplemented PUFA (either 200μm or 2mM) and length of exposure to supplemented PUFA (either from crosses/larval stage or from adult stage). 1% ethanol (etOH) groups were used as additional controls, given that ethanol contained by PUFA solutions supplemented in media is equivalent to 1% etOH in the media. For statistical analysis, a three-way ANOVA test was performed, followed by Sidak's multiple comparison test to compare selected pairs of data). p-values: ns= non-significant; *= p<0.05 **= p<0.01; **= p<0.001; ****=p<0.0001. Individual values from each fly are plotted in the graph as dots. Data is shown as mean ± SEM. Displayed data comes from a single experimental repeat. ii) Diagram illustrating the protocol for dietary manipulations in i). H-LIN = linoleic-acid; H-LNN= linolenic-acid; etOH = ethanol.

(2) Testing the effect of supplementing Drosophila food media with D-PUFAs on sleep.

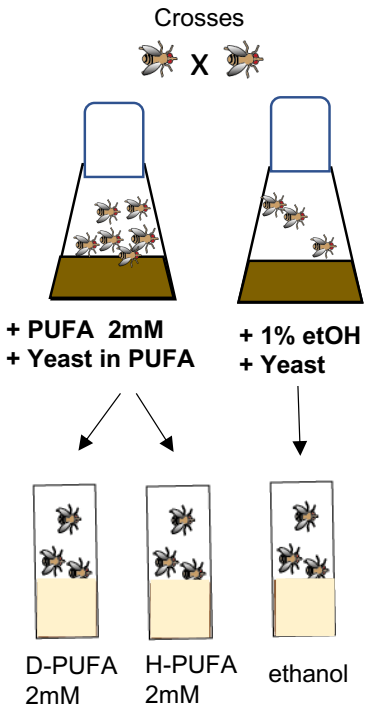
Next, I wanted to test whether supplementing *Drosophila*'s diet with D-PUFAs would lead to a reduction in sleep. Since I previously saw that neither adding 200μM nor 2mM of non-deuterated PUFA into *Drosophila*'s diet altered sleep, I decided to supplement D-PUFAs at a 2mM concentration. Like in the previous control experiments, I also sprinkled PUFA-treated yeast onto *Drosophila* media, this time since the larval stage. Given that it is not possible to control the amount of PUFA already contained in the standard food media, I decided to first try the experiments using the sucrose-agar media after flies eclosed. This way, larvae would grow in a standard (brown) media supplemented with PUFA (either D-PUFA or its equivalent H-PUFA control) and, once in the adult stage, flies would be transferred onto a fresh sucrose-agar media supplemented with PUFA (Fig 3.7.A) i)). This would allow me to

control, at the adult stage, the exact D-PUFA concentration to 2mM and ensure that flies are not exposed to other PUFA contained by the standard molasses-based brown food medium. I tested 3 types of D-PUFA treatments: 1:1 D-LIN:D-LNN (2mM), D-LIN alone (2mM) and D-LNN alone (2mM). Baseline sleep was measured after 4-7 days into the adult stage, finding no significant difference between flies treated with D-PUFAs and control groups (Fig 3.7 A) ii)). In addition, I also tested whether D-PUFA treatment would decrease rebound sleep after sleep depriving flies for 12h through mechanical sleep deprivation overnight. I hypothesised the following: by being in a state of heightened oxidative stress and lipid peroxidation, as it should be during and following sleep deprivation, the protective effect of D-PUFAs against lipid peroxidation may be more prominent than under baseline conditions, when lipid peroxidation is not as high. I believed that this may strengthen the protective effect of D-PUFA against ROS, which, if our model is correct, should be reflected in decreased rebound sleep following sleep deprivation. However, while there was a small decrease in rebound sleep (measured as % of sleep recovered after sleep deprivation) in flies treated with D-PUFAs compared to control flies treated with H-PUFAs, the decrease was not statistically significant (Fig 3.7 A) ii)).

Because flies sleep significantly less when on a sucrose-agar media that when fed standard brown food (Fig 3.6 i)), the low baseline sleep levels could be making it more difficult to bring sleep levels down even more with the D-PUFA treatment. Therefore, I decided to test the D-PUFA treatment using standard brown food throughout the experimental protocol (Fig 3.7 B)i)). However, this did not lead to any significant differences in baseline sleep between D-PUFA-treated and control flies (Fig 3.7 B)ii)).

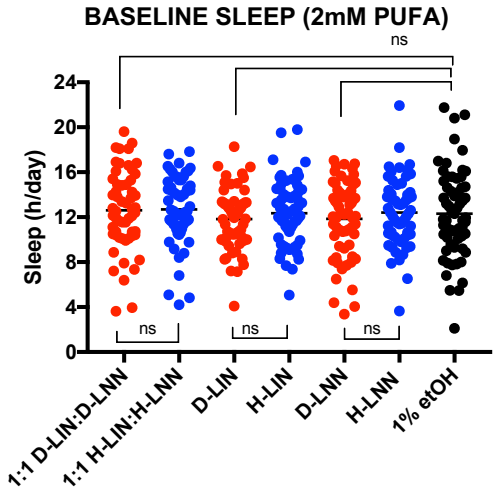
A)

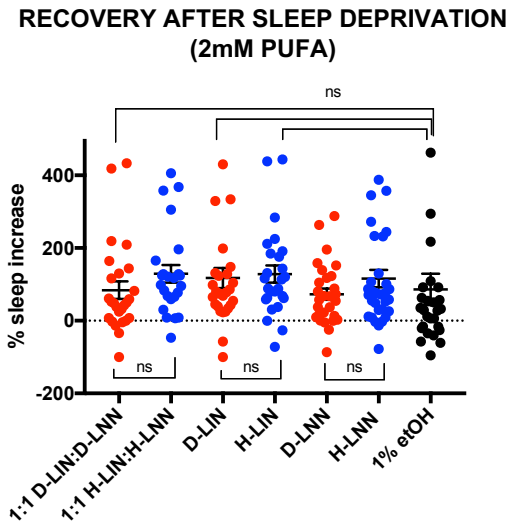
i.



Ageing on **sucrose-agar (5-6 days)** food +PUFA 2mM + Yeast in PUFA (or 1% etOH for control group)

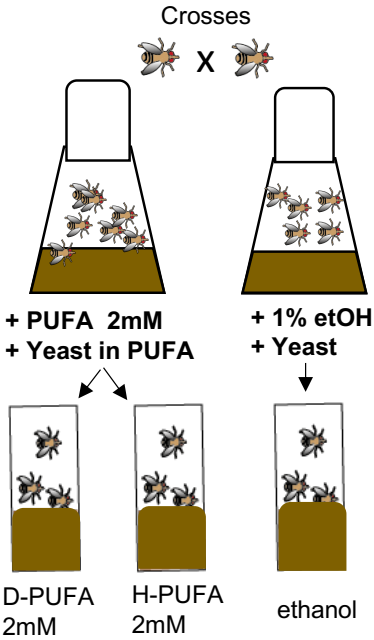
ii.





B)

i.



Ageing on **brown standard (5-6 days)** food +PUFA **2mM** + Yeast in PUFA (or 1% etOH for control group)

ii.

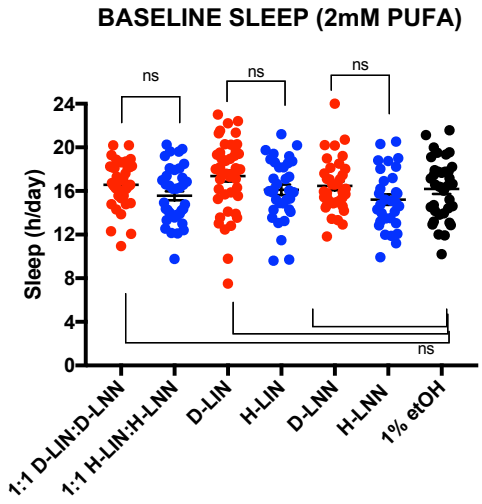


Figure 3.7. Dietarily supplementing 2mM D-PUFA through a sucrose-agar or a standard brown molasses-based *Drosophila* media does not reduce baseline or rebound sleep. A) i) Diagram illustrating the experimental protocol for dietary manipulations, where fly crosses were set up and larvae grew in a standard brown media supplemented with 2mM of D- or H-PUFA (or 1% etOH in the etOH control groups) and adult flies were transferred and aged in sucrose-agar media supplemented with the corresponding D- or H-PUFA (or 1% etOH). ii) On the top, baseline sleep. On the bottom, sleep rebound (recovery sleep after sleep deprivation), measured as % of sleep increase in the light period after sleep deprivation compared to baseline sleep in the light period prior sleep deprivation. For statistical analysis, a one-way ANOVA test was performed, followed by Sidak's multiple comparison test to compare selected pairs of data. p-values: ns= non-significant. Individual values from each fly are plotted in the graph as dots. Data is shown as mean ± SEM. Displayed data was pooled from two independent experimental repeats. B) i) Diagram illustrating the experimental protocol for dietary manipulations, where fly crosses were set up and larvae grew in a standard brown media supplemented with 2mM of D- or H-PUFA (or 1% etOH in the etOH control groups) and adult flies were also aged in standard brown food supplemented with the corresponding D- or H-PUFA (or 1% etOH). ii) Baseline sleep graph. For statistical analysis, a one-way ANOVA test was performed, followed by Sidak's multiple comparison test to compare selected pairs of data. p-values: ns= non-significant. Individual values from each fly are plotted in the graph as dots. Data is shown as mean ± SEM. Displayed data was pooled from two independent experimental repeats. H-LIN = linoleic-acid; H-LNN= linolenic-acid; etOH = ethanol; D-LIN= D-linoleic acid; D-LIN= D-linolenic acid.

Given that the previous treatment protocols were not effective at generating the expected decrease in sleep with D-PUFA feeding, another possibility was that higher D-PUFA concentrations and/or longer feeding times were necessary so that enough D-PUFAs integrate into *Drosophila*'s lipid membranes to effectively reduce lipid peroxidation and, in consequence, reduce sleep. Therefore, I performed another experiment where the concentration of supplemented PUFA in the diet was increased to 10mM, and where flies were exposed to the treatment from the larval stage and aged from eclosion for an additional 11-13 days before they were loaded into *Drosophila Activity Monitors* to perform sleep measurements. Nevertheless, these manipulations did not lead to any significant changes on sleep either (Fig. 3.8.)

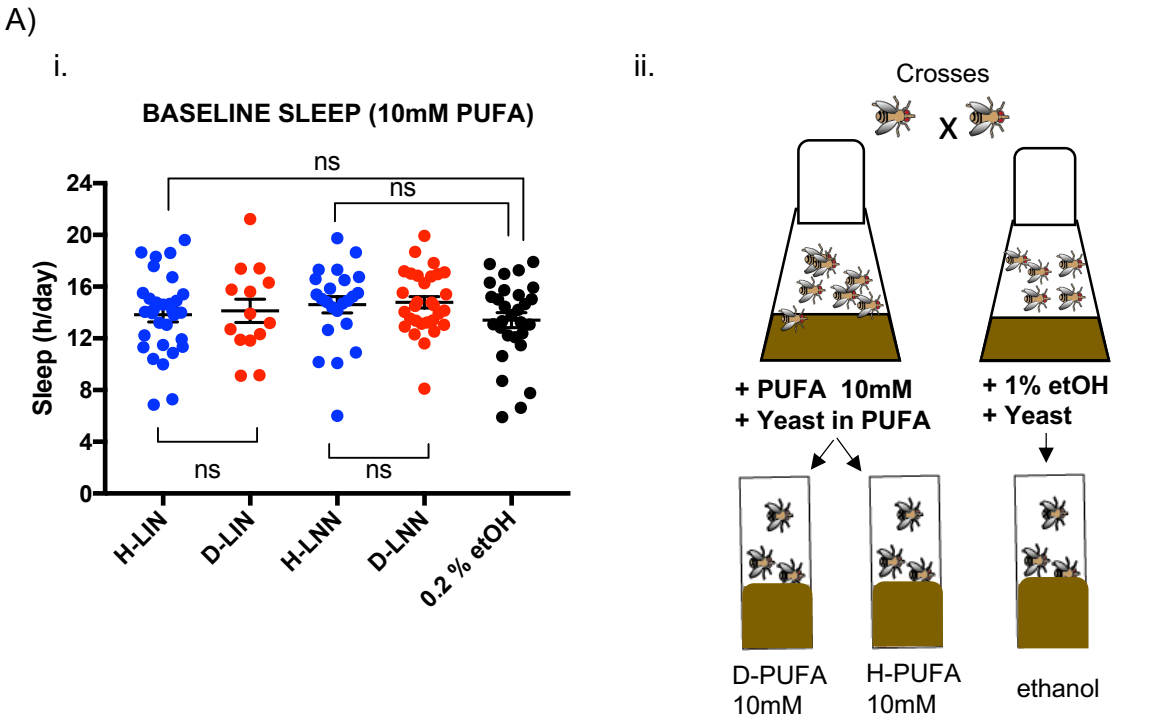


Figure 3.8. Increasing dietarily supplemented D-PUFA to 10mM and a longer exposure time does not significantly decrease sleep. A) i) Baseline sleep on a 10mM PUFA diet. For statistical analysis, a one-way ANOVA test was performed, followed by Sidak's multiple comparison test to compare selected pairs of data. p-values: ns= non-significant. Individual values from each fly are plotted in the graph as dots. Data is shown as mean ± SEM. Displayed data was pooled from two independent experimental repeats. H-LIN = linoleic-acid; H-LNN= linolenic-acid; etOH = ethanol; D-LIN= D-linoleic acid; D-LIN= D-linolenic acid. A) ii) Diagram illustrating the experimental protocol for dietary manipulations, where fly crosses were set up and larvae grew in a standard brown media supplemented with 10mM of D- or H-PUFA (or 1% etOH in the etOH control groups) and adult flies were transferred and aged in a standard brown food media supplemented with the corresponding D- or H-PUFA (or 1% etOH) for a further 11-13 days until sleep measurements were recorded.

(3) Using a chemically defined food (CDF) media to supplement D-PUFAs into Drosophila diet and measure the effects of this manipulation on sleep.

Using the standard brown and the sucrose-agar media for dietary manipulations presents the following challenges, which could have hindered the effectivity of D-PUFAs in my previous experiments: (1) with standard brown food one cannot control the exact PUFA content found in the media and, therefore, one cannot be certain that flies are eating non-deuterated PUFA in addition to the supplemented D-PUFAs and (2) with the sucrose-agar media, baseline sleep is low, which may make it harder to observe any further decreases in sleep. To overcome these issues, I decided to use the chemically defined food (CDF) recipe developed by Lee and Micchelli (2013). While the CDF is associated with a delay in larval development, it has been shown to sufficiently support the long-term culture of *Drosophila* across several generations (Lee and Micchelli, 2013). The only source of lipids in this diet comes from cholesterol and lecithin (where PUFA content comes from) in defined amounts. Therefore, I

substituted the lecithin in the recipe for D-PUFA (either D-linoleic acid or D-linolenic acid) or H-PUFA (linoleic acid or linolenic acid) at a 2mM concentration, which is approximately equivalent to the initial concentration of lecithin in the CDF recipe (Lee and Micchelli., 2013). In addition, there is evidence that remaining linoleic acid can be passed from *Drosophila* mother to progeny across generations in a fatty-acid free and microorganism free diet (Rapport et al., 1983). Therefore, to minimise the potential amount of non-deuterated PUFAs transferred from mother to progeny, I decided to grow two generations of *Drosophila* in a PUFA-supplemented CDF. Furthermore, once flies in the second generation reached adult stage, they continued to be fed with a PUFA-supplemented CDF until the end of the experiment (including aging for 5-7 days and once loaded into the *Drosophila Activity Monitors* for sleep measurements) (Fig 3.9. i)). The results shows a small, but significant, decrease in baseline sleep in D-LIN-treated flies compared to those treated with non-deuterated H-LIN acid. D-LNN-treated flies also slept less than H-LNN-treated flies, but the sample size was too small to reach statistical significance. Therefore, more experiments are necessary to determine whether this effect is replicated consistently across independent trials and with a larger sample size (see Fig. 3.9. legend for power calculation). If confirmed, this would directly prove the connection between lipid peroxidation and sleep.

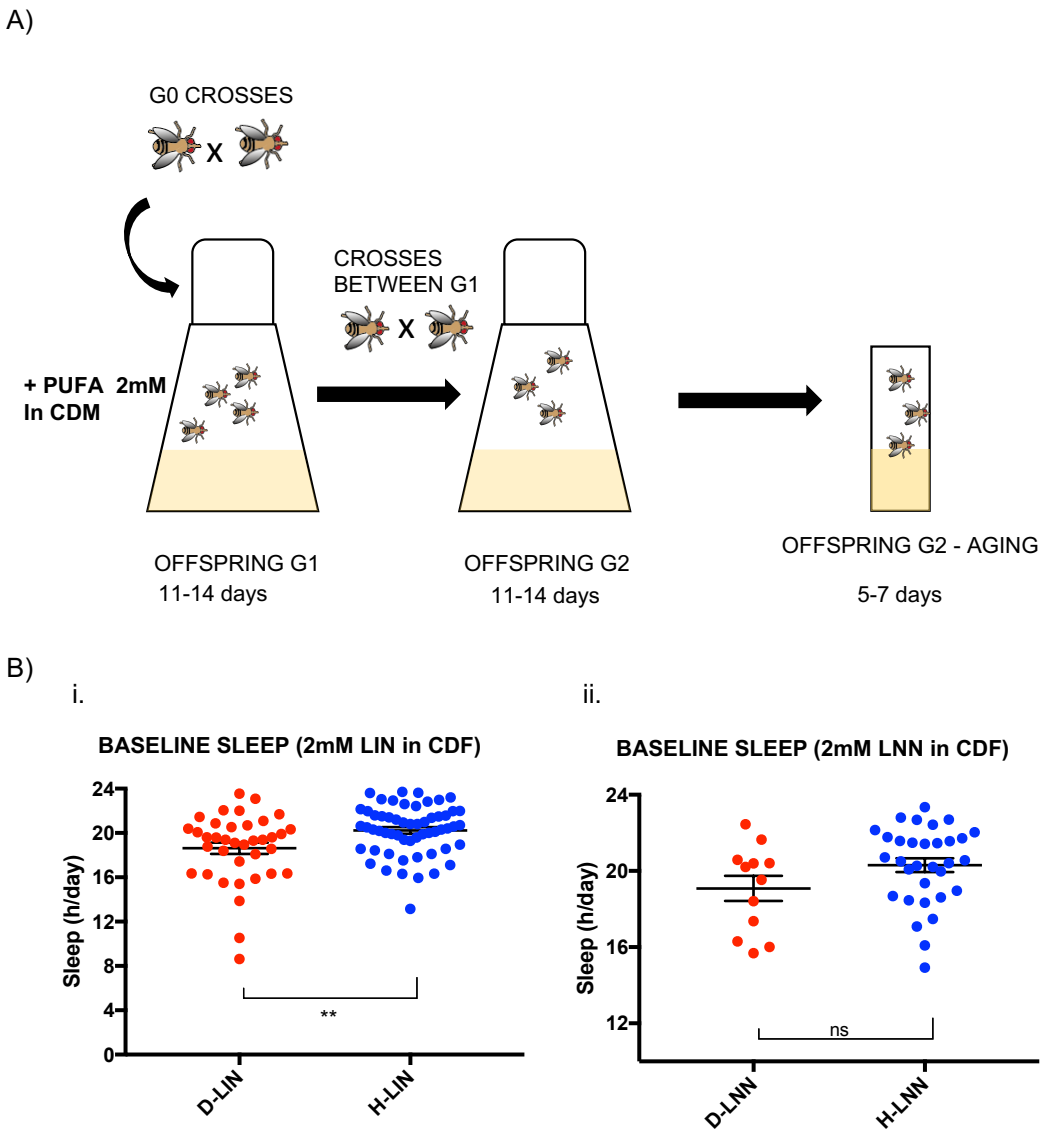


Figure 3.9. Using chemically defined food (CDF) media and longer culture time to selectively feed *Drosophila* with 2mM of D-PUFA. A) i) Diagram illustrating the experimental protocol for dietary manipulations. Fly crosses (G0) are set up in a CDF media containing either supplemented D-PUFA or H-PUFA as the only source of fatty acids. Progeny from these crosses (G1) was transferred into new bottles containing the same PUFA-supplemented CDF diet. Progeny from G1 crosses (G2 flies) were then transferred into vials right after eclosion and aged for 5-7 days until loaded into the *Drosophila Activity Monitors* for sleep recordings, also in tubes containing PUFA-supplemented CDF (not shown). B) Baseline sleep on a 2mM PUFA CDF diet (i. linoleic acid; ii. Linolenic acid). For statistical analysis

a two-tail t-test to compare selected pairs of data. p-values: ns= non-significant; **= $p<0.01$. Individual values from each fly are plotted in the graph as dots. Power calculation indicates that a sample size of a minimum of 41 subjects per group is required to reach a statistical power of 0.6 (assuming the following factors: two-tail t-test; 0.5 effect size; 0.05 significance level). Data shown as mean ± SEM and pooled from independent trial repeats. H-LIN = linoleic-acid; H-LNN= linolenic-acid D-LIN= D-linoleic acid; D-LIN= D-linolenic acid.

Chapter 4. Discussion and Future Directions.

4.1 Drosophila's dFB sleep neurons: a recap

In 2011, Donlea et al. discovered *Drosophila's* dFB sleep neurons, a cluster of about a dozen neurons in each hemisphere of the fly's brain whose activation induces sleep on demand (Donlea et al., 2011). These neurons are necessary for baseline and rebound sleep, and they adjust their electrical output according to sleep need. They oscillate between the OFF (electrically silent) state during wake and the ON (electrically excitable) state as sleep need increases, leading to sleep (Donlea et al., 2014). Dopamine signalling into the dFB operates the ON (sleep) to OFF (wake) switch through a dopamine D1-like receptor and involves the antagonistic modulation of two potassium channels: the downregulation of Shaker's A-type currents and the upregulation of the two-pore potassium channel Sandman's voltage-independent leak currents (Pimentel et al., 2016). An increase in mitochondrial ROS drives at least part of the switch from the OFF to the ON state: Kempf et al. (2019) showed that ROS accumulate in the mitochondria during sleep deprivation and increase the excitability of dFB neurons. This is achieved through the oxidative conversion of the Shaker beta-subunit Hyperkinetic into its NADP+-bound form, slowing the inactivation of Shaker's A-type current and increasing spiking, which promotes sleep (Kempf et al., 2019).

These findings form the foundation of my work. On the one hand, I focused on identifying the dopaminergic neuronal inputs that modulate the dFB ON to OFF switch. On the other, my aim was to better understand how ROS are involved in sleep control.

4.2 Wake-promoting inputs to the dFB.

4.2.1 Refined access to Drosophila's wake-promoting dopamine neurons: inputs to the dFB.

Dopamine plays a crucial role in *Drosophila's* dFB sleep homeostasis circuitry: it operates the switch from the ON to OFF state, silencing dFB neurons and waking flies up (Pimentel et al., 2016). But how are the dopamine neurons themselves regulated? What are the intrinsic molecular mechanisms and rules governing their activity? The answers to these questions are important to fully understand how sleep is regulated, but obtaining them requires that we gain access to the relevant dopaminergic inputs to the dFB. Bringing the sleep field closer to understanding *Drosophila's* wake-promoting circuits, I have significantly refined genetic access to *Drosophila's* waking neurons by identifying small subsets of wake-promoting dopaminergic neurons with putative projections to the dFB.

My results revealed that *R91D10p65;TH-DBD*, a line labelling one PPL1 and two PAL dopamine neurons in each brain hemisphere, has a strong wake-promoting phenotype (Fig 2.10). Anatomical characterisation of the line revealed that the two PPL1 dopamine neurons' projections closely overlap with the dFB neurons' dendritic tuft and, to a lesser extent, with the dFB neurons' axons in the fan-shaped body (Fig 2.8). These findings are in line with observations by Pimentel et al. (2016) that focal application of dopamine onto dFB neuron's dendritic tuft effectively hyperpolarised and suppressed spiking of dFB neurons. More recently, Ni et al. (2019) reported that dopamine neurons primarily synapse onto the dFB neurons dendritic tufts and, more

weakly, onto the axons in the dorsal layer of the FB. In addition, a study by Liu et al. (2012) had previously suggested that neurons within the PPL1 cluster project to the dFB, with two PPL1 neurons being wake-promoting (one per cluster). However, in contrast to my work, this study failed to identify which neuron drives the observed wake-promoting phenotype, out of the 24 PPL1 dopamine neurons present in the *Drosophila* brain (Claridge-Chang et al., 2009; Liu et al., 2012; Mao and Davis., 2009).

Further work is now needed to verify the direct functional connection between the *R91D10p65;TH-DBD* PPL1 neurons and the dFB sleep neurons. The involvement of *R91D10p65;TH-DBD* PAL neurons in driving the wake-promoting phenotype still remains to be fully ruled out. The possibility is, however, remote: PAL neurons do not project to the dFB, where dopamine is the key input, and have never been linked to sleep (Liu et al., 2012; Ueno et al., 2012; Sitaraman et al., 2015). The results presented here support the model that *R91D10p65;TH-DBD* PPL1 neurons drive the wake promoting phenotype by directly inhibiting the dFB sleep neurons. Upon performing further functional validation, the powerful tool here presented may assist in addressing the mechanisms and rules governing the activity of the dopamine inputs to the dFB.

In addition, I reported that *TH-C-AD; Ddc-R60F07-DBD*, a line with projections in areas including the dorsal fan-shaped body (dFB), has a wake promoting phenotype. This line contains two PPL1 and one PPM2 dopamine neurons in each brain hemisphere, as well as a small number of non-dopaminergic neurons. My work showed that dopamine neurons within this line drive the wake-promoting phenotype, but failed to refine which one(s) are causally involved (Fig 2.10). Furthermore, *TH-C-AD; Ddc-R60F07-DBD* has projections in areas other than the dFB, including the vFB and MB.

Previous studies have shown that subsets of PAM and PPL1 dopamine neurons inhibit sleep by regulating sleep-control circuits in the MB (Sitaraman et al., 2015; Driscoll et al., 2020; Joiner et al., 2006). Therefore, *TH-C-AD; Ddc-R60F07-DBD* dopamine neurons may be regulating sleep through a target other than dFB neurons, such as the MB sleep circuitry. Accordingly, experimental evaluation of the target of *TH-C-AD; Ddc-R60F07-DBD* dopamine neurons will be the subject of future studies.

4.2.2 Non-dopaminergic wake promoting circuits in Drosophila.

My work also outlines the relevance of non-dopaminergic neurons in wake-inducing phenotypes. For instance, given that *R12D12p65;TH-DBD* neurons are not wake-inducing, this suggests that the wake-promoting phenotype of the full *R12D12-GAL4* line is not due to dopaminergic neurons. In addition, although the dopaminergic *R91D10p65;TH-DBD* neurons have a strong wake-promoting phenotype, the split-GAL4 line does not fully recapitulate the wake-inducing effect of the full *R91D10-GAL4* line*,* whose activation almost completely abolished sleep. While this difference may be caused by a decrease in strength of the split-GAL4 construct, it remains possible that other neurotransmitters contribute to the stronger wake-inducing effect of the full *R91D10-GAL4* pattern.

Previous studies have shown that octopamine, like its mammalian analogue norepinephrine, promotes wake in *Drosophila* (Neckameyer and Leal, 2009; Liu et al., 2012; Crocker et al., 2010). However, my immunohistochemistry experiments showed that neither *R12D12-GAL4* nor *R91D10-GAL4* contain octopaminergic neurons (Fig 2.4 and Fig 2.5). Instead, both lines contained different subsets of serotoninergic

neurons. In vertebrate models, the role of serotonin in sleep homeostasis is controversial: Both sleep-promoting and wake-promoting phenotypes have been reported (Oikonomu et al., 2019; Torda, 1967, Weitzman et al., 1968; Cespuglio et al., 1976). In contrast, research in flies agrees on attributing a sleep-promoting function to serotonin (Pooryasin and Fiala, 2015; Yuan et al., 2006; Qian et al 2017). Indeed, a recent study suggested that serotoninergic signalling in a specific subset of dFB neurons is required for sleep homeostasis (Qian et al 2017). But, could the subset of serotoninergic neurons in *R12D12-GAL4* and/or *R91D10-GAL4* promote wake? Some neurotransmitters, such as glutamate and acetylcholine, can promote wake or sleep in *Drosophila* depending on the target circuit (Zimmerman, 2017; Tomita et al., 2015). By isolating the subset of serotoninergic neurons in *R12D12-GAL4* and *R91D10-GAL4* or by inhibiting their serotoninergic transmission one could investigate whether these neurons are wake-promoting. Alternatively, if serotonin neurons do not regulate sleep in this context, other neurons must be driving the wake-promoting phenotype of these GAL4 lines. In addition to dopamine and octopamine, molecules including glutamate, acetylcholine, PDF and NPY have been shown to promote wake (Chung et al., 2017; Parisky et al., 2009; Zimmerman, 2017; Tomita et al., 2015).

4.2.3 Future directions:

What are the rules governing the activity of the dopaminergic inputs to the dFB? Which are the intrinsic molecular mechanisms that mediate their wake-promoting function? How and when are they activated? By which signals and neurons? As I have gained genetic access to the small population of dopaminergic wake-promoting neurons labelled by *R91D10p65;TH-DBD* and *TH-C-AD; Ddc-R60F07-DBD*, my work brings us

a step closer to finally answering these questions. Yet, while dopaminergic *R91D10p65;TH-DBD* and *TH-C-AD; Ddc-R60F07-DBD* neurons are both wake-promoting and have anatomical projections in close proximity to the dFB neurons, it is necessary to experimentally prove that they are the functional inputs to the dFB. Previous work by Pimentel et al. (2016) demonstrated that optogenetically activating *TH-GAL4* neurons (i.e. the majority of dopaminergic neurons in the fly brain) can effectively block spiking and hyperpolarise dFB neurons. Therefore, if *R91D10p65;TH-DBD* and *TH-C-AD; Ddc-R60F07-DBD* are inputs to the dFB neurons, I expect to see that optogenetically activating these dopamine neurons will silence the dFB neurons in a similar fashion. These experiments are currently in progress.

My work also suggests that neurotransmitters other than dopamine and octopamine promote wake in *Drosophila*. Interestingly, I here identify two wake-promoting GAL4 lines that label a broad subset of serotoninergic neurons. Collectively, identifying the neurotransmitter identity of the wake-promoting neurons in *R12D12-GAL4* and *R91D10-GAL4* may reveal undiscovered wake-promoting circuits in *Drosophila's* brain in the future.

4.3. ROS, lipid peroxidation and sleep in Drosophila.

4.3.1 ROS in the gut may promote sleep.

Does the accumulation of ROS in tissues other than the dFB cause sleep? More precisely, can ROS in non-neuronal tissues, such as the gut, increase sleep? Recently, Vaccaro et al. (2020) found that sleep deprivation increases ROS in the gut of flies and mice. However, they failed to show the existence of a bidirectional relationship, in which an increase of ROS in the gut directly promotes sleep. To address these questions, I generated chemogenetic tools based on the DAAO enzyme, which generates H_2O_2 upon binding to D-amino acids. Chemogenetically inducing ROS in *Myo1A-GAL4*, which expresses primarily in the fly's midgut enterocytes, increased sleep (Fig 3.4). However, *Myo1A-GAL4* also displayed leaky expression in the brain, including in areas such as the PI, which has been previously linked to sleep (Foltenyi et al., 2007). In this light, it remains possible that increases of ROS in the brain are either partially or fully contributing to the observed increase in sleep amount. To confirm the connection between the accumulation of ROS in the gut and sleep promotion, the chemogenetic induction of ROS should be achieved using a GAL4 line which exclusively labels the gut of *Drosophila*, such as *Mex1-GAL4* (Vaccaro et al., 2020).

4.3.2 Chemogenetically inducing ROS in the dFB neurons does not increase sleep: what could have caused this?

The DAAO-based chemogenetic system here presented effectively induced ROS in the dFB neurons *ex-vivo* (Fig 3.2). As previously stated, *in vivo* induction of ROS in the gut using this system led to an increase in sleep. Using the ROS-generating miniSOG optogenetic system, Kempf et al. (2019) demonstrated that inducing ROS in the dFB neurons increases sleep. Similarly, expressing the pro-oxidant mutant enzyme $SOD1^{A4V}$ in the dFB neurons also increases sleep (Kempf et al., 2019). In contrast, expressing the ROS-generating DAAO-based system in the dFB neurons to chemogenetically induce ROS *in vivo* failed to promote sleep (Fig 3.3). What could have caused this? Various potential explanations come to mind:

To effectively bypass the chain of events that couples mitochondrial respiration to the oxidation of the Hyperkinetic-bound NADPH co-factor and induce sleep, Kempf et al. (2019) anchored miniSOG to the cytosolic face of the plasma membrane. This way, miniSOG is placed in close proximity to Hyperkinetic to release ROS and oxidise NADPH directly or indirectly via local membrane lipid peroxidation. In contrast, the DAAO-based chemogenetic tool floats in the cytoplasm, which might prevent the extremely short-lived H_2O_2 to target Hyperkinetic effectively.

An alternative explanation involves the substrate of DAAO, D-ALA, not reaching the target neurons at the right concentration. *Ex-vivo*, 10 mM D-ALA was used to effectively increase ROS in dFB neurons. Furthermore, my results indicate that at least a 15-mM concentration of dietarily supplemented D-ALA is needed to increase sleep

by expressing the DAAO chemogenetic system in *Myo1A-GAL4,* which expresses most strongly in the gut. In addition, toxic/non-specific effects were observed when feeding flies with D-ALA at concentrations as low as 30 mM. In *Drosophila*, dietary amino acids are absorbed through the gut wall from the lumen of the digestive tract to the haemolymph (Maniére et al., 2020). Once in the haemolymph, circulating amino acids enter the brain via amino acid transporters before reaching the target DAAO-based chemogenetic system (Reynolds et al., 2007; Aggarwal et al., 2020). Thus, at a 15 mM D-ALA concentration in fly food, the concentration of D-ALA reaching the dFB neurons may be below the minimum required to effectively induce ROS and trigger sleep. In future experiments, concentrations ranging from 15 mM to 30 mM should then be tested.

4.3.3 Diet composition affects sleep amount.

My results show that *Drosophila's* diet composition can alter sleep duration. Flies fed with a standard molasses-based brown media sleep significantly more than flies on a 5% sucrose media (Fig. 3.6). What might underlie these differences in sleep amount? Previous studies have shown that the calories a diet provides impact sleep. Starvation decreases sleep amount in flies and mammals, while chronically feeding flies with a high caloric diet can also alter sleep (Brown et al., 2020; Catterson et al., 2010; Yamazaki et al., 2012). Interestingly, research has suggested that, under a calory-restricted diet, some tissues have reduced mitochondrial ROS generation and oxidative damage (Gredilla and Barja., 2005). Accordingly, the difference in caloric content between the two diets may explain the difference in sleep amount. According to Lee and Micchelli (2013), a standard molasses-based diet has approximately 50

Kcal per 100 mL. Meanwhile, the caloric content of the 5% sucrose diet can be estimated as 20 Kcal per 100mL, considering that 1 g of sucrose contains approximately 4 Kcal (Diabetes Education Online).

In addition, distinct macronutrients in a diet may regulate sleep differently. Pamboro et al. (2020) recently showed that medium and long chain, but not short chain, saturated fatty acids promote sleep amount in *Drosophila*. Although the caloric content of individual macronutrients may account for these differences, other mechanisms may be involved. For example, it has been shown that different fatty acids have different rates of oxidation (DeLany et al., 2000). In addition, studies show that fatty foods promote food intake, which may lead to higher calory consumption (Masek and Keene, 2013; Erlanson-Albertsson, 2010). However, supplementing *Drosophila*'s molasses-based and 5% sucrose diets with 200 μM to 2 mM PUFAs (linoleic or linolenic acid) has no significant effect on sleep amount (Fig. 3.6). While Pamboro et al. (2020) reported that some fatty acids promote sleep, high concentrations were required to cause significant effects. The total fat concentration in a standard molasses-based diet is approximately 0.24% (w/v) (Lee and Micchelli, 2013). To promote sleep, a sucrose media with a concentration of at least 0.4% (w/v) hexanoic acid was necessary, and at least 1% (w/v) of hexanoic acid was necessary to cause a sleep increase when using a standard, nutrient-rich, diet (Pamboro et al., 2020). In contrast, the PUFA concentrations used in my experiment were significantly lower: 200 μM of linoleic or linolenic acid is equivalent to a 0.0056% (w/v) concentration, while 2 mM is equivalent to 0.056% (w/v). This way, significantly higher concentrations may be needed to see if overconsumption of PUFAs can cause an increase in sleep.

4.3.4 D-PUFAs may link lipid peroxidation to sleep in Drosophila.

What are the intermediate steps that couple mitochondrial ROS production with the modulation of Hyperkinetic at the plasma membrane to induce sleep? The leading hypothesis is that longer-lived lipid peroxidation by-products, such as aldehydes (Long et al., 2005; Weng et al., 2006), link mitochondrial ROS with Hyperkinetic and sleep (Kempf et al., 2019). To test this, I supplemented *Drosophila* diet with reinforced, lipid peroxidation-resistant D-PUFAs. Results showed that supplementing 2 mM linoleic acid into a CDF diet significantly decreased sleep amount in flies (Fig. 3.9) A similar, albeit not-significant, trend was observed when supplementing the CDF with 2 mM linolenic. The results should be verified in additional replicates and with larger sample sizes in order to provide strong evidence that lipid peroxidation promotes sleep in *Drosophila*.

In interpreting these experiments it is important to bear in mind that several variables could affect the efficacy of D-PUFA dietary manipulations. First, it is unclear how effectively D-PUFAs are being integrated into *Drosophila's* brain to replace membrane PUFAs and whether they are reaching the minimum integration threshold to significantly reduce lipid peroxidation and decrease sleep. In yeast and mammalian cell cultures, integration of a small amount of D-PUFAs into the lipid membranes (20% in the total pool of membrane PUFAs) is sufficient to profoundly inhibit lipid peroxidation (Firsov et al., 2019. Andreyev et al., 2015; Hill et al., 2012). However, a recent study showed that after 18 weeks on a D-PUFA diet the rate of incorporation of D-PUFA into the brain of mice was approximately 35% (Elharram et al., 2017). In a separate study with a transgenic mouse model of Alzheimer's disease, 5 months on a

D-PUFA diet led to high levels of D-PUFA incorporation and a reduction of brain lipid peroxidation. Yet, this was not sufficient to cause any discernible behavioural effects, which might indicate that the time of initiation/or duration of the D-PUFA treatment were not sufficient to reduce lipid peroxidation enough to improve cognitive deficits (Raefsky, 2018). Thus, to fully understand the implications of my results it would be necessary to quantify the levels of D-PUFA incorporation in *Drosophila's* brain. Unfortunately, quantifying the integration of D-PUFAs by mass spectrometry has so far proven difficult due to the low mass of the fly brain.

In contrast with the CDF experiments, supplementing a standard molasses-based medium or a 5 % sucrose-agar medium with D-PUFA produced no significant alterations on sleep (Fig 3.7). As outlined in the previous section, diet composition alone has a significant effect on sleep, which can hinder the effect of any additional supplemented nutrients. This highlights the importance of using CDF media when performing experiments to understand the role of specific nutrients or dietary manipulations on sleep. In addition, in previous experiments with standard and sucrose media flies were exposed to D-PUFAs for only one generation from larval stage; however, in the CDF experiments, the exposure to D-PUFAs was extended for two consecutive generations from larval stage. The aim of this extension was to maximise the integration of D-PUFAs into *Drosophila*'s lipid membranes over non-deuterated PUFAs, since a previous study suggested that linoleic acid can be passed from the *Drosophila* mother to the progeny across several generations (Rapport et al., 1983). To understand whether length of exposure played a significant effect in this context, experiments in CDF media should be performed using shorter exposure times.

4.3.5 Future directions.

In *Drosophila*'s dFB neurons, increases in mitochondrial ROS promote sleep. Does this phenomenon occur outside the dFB, in non-neuronal tissues? Using the DAAO-based chemogenetic tool newly developed here, I have shown that the sleep-promoting function of ROS is not exclusive to the dFB neurons: My results and those of Vaccaro et al. (2020) suggest that accumulation of ROS in the fly's gut may increase sleep. Provided that the results are validated in subsequent analyses, this will pave the way for a new exciting line of research: Is there a gut-brain pathway regulating sleep? Does the gut promote sleep through the dFB neurons? Or does it use a dFB-independent mechanism? The DAAO-based chemogenetic system can be employed to address these questions by inducing ROS in the gut while simultaneously blocking the activity of the dFB neurons. In addition, a recent study has shown that gut-innervating thoracic-abdominal ganglion neurons and enterocyte cells in the gut express the neuropeptide Allatostatin A, and that secretion by enterocyte cells in the gut reduces feeding and may promote sleep (Chen et al., 2016; Kubrak et al., 2020). Interestingly, Allatostatin A is also one of the neuropeptides secreted by dFB neurons to promote sleep (Donlea et al., 2018). In addition, my work also showed that diet composition has a significant impact on sleep, likely caused by changes in caloric content. This way, could intestinal ROS be the missing link between diet, metabolism, and sleep? An open question for future research.

Finally, I have investigated the hypothesis that lipid peroxidation is the intermediate step between mitochondrial ROS and sleep in *Drosophila*. Preliminary experiments using lipid peroxidation-resistant D-PUFAs on a CDF diet provide support for this

model, since the dietary manipulation decreased sleep. In addition, with the objective of characterising sleep-related changes on lipid membranes reflective of lipid peroxidation I am currently performing mass spectrometry measurements of rested and sleep-deprived *Drosophila* brains in collaboration with the Bernhard Spengler group from the University of Giessen.

Chapter 5: Materials and Methods

5.1 Fly husbandry methods

Unless specified, fly strains were grown on a standard molasses-based cornmeal media (yeast 2.5% (m/v), cornmeal 6.25 % (m/m), molasses 3.75% (v/v) agar 0.7% (m/v), acid mix 0.42% (v/v), tegosept 0.14% (m/v) and ethanol 0.7% (v/v) in water) and kept on a 12-h light: 12-h dark schedule at 25 °C and controlled humidity levels. The crosses for the thermogenetic activation experiments were housed at 21 °C.

Fly stocks were obtained from in-house stock collections at the CNCB, from the Bloomington Drosophila Stock centre (BDSC), generated in-house or obtained as gifts from academic research groups, as specified in the table below.

Table 5.1.1 GAL4 and LexA driver stocks

Fly Stock	**Source**
R12D12-GAL4	BDSC #48506
R91D10-GAL4	BDSC #40582
R23E10-GAL4	BDSC #49032
Myo1A-GAL4 (NP0001)	BDSC #67057
ple-GAL4 (TH-GAL4)	BDSC #8848
R23E10-LexA	BDSC #52693

Table 5.1.2 split-GAL4 driver stocks

Fly Stock	Source
TH-C-AD	Gift from Mark Wu lab (Xie et al., 2018)
Ddc-R60F07-DBD	Gift from Mark Wu lab (Xie et al., 2018)
R91D10-p65AD	BDSC #70848
R12D12-p65AD	BDSC #70539
ple-GAL4-DBD (TH-DBD)	BDSC #70197

Table 5.1.3 UAS and LexAop responder stocks

Fly Stock	Source
UAS-dTrpA1	BDSC #26263
UAS-TH-miR	Gift from Mark Wu lab (Liu et al., 2017).
UAS-mCD8::GFP	From CNCB collection
UAS-myr-mRFP	BDSC #7118
LexAop-mCherry	From CNCB collection
UAS-20xUAS6xmCD8::GFP	From CNCB collection
LexAop-mCD8::GFP	From CNCB collection
UAS-DAAO	Generated in-house
UAS-HyPer-DAAO	Generated in-house
UAS-SypHer-DAAO	Generated in-house
LexAop-DAAO	Generated in-house
LexAop-HyPer-DAAO	Generated in-house
LexAop-SypHer-DAAO	Generated in-house

Table 5.1.4 Mutant stocks

Fly Stock	Source
DAAO DKO	Gift from Yi Rao lab (Dai et al., 2019)

A separate set of split-GAL4 hemidriver lines based on the R91D10-GAL4 and R12D12-GAL4 sequences were also generated in-house. All D-amino acid oxidase (DAAO) constructs were generated in-house as specified in the next section.

5.2 Molecular biology methods for the generation of transgenic flies

5.2.1 Generation of split-GAL4 constructs with traditional and Gateway cloning.

Traditional restriction site-based cloning was used to generate the *R91D10-VP16, R12D12-VP16, R91D10-DBD* and *R12D12-DBD* split-GAL4 hemidriver constructs. The enhancer sequences that drive transgene expression in the *R91D10-GAL4* line, associated with the *Drp12* gene, and the *R12D12-GAL4* line, associated with the *dnc* gene, were used to generate these constructs. The New England Biolabs (NEB) Polymerase Chain Reaction (PCR) protocol for Phusion high-fidelity DNA Polymerase (#M0530, NEB, Ipswich, MA, USA) was used to generate DNA inserts. DNA sequences were amplified from genomic DNA of the *R91D10* and *R12D12* GAL4 strains, using the primers specified in Table 1. The QIAquick Gel Extraction kit (#28706X4, Qiagen, Hilden, Germany) was used to extract DNA from the amplified fragments. The restriction enzymes EcoRI-HF (#3101, NEB) and NotI-HF (#R3189, NEB) were used for digestion of the amplified fragments containing the *R12D12-GAL4*-associated enhancer sequence and the empty vector, as described in the manufacturer's protocol. AvrII (#R0174, NEB) and NotI-HF (#R3189, NEB) were used for restriction of the fragments containing the *R91D10-GAL4*-associated enhancer

sequence and the empty vector. Digested products were ligated into the X11-pCast-GAL4DBD and the pCaST-dVP16AD vectors using the T4 DNA ligase (#M0202, NEB) as per manufacturer's indications. Ligation reactions were then transformed into OneShot TOP10 competent *E. coli* cells (#C404006, NEB). The Macherey-Nagel DNA purification kit (#740588, Macherey-Nagel, Duren, Germany) was used to isolate and purify DNA from bacterial colonies. Constructs were sent to BestGene Inc. for injection and genomic insertion using phiC31-mediated integration (Bischof et al., 2007).

The *R91D10-p65AD* and *R12D12-p65AD* constructs were generated using Gateway cloning, as described by the Thermo Fisher Scientific protocol. DNA inserts were amplified through PCR from vectors containing the DNA sequences of interest, using the primers specified in Table 1. The Gateway BP Clonase II Enzyme mix (#11789020, Thermo Fisher Scientific, Waltham, MA, USA) and Gateway LR Clonase II Enzyme mix (#11791020, Thermo Fisher Scientific) were used for the BP and LR reactions, respectively. pDONRP4-P1R was used as the donor vector. The pPIp65AD, containing the p65AD, was the destination vector. Constructs were sent to BestGene Inc. for injection and P-element random-mediated genomic insertion.

The X11-pCast-GAL4DBD, pCaST-dVP16AD, pDONRP4-P1R and pPIp65AD vectors were a gift from the Goodwin lab. Restriction digestion and Sanger sequencing were used to verify the sequences of the constructs.

Table 5.2.1.1 Primers for initial amplification of enhancer sequences for traditional cloning

R91D10 FW	5' AAATATCCTAGGCCCGGAAGCGATGGTTTGAGGGTAT (AvrII restriction site)
R91D10 RV	5' TTTTTTCCTTGCGGCCGCCCGCGCATCCATGCTTCTTCCAAT (Not1 restriction site)
R12D12 FW	5' CGCCGAATTCCCTTTGCGGCTTTTTGTGGTGTTCA (EcoRI restriction site)
R12D12 RV	5' TTTTTTCCTTGCGGCCGCCCGCGTCTAACTGAGATCACAATTC (Not1 restriction site)

Table 5.2.1.2 Primers for initial amplification of enhancer sequences for gateway cloning.

R91D10 FW	5' GGGGACAACTTTGTATAGAAAAGTTGCCCGGAAGCGATGGTTTGAGGGTAT
R91D10 RV	5' GGGGACTGCTTTTTTGTACAAACTTGACCGCGCATCCATATAGCTTCTTCC
R12D12 FW	5' GGGGACAACTTTGTATAGAAAAGTTGCCTTTGCGGCTTTTTGTGGTGTGTT
R12D12 RV	5' GGGGACTGCTTTTTTGTACAAACTTGACCGCGTCTAACTGAGATCACAATTC

5.2.2 Generation of DAAO constructs using traditional restriction site-based cloning.

The following constructs containing the yeast DAAO sequence were generated using traditional cloning:

UAS-HyPer-DAAO

UAS-SypHer-DAAO

UAS-DAAO

LexAop-HyPer-DAAO

LexAop-SypHer-DAAO

LexAop-DAAO

Phusion high-fidelity DNA Polymerase (#M0530, NEB) was used to generate DNA inserts according to manufacturer's instructions. DNA inserts were amplified from the commercially available plasmids by Steinhorn et al. (2018*) pAAV-SypHer2-DAAO-NES* (Addgene plasmid #119184) and *pAAV-HyPer-DAAO-NES* (Addgene plasmid #119164) using the primers specified in Table 4.2.2.1. The QIAquick Gel Extraction kit (#28706X4, Qiagen) was used to isolate the amplified DNA fragments upon electrophoresis-based gel separation. The restriction enzymes XhoI (#R0146, NEB) and XbaI (#R0145, NEB) were used for digestion of the amplified fragments and the empty vector, as described in the NEB protocol. Each digested product was ligated to the commercially available vectors pJFRC-MUH (Addgene plasmid #26213) and pJFRC19-13XLexAop2-IVS-myr::GFP (Addgene plasmid #26224) using the T4 DNA ligase (#M0202, NEB). Ligation reactions were then transformed into OneShot TOP10 competent *E. coli* cells (C404006, NEB). The Macherey-Nagel DNA purification kit (#740588) was used to isolate and purify DNA from bacterial colonies. All sequences were verified through restriction digestion and Sanger sequencing. Constructs were sent to BestGene Inc. for injection and genomic insertion using phiC31-mediated integration (Bischof et al., 2007). Two separate transgenic stock versions were generated for each construct by inserting the respective constructs into either the second or the third chromosome.

Table 5.2.2.1 Primers for amplification of DAAO sequences.

1 FW	5' CCG CTCGAG ACAAA atg gagatggcaagccagca 3' (XhoI restriction site) (Kozak sequence)
1 RV	5' CTAG TCTAGA tta cagggtcagccgctcca 3' (XbaI restriction site)
2 FW	5' CCG CTCGAG ACAAA atg gtcacagccagaagagggtg 3'. (XhoI restriction site) (Kozak sequence)
2 RV	5' CTAG TCTAGA tta cagggtcagccgctcca 3' (XbaI restriction site)

5.3 Imaging methods

5.3.1 Immunohistochemistry and confocal imaging.

Adult fly brains were dissected in phosphate-buffered saline (PBS) and fixed immediately after for 20 min in 4% (w/v) paraformaldehyde, followed by three 20-min washes in 0.7% (v/v) Triton-X100 in PBS (hereinafter PBT) and incubation in blocking solution (10% (w/v) Normal Goat Serum (NGS) in PBT) for 8 hours, at room temperature. For immunostaining, brains were incubated with the relevant primary antibody solution diluted 1:1000 in blocking solution for 48 h at 4 °C, followed by four one-hour washes in PBT at room temperature and incubation with the relevant secondary antibody solution diluted 1:500 in blocking solution for 24 h at 4 °C. After incubation, brains were subject to four 1 h washes in PBT. Samples were either, (1) placed in a 70% (v/v) glycerol solution and stored at -20 °C until needed, or (2) immediately mounted in Vectashield (Vector Laboratories, Burlingame, CA, USA) and imaged on a Leica TCS SP 5 confocal microscope with an HCX IRAPO L 25X/0.95W

objective (Leica, Wetzlar, Germany). Fiji ImageJ (Schindelin et al., 2012) was used for image processing.

Table 5.3.1.1 Primary antibodies

Antibody	**Source**
anti-mouse tyrosine hydroxylase monoclonal	#22941, Immunostar, Hudson, WI, USA
anti-rabbit serotonin polyclonal	#S5545, Sigma-Aldrich, St Louis, MO, USA
anti-rabbit Tdc2 polyclonal	#ab128225, Abcam, Cambridge, UK
anti-rabbit GFP polyclonal	#A6455, Thermo Fisher Scientific
anti-chicken GFP polyclonal	#ab92456, Abcam
anti-rat mCherry monoclonal	#M11217, Thermo Fisher Scientific
Living Colors DsRed monoclonal	#632392, Takara Bio, Kusatsu, Japan

Table 5.3.1.2 Secondary antibodies

Antibody	**Source**
goat anti-rabbit Alexa Fluor 488	#A11034, Thermo Fisher Scientific
goat anti-chicken Alexa Fluor 488	#A11039, Thermo Fisher Scientific
goat anti-mouse Alexa Fluor 546	#A11003, Thermo Fisher Scientific
goat anti-rabbit Alexa Fluor 633	#A21070, Thermo Fisher Scientific
goat anti-rat Alexa Fluor 633	#A21094, Thermo Fisher Scientific

5.3.2 In vitro chemogenetic tests, confocal imaging, and quantification of fluorescence.

Adult fly brains were dissected in PBS and immediately transferred to either a 10 mM D-Alanine (#A7377, Sigma-Aldrich) solution in PBS, 10 mM L-Alanine (#A7627, Sigma-Aldrich) solution in PBS, or a control PBS-only solution. Incubations were carried out in the respective solution for 1 h at room temperature and, immediately after, mounted in Vectashield (Vector Laboratories) and imaged on a Leica TCS SP 5 confocal microscope with an HCX IRAPO L 25X/0.95W objective (Leica). Fiji ImageJ (Schindelin et al., 2012) was used for image processing. To quantify fluorescence levels, sum intensity projection images were generated from each stack. From each image, a region of interest (ROI) was selected, as well as four regions near the ROI with no fluorescence to serve as background. From each selected region, the following measurements were taken: area, integrated density, and mean fluorescence. The corrected total cell fluorescence (CTCF) of each image was calculated using the following formula:

$$CTCF = Integrated\ density - (Cell\ area \times Mean\ fluorescence\ of\ background)$$

5.4 Diet manipulation methods

5.4.1 In vivo chemogenetics.

For manipulations with the DAAO-based chemogenetic system, D-Alanine (#A7377, Sigma-Aldrich) or L-Alanine (#A7627, Sigma-Aldrich) were mixed in a 5% (w/v) sucrose and 2% (w/v) agar medium at the concentrations specified in the figure

legends. Flies were maintained on food containing either D-Alanine, or L-Alanine, or amino acid-free control food after eclosion for 3 full days before being individually transferred to glass tubes with the equivalent fresh medium.

5.4.2 Deuterated PUFA feeding experiments.

5.4.2.1 PUFA aliquots and storage

PUFA stocks were diluted in ethanol at 200 mM and kept at -80 °C until used.

Table 5.4.2.1.1 PUFAs used in this study

PUFA	Source
D2-Linoleic-acid	Gift from Misha Shchepinov, Retrotope
D4-Linolenic-acid	Gift from Misha Shchepinov, Retrotope
Linoleic acid	#1376, Sigma-Aldrich
Linolenic acid	#2376, Sigma-Aldrich

5.4.2.2 PUFA-containing media

In a first set of experiments, the corresponding D-PUFA, H-PUFA or an ethanol control aliquot, were directly added and mixed in liquid standard cornmeal medium or a liquid 5% (w/v) sucrose, 2% (w/v) agar medium at the concentrations specified in the figure legends. 10mL-15mL of media preparations were then poured into empty *Drosophila* vials and left to dry overnight. When specified, 20 μl of *Saccharomyces cerevisiae* solution treated

with the corresponding D- or H-PUFA was sprinkled on top of the medium surface (see yeast culture methods section below).

In a second set of experiments, a chemically defined diet was used where the only source of fat was cholesterol and the selected PUFA at the concentrations specified in the figure legends, either deuterated, or hydrogenated in the control groups. The chemically defined food (CDF) media recipe was adapted from the Lee & Micchelli (2013) CDF 400Kcal/L medium, by substituting lecithin with the corresponding PUFA at a final concentration of 2 mM. All chemicals were sourced from the same distributors as in the original Lee & Micchelli (2013) medium.

5.4.2.3 Yeast culture.

Saccharomyces Cerevisiae wildtype yeast WT W303 Mat alpha strain from the Kornmann lab were used. Yeast were stored on YPD plates at room temperature and stroked into new plates weekly.

Yeast were grown overnight in a liquid yeast peptone dextrose (YPD) medium at 30 °C 250 rpm and harvested while in logarithmic phase (OD600nm= 0.1–1.0). The yeast cells were washed twice with sterile water and resuspended in a 0.10M phosphate buffer, pH 6.2, with 0.2% dextrose, to an optical density of 0.20 OD600nm. Aliquots of 1mL were placed in sterile 5mL culture tubes and the corresponding PUFAs were added (from stocks prepared in ethanol) to a final concentration of 200 µM. For a control yeast preparation, ethanol was

added in lieu of PUFA. Aliquots were incubated at 30 °C 250 rpm for 4h before sprinkling 20 ml of the *Drosophila* medium.

YPD media was prepared as described in the Methods in Yeast Genetics Manual by Burke et al. (2000) using 1% (w/v) yeast extract (#210929, Thermo Fisher Scientific), 2% (w/v) peptone (#211910, Thermo Fisher Scientific) and 2% (w/v) dextrose (#50997, Thermo Fisher Scientific). For YPD solid plates, medium also contained 2% Bacto agar (#10455513, Fisher Scientific).

5.5 Behavioural analyses methods

5.5.1 Sleep assays

Adult female flies (3 to 5 days old) were inserted individually into 65-mm glass tubes and loaded into the *Trikinetics Drosophila* Activity Monitor (DAM) system. The monitors were placed inside an incubator with a 12-h light: 12-h dark cycle and controlled humidity. Unless otherwise indicated, the temperature of the incubator was kept at 25 °C throughout the experiments. Sleep was classified as periods of inactivity, no beam breaks, lasting for a minimum of 5 minutes. To quantify the sleep parameters used in this study, raw data was processed using the Sleep and Circadian Analysis MATLAB Program (S.C.A.M.P.).

5.5.2 Sleep deprivation methods

Mechanical sleep deprivation was achieved using a vibrating vortexer *Trikinetics* mounting plate, which can hold up to 8 DAMs. The vortexer was controlled by software (Trikinetics, Waltham MA), which activated the vortexer for 2s duration at

random intervals within every 20s. The intensity of the vortexer vibrations was set to level 4.

5.6 Statistical analyses

Statistical analyses were carried out using the GraphPad Prism version 7 for Mac, GraphPad Software, San Diego, California USA, www.graphpad.com. The specific statistical tests used for the analysis of individual experiments and the corresponding p-values are specified in the figure legends.

Chapter 6: Bibliography

- Aggarwal, T., Patil, S., Ceder, M., Hayder, M., Fredriksson, R., 2020. Knockdown of SLC38 Transporter Ortholog – CG13743 Reveals a Metabolic Relevance in Drosophila. Frontiers in Physiology 10, 1592.
- Allada, R., Cirelli, C., Sehgal, A., 2017. Molecular Mechanisms of Sleep Homeostasis in Flies and Mammals. Cold Spring Harb Perspect Biol 9, a027730.
- Alonso, J., Barredo, J.L., Díez, B., Mellado, E., Salto, F., García, J.L., Cortés, E., 1998. D-amino-acid oxidase gene from Rhodotorula gracilis (Rhodosporidium toruloides) ATCC 26217. Microbiology (Reading) 144 (Pt 4), 1095–1101.
- Anafi, R.C., Pellegrino, R., Shockley, K.R., Romer, M., Tufik, S., Pack, A.I., 2013. Sleep is not just for the brain: transcriptional responses to sleep in peripheral tissues. BMC Genomics 14, 362.
- Andreyev, A.Y., Tsui, H.S., Milne, G.L., Shmanai, V.V., Bekish, A.V., Fomich, M.A., Pham, M.N., Nong, Y., Murphy, A.N., Clarke, C.F., Shchepinov, M.S., 2015. Isotope-reinforced polyunsaturated fatty acids protect mitochondria from oxidative stress. Free Radic Biol Med 82, 63–72.
- Barski, O.A., Tipparaju, S.M., Bhatnagar, A., 2008. The Aldo-Keto Reductase Superfamily and its Role in Drug Metabolism and Detoxification. Drug Metab Rev 40, 553–624.
- Beccuti, G., Pannain, S., 2011. Sleep and obesity. Curr Opin Clin Nutr Metab Care 14, 402–412.

- Bellen, H.J., Tong, C., Tsuda, H., 2010. 100 years of Drosophila research and its impact on vertebrate neuroscience: a history lesson for the future. Nat Rev Neurosci 11, 514–522.
- Belousov, V.V., Fradkov, A.F., Lukyanov, K.A., Staroverov, D.B., Shakhbazov, K.S., Terskikh, A.V., Lukyanov, S., 2006. Genetically encoded fluorescent indicator for intracellular hydrogen peroxide. Nat Methods 3, 281–286.
- Benca, R.M., Okawa, M., Uchiyama, M., Ozaki, S., Nakajima, T., Shibui, K., Obermeyer, W.H., 1997. Sleep and mood disorders. Sleep Med Rev 1, 45–56.
- Bischof, J., Maeda, R.K., Hediger, M., Karch, F., Basler, K., 2007. An optimized transgenesis system for Drosophila using germ-line-specific ϕC31 integrases. PNAS 104, 3312–3317.
- Borbély, A.A., 1982. A two process model of sleep regulation. Hum Neurobiol 1, 195–204.
- Brand, A.H., Perrimon, N., 1993. Targeted gene expression as a means of altering cell fates and generating dominant phenotypes. Development 118, 401–415.
- Brown, E.B., Shah, K.D., Faville, R., Kottler, B., Keene, A.C., 2020. Drosophila insulin-like peptide 2 mediates dietary regulation of sleep intensity. PLOS Genetics 16, e1008270.
- Buchon, N., Broderick, N.A., Kuraishi, T., Lemaitre, B., 2010. Drosophila EGFR pathway coordinates stem cell proliferation and gut remodeling following infection. BMC Biol 8, 152.

- Burke, D., Dawson, D., Stearns, T., 2000. Methods in yeast genetics: a Cold Spring Harbor Laboratory course manual, 2000 ed. ed. Cold Spring Harbor Laboratory Press, Plainview, N.Y.
- Bushey, D., Huber, R., Tononi, G., Cirelli, C., 2007. Drosophila Hyperkinetic Mutants Have Reduced Sleep and Impaired Memory. J. Neurosci. 27, 5384–5393.
- Carrillo, R.A., Özkan, E., Menon, K.P., Nagarkar-Jaiswal, S., Lee, P.-T., Jeon, M., Birnbaum, M.E., Bellen, H.J., Garcia, K.C., Zinn, K., 2015. Control of Synaptic Connectivity by a Network of Drosophila IgSF Cell Surface Proteins. Cell 163, 1770–1782.
- Catterson, J.H., Knowles-Barley, S., James, K., Heck, M.M.S., Harmar, A.J., Hartley, P.S., 2010. Dietary Modulation of Drosophila Sleep-Wake Behaviour. PLOS ONE 5, e12062.
- Cespuglio, R., Walker, E., Gomez, M.-E., Musolino, R., 1976. Cooling of the nucleus raphe dorsalis induces sleep in the cat. Neuroscience Letters 3, 221–227.
- Chang, H.-M., Mai, F.-D., Chen, B.-J., Wu, U.-I., Huang, Y.-L., Lan, C.-T., Ling, Y.-C., 2008. Sleep deprivation predisposes liver to oxidative stress and phospholipid damage: a quantitative molecular imaging study. J Anat 212, 295–305.
- Chang, H.-M., Wu, U.-I., Lin, T.-B., Lan, C.-T., Chien, W.-C., Huang, W.-L., Shieh, J.-Y., 2006. Total sleep deprivation inhibits the neuronal nitric oxide synthase and cytochrome oxidase reactivities in the nodose ganglion of adult rats. J Anat 209, 239–250.

- Chen, J., Reiher, W., Hermann-Luibl, C., Sellami, A., Cognigni, P., Kondo, S., Helfrich-Förster, C., Veenstra, J.A., Wegener, C., 2016. Allatostatin A Signalling in Drosophila Regulates Feeding and Sleep and Is Modulated by PDF. PLOS Genetics 12, e1006346.
- Chung, B.Y., Ro, J., Hutter, S.A., Miller, K.M., Guduguntla, L.S., Kondo, S., Pletcher, S.D., 2017. Drosophila Neuropeptide F Signaling Independently Regulates Feeding and Sleep-Wake Behavior. Cell Rep 19, 2441–2450.
- Cirelli, C., Bushey, D., Hill, S., Huber, R., Kreber, R., Ganetzky, B., Tononi, G., 2005. Reduced sleep in Drosophila Shaker mutants. Nature 434, 1087–1092.
- Crocker, A., Sehgal, A., 2008. Octopamine regulates sleep in drosophila through protein kinase A-dependent mechanisms. J Neurosci 28, 9377–9385.
- Crocker, A., Shahidullah, M., Levitan, I.B., Sehgal, A., 2010. Identification of a neural circuit that underlies the effects of octopamine on sleep:wake behavior. Neuron 65, 670–681.
- Dai, X., Zhou, E., Yang, W., Zhang, X., Zhang, W., Rao, Y., 2019. D-Serine made by serine racemase in Drosophila intestine plays a physiological role in sleep. Nat Commun 10, 1986.
- de Oliveira, A.C., D'Almeida, V., Hipólide, D.C., Nobrega, J.N., Tufik, S., 2002. Sleep deprivation reduces total plasma homocysteine levels in rats. Can J Physiol Pharmacol 80, 193–197.
- DeLany, J.P., Windhauser, M.M., Champagne, C.M., Bray, G.A., 2000. Differential oxidation of individual dietary fatty acids in humans. Am J Clin Nutr 72, 905–911.

- Demystifying Sugar :: Diabetes Education Online, n.d. URL https://dtc.ucsf.edu/living-with-diabetes/diet-and-nutrition/understanding-carbohydrates/demystifying-sugar/.
- Diekelmann, S., Born, J., 2010. The memory function of sleep. Nat Rev Neurosci 11, 114–126.
- Donlea, J.M., 2019. Roles for sleep in memory: Insights from the fly. Curr Opin Neurobiol 54, 120–126.
- Donlea, J.M., Pimentel, D., Miesenböck, G., 2014. Neuronal machinery of sleep homeostasis in Drosophila. Neuron 81, 860–872.
- Donlea, J.M., Pimentel, D., Talbot, C.B., Kempf, A., Omoto, J.J., Hartenstein, V., Miesenböck, G., 2018a. Recurrent Circuitry for Balancing Sleep Need and Sleep. Neuron 97, 378-389.e4.
- Donlea, J.M., Pimentel, D., Talbot, C.B., Kempf, A., Omoto, J.J., Hartenstein, V., Miesenböck, G., 2018b. Recurrent Circuitry for Balancing Sleep Need and Sleep. Neuron 97, 378-389.e4.
- Donlea, J.M., Thimgan, M.S., Suzuki, Y., Gottschalk, L., Shaw, P.J., 2011. Inducing Sleep by Remote Control Facilitates Memory Consolidation in Drosophila. Science 332, 1571–1576.
- Driscoll, M., Buchert, S., Coleman, V., McLaughlin, M., Nguyen, A., Sitaraman, D., 2020. Dopamine neurons promotes wakefulness via the DopR receptor in the Drosophila mushroom body. bioRxiv 2020.04.29.069229.
- Dudai, Y., Jan, Y.N., Byers, D., Quinn, W.G., Benzer, S., 1976. dunce, a mutant of Drosophila deficient in learning. Proc Natl Acad Sci U S A 73, 1684–1688.

- Duffy, J.B., 2002. GAL4 system in drosophila: A fly geneticist's swiss army knife. genesis 34, 1–15.
- Eban-Rothschild, A., Rothschild, G., Giardino, W.J., Jones, J.R., de Lecea, L., 2016. VTA dopaminergic neurons regulate ethologically relevant sleep-wake behaviors. Nat Neurosci 19, 1356–1366.
- Elharram, A., Czegledy, N.M., Golod, M., Milne, G.L., Pollock, E., Bennett, B.M., Shchepinov, M.S., 2017. Deuterium-reinforced polyunsaturated fatty acids improve cognition in a mouse model of sporadic Alzheimer's disease. The FEBS Journal 284, 4083–4095.
- Erlanson-Albertsson, C., 2010. Fat-Rich Food Palatability and Appetite Regulation, in: Montmayeur, J.-P., le Coutre, J. (Eds.), Fat Detection: Taste, Texture, and Post Ingestive Effects, Frontiers in Neuroscience. CRC Press/Taylor & Francis, Boca Raton (FL).
- Everson, C.A., Crowley, W.R., 2004. Reductions in circulating anabolic hormones induced by sustained sleep deprivation in rats. Am J Physiol Endocrinol Metab 286, E1060-1070.
- Everson, C.A., Laatsch, C.D., Hogg, N., 2005. Antioxidant defense responses to sleep loss and sleep recovery. Am J Physiol Regul Integr Comp Physiol 288, R374-383.
- Everson, C.A., Toth, L.A., 2000. Systemic bacterial invasion induced by sleep deprivation. Am J Physiol Regul Integr Comp Physiol 278, R905-916.
- Finkel, T., 2011. Signal transduction by reactive oxygen species. J Cell Biol 194, 7–15.

- Firsov, A.M., Fomich, M.A., Bekish, A.V., Sharko, O.L., Kotova, E.A., Saal, H.J., Vidovic, D., Shmanai, V.V., Pratt, D.A., Antonenko, Y.N., Shchepinov, M.S., 2019. Threshold protective effect of deuterated polyunsaturated fatty acids on peroxidation of lipid bilayers. The FEBS Journal 286, 2099–2117.
- Foltenyi, K., Greenspan, R.J., Newport, J.W., 2007. Activation of EGFR and ERK by rhomboid signaling regulates the consolidation and maintenance of sleep in Drosophila. Nat Neurosci 10, 1160–1167.
- Goodwin, J.S., Larson, G.A., Swant, J., Sen, N., Javitch, J.A., Zahniser, N.R., De Felice, L.J., Khoshbouei, H., 2009. Amphetamine and Methamphetamine Differentially Affect Dopamine Transporters in Vitro and in Vivo. J Biol Chem 284, 2978–2989.
- Gredilla, R., Barja, G., 2005. Minireview: The Role of Oxidative Stress in Relation to Caloric Restriction and Longevity. Endocrinology 146, 3713–3717.
- Gulbis, J.M., Mann, S., MacKinnon, R., 1999. Structure of a voltage-dependent K+ channel beta subunit. Cell 97, 943–952.
- Halliwell, B., Gutteridge, J.M.C., 2015. Free Radicals in Biology and Medicine, Fifth Edition. ed. Oxford University Press, Oxford, New York.
- Hendricks, J.C., Finn, S.M., Panckeri, K.A., Chavkin, J., Williams, J.A., Sehgal, A., Pack, A.I., 2000. Rest in Drosophila is a sleep-like state. Neuron 25, 129–138.
- Hendricks, J.C., Kirk, D., Panckeri, K., Miller, M.S., Pack, A.I., 2003. Modafinil maintains waking in the fruit fly drosophila melanogaster. Sleep 26, 139–146.
- Hill, S., Hirano, K., Shmanai, V.V., Marbois, B.N., Vidovic, D., Bekish, A.V., Kay, B., Tse, V., Fine, J., Clarke, C.F., Shchepinov, M.S., 2011. Isotope-Reinforced

Polyunsaturated Fatty Acids Protect Yeast Cells from Oxidative Stress. Free Radic Biol Med 50, 130–138.

- Hill, S., Lamberson, C.R., Xu, L., To, R., Tsui, H.S., Shmanai, V.V., Bekish, A.V., Awad, A.M., Marbois, B.N., Cantor, C.R., Porter, N.A., Clarke, C.F., Shchepinov, M.S., 2012. Small amounts of isotope-reinforced polyunsaturated fatty acids suppress lipid autoxidation. Free Radic Biol Med 53, 893–906.
- Hill, V.M., O'Connor, R.M., Sissoko, G.B., Irobunda, I.S., Leong, S., Canman, J.C., Stavropoulos, N., Shirasu-Hiza, M., 2018. A bidirectional relationship between sleep and oxidative stress in Drosophila. PLoS Biol 16, e2005206.
- Hoang, D., Kopp, A., Chandler, J.A., 2015. Interactions between Drosophila and its natural yeast symbionts—Is Saccharomyces cerevisiae a good model for studying the fly-yeast relationship? PeerJ 3, e1116.
- Honda, K., Komoda, Y., Inoue´, S., 1994. Oxidized glutathione regulates physiological sleep in unrestrained rats. Brain Research 636, 253–258.
- Ikeda, M., Ikeda-Sagara, M., Okada, T., Clement, P., Urade, Y., Nagai, T., Sugiyama, T., Yoshioka, T., Honda, K., Inoué, S., 2005. Brain oxidation is an initial process in sleep induction. Neuroscience 130, 1029–1040.
- Irwin, M.R., Opp, M.R., 2017. Sleep Health: Reciprocal Regulation of Sleep and Innate Immunity. Neuropsychopharmacol 42, 129–155.
- Isaac, S.O., Berridge, C.W., 2003. Wake-promoting actions of dopamine D1 and D2 receptor stimulation. J Pharmacol Exp Ther 307, 386–394.
- Jenett, A., Rubin, G.M., Ngo, T.-T.B., Shepherd, D., Murphy, C., Dionne, H., Pfeiffer, B.D., Cavallaro, A., Hall, D., Jeter, J., Iyer, N., Fetter, D., Hausenfluck, J.H., Peng, H., Trautman, E.T., Svirskas, R.R., Myers, E.W., Iwinski, Z.R., Aso,

Y., DePasquale, G.M., Enos, A., Hulamm, P., Lam, S.C.B., Li, H.-H., Laverty, T.R., Long, F., Qu, L., Murphy, S.D., Rokicki, K., Safford, T., Shaw, K., Simpson, J.H., Sowell, A., Tae, S., Yu, Y., Zugates, C.T., 2012. A GAL4-driver line resource for Drosophila neurobiology. Cell Rep 2, 991–1001.

- Jennings, B.H., 2011. Drosophila – a versatile model in biology & medicine. Materials Today 14, 190–195. https://doi.org/10.1016/S1369-7021(11)70113-4
- Jiang, H., Grenley, M.O., Bravo, M.-J., Blumhagen, R.Z., Edgar, B.A., 2011. EGFR/Ras/MAPK signaling mediates adult midgut epithelial homeostasis and regeneration in Drosophila. Cell Stem Cell 8, 84–95.
- Joiner, W.J., Crocker, A., White, B.H., Sehgal, A., 2006. Sleep in Drosophila is regulated by adult mushroom bodies. Nature 441, 757–760.
- Kempf, A., Song, S.M., Talbot, C.B., Miesenböck, G., 2019. A Potassium Channel β Subunit Couples Mitochondrial Electron Transport to Sleep. Nature 568, 230–234. https://doi.org/10.1038/s41586-019-1034-5
- Kimura, M., Kapás, L., Krueger, J.M., 1998. Oxidized Glutathione Promotes Sleep in Rabbits. Brain Research Bulletin 45, 545–548.
- Klein, M.O., Battagello, D.S., Cardoso, A.R., Hauser, D.N., Bittencourt, J.C., Correa, R.G., 2019. Dopamine: Functions, Signaling, and Association with Neurological Diseases. Cell Mol Neurobiol 39, 31–59.
- Koh, K., Evans, J.M., Hendricks, J.C., Sehgal, A., 2006. A Drosophila model for age-associated changes in sleep:wake cycles. Proc Natl Acad Sci U S A 103, 13843–13847.
- Kohl, J., Jefferis, G.S.X.E., 2011. Neuroanatomy: Decoding the Fly Brain. Current Biology 21, R19–R20.

- Komoda, Y., Honda, K., Inoue, S., 1990. SPS-B, a physiological sleep regulator, from the brainstems of sleep-deprived rats, identified as oxidized glutathione. Chem Pharm Bull (Tokyo) 38, 2057–2059.
- Konopka, R.J., Benzer, S., 1971. Clock mutants of Drosophila melanogaster. Proc Natl Acad Sci U S A 68, 2112–2116.
- Koren, D., Dumin, M., Gozal, D., 2016. Role of sleep quality in the metabolic syndrome. Diabetes Metab Syndr Obes 9, 281–310.
- Kubrak, O., Jensen, L., Ahrentløv, N., Koyama, T., Malita, A., Naseem, M.T., Lassen, M., Nagy, S., Texada, M.J., Halberg, K.A., Rewitz, K., 2020. The gut hormone Allatostatin C regulates food intake and metabolic homeostasis under nutrient stress.
- Kume, K., Kume, S., Park, S.K., Hirsh, J., Jackson, F.R., 2005. Dopamine Is a Regulator of Arousal in the Fruit Fly. J. Neurosci. 25, 7377–7384.
- Lai, S.-L., Lee, T., 2006. Genetic mosaic with dual binary transcriptional systems in Drosophila. Nat Neurosci 9, 703–709.
- Lee, W.-C., Micchelli, C.A., 2013. Development and Characterization of a Chemically Defined Food for Drosophila. PLoS One 8, e67308.
- Levine, J.D., Casey, C.I., Kalderon, D.D., Jackson, F.R., 1994. Altered circadian pacemaker functions and cyclic AMP rhythms in the Drosophila learning mutant dunce. Neuron 13, 967–974.
- Lima, A.M.A., de Bruin, V.M.S., Rios, E.R.V., de Bruin, P.F.C., 2014. Differential effects of paradoxical sleep deprivation on memory and oxidative stress. Naunyn-Schmiedeberg's Arch Pharmacol 387, 399–406.

- Liu, Q., Tabuchi, M., Liu, S., Kodama, L., Horiuchi, W., Daniels, J., Chiu, L., Baldoni, D., Wu, M.N., 2017. Branch-Specific Plasticity of a Bifunctional Dopamine Circuit Encodes Protein Hunger. Science 356, 534–539.
- Liu, S., Liu, Q., Tabuchi, M., Wu, M.N., 2016. Sleep Drive Is Encoded by Neural Plastic Changes in a Dedicated Circuit. Cell 165, 1347–1360.
- Long, S.B., Campbell, E.B., Mackinnon, R., 2005. Crystal structure of a mammalian voltage-dependent Shaker family K+ channel. Science 309, 897–903.
- Lu, J., Jhou, T.C., Saper, C.B., 2006. Identification of wake-active dopaminergic neurons in the ventral periaqueductal gray matter. J Neurosci 26, 193–202.
- Luan, H., Peabody, N.C., Vinson, C.R., White, B.H., 2006. Refined Spatial Manipulation of Neuronal Function by Combinatorial Restriction of Transgene Expression. Neuron 52, 425–436.
- Lungato, L., Marques, M.S., Pereira, V.G., Hix, S., Gazarini, M.L., Tufik, S., D'Almeida, V., 2013. Sleep deprivation alters gene expression and antioxidant enzyme activity in mice splenocytes. Scand J Immunol 77, 195–199.
- Manière, G., Alves, G., Berthelot-Grosjean, M., Grosjean, Y., 2020. Growth regulation by amino acid transporters in Drosophila larvae. Cell. Mol. Life Sci. 77, 4289–4297.
- Mao, Z., Davis, R.L., 2009. Eight Different Types of Dopaminergic Neurons Innervate the Drosophila Mushroom Body Neuropil: Anatomical and Physiological Heterogeneity. Front Neural Circuits 3, 5.
- Masek, P., Keene, A.C., 2013. Drosophila Fatty Acid Taste Signals through the PLC Pathway in Sugar-Sensing Neurons. PLOS Genetics 9, e1003710.

- Matlashov, M.E., Belousov, V.V., Enikolopov, G., 2014. How Much H2O2 Is Produced by Recombinant D-Amino Acid Oxidase in Mammalian Cells? Antioxid Redox Signal 20, 1039–1044.
- Matlashov, M.E., Bogdanova, Y.A., Ermakova, G.V., Mishina, N.M., Ermakova, Y.G., Nikitin, E.S., Balaban, P.M., Okabe, S., Lukyanov, S., Enikolopov, G., Zaraisky, A.G., Belousov, V.V., 2015. Fluorescent ratiometric pH indicator SypHer2: Applications in neuroscience and regenerative biology. Biochim Biophys Acta 1850, 2318–2328.
- McGill, M.R., Jaeschke, H., 2013. Chapter 4 - Oxidant Stress, Antioxidant Defense, and Liver Injury, in: Kaplowitz, N., DeLeve, L.D. (Eds.), Drug-Induced Liver Disease (Third Edition). Academic Press, Boston, pp. 71–84.
- Mehta, S.H., Morgan, J.C., Sethi, K.D., 2008. Sleep disorders associated with Parkinson's disease: role of dopamine, epidemiology, and clinical scales of assessment. CNS Spectr 13, 6–11.
- Nakamura, M., Baldwin, D., Hannaford, S., Palka, J., Montell, C., 2002. Defective Proboscis Extension Response (DPR), a Member of the Ig Superfamily Required for the Gustatory Response to Salt. J. Neurosci. 22, 3463–3472.
- Nall, A., Sehgal, A., 2014. Monoamines and sleep in Drosophila. Behav Neurosci 128, 264–272.
- Neckameyer, W.S., Leal, S.M., 2009. 28 - Biogenic Amines as Circulating Hormones in Insects, in: Pfaff, D.W., Arnold, A.P., Etgen, A.M., Fahrbach, S.E., Rubin, R.T. (Eds.), Hormones, Brain and Behavior (Second Edition). Academic Press, San Diego, pp. 967–1003.

- Ni, J.D., Gurav, A.S., Liu, W., Ogunmowo, T.H., Hackbart, H., Elsheikh, A., Verdegaal, A.A., Montell, C., 2019. Differential regulation of the Drosophila sleep homeostat by circadian and arousal inputs. eLife 8, e40487.
- Nitz, D.A., van Swinderen, B., Tononi, G., Greenspan, R.J., 2002. Electrophysiological correlates of rest and activity in Drosophila melanogaster. Curr Biol 12, 1934–1940.
- Oikonomou, G., Altermatt, M., Zhang, R., Coughlin, G.M., Montz, C., Gradinaru, V., Prober, D.A., 2019. The Serotonergic Raphe Promote Sleep in Zebrafish and Mice. Neuron 103, 686-701.e8.
- Pamboro, E.L.S., Brown, E.B., Keene, A.C., 2020. Dietary fatty acids promote sleep through a taste-independent mechanism. Genes Brain Behav 19, e12629.
- Parisky, K.M., Agosto, J., Pulver, S.R., Shang, Y., Kuklin, E., Hodge, J.J.L., Kang, K., Liu, X., Garrity, P.A., Rosbash, M., Griffith, L.C., 2008. PDF cells are a GABA-responsive wake-promoting component of the Drosophila sleep circuit. Neuron 60, 672–682.
- Patke, A., Young, M.W., Axelrod, S., 2020. Molecular mechanisms and physiological importance of circadian rhythms. Nat Rev Mol Cell Biol 21, 67–84.
- Pfeiffenberger, C., Allada, R., 2012. Cul3 and the BTB Adaptor Insomniac Are Key Regulators of Sleep Homeostasis and a Dopamine Arousal Pathway in Drosophila. PLOS Genetics 8, e1003003.

- Pfeiffer, B.D., Ngo, T.-T.B., Hibbard, K.L., Murphy, C., Jenett, A., Truman, J.W., Rubin, G.M., 2010. Refinement of Tools for Targeted Gene Expression in Drosophila. Genetics 186, 735–755.
- Piéron, H., 1913. Le probleme physiologique du sommeil. Masson, Paris.
- Pimentel, D., Donlea, J.M., Talbot, C.B., Song, S.M., Thurston, A.J.F., Miesenböck, G., 2016. Operation of a homeostatic sleep switch. Nature 536, 333–337.
- Pitman, J.L., McGill, J.J., Keegan, K.P., Allada, R., 2006. A dynamic role for the mushroom bodies in promoting sleep in Drosophila. Nature 441, 753–756.
- Pollegioni, L., Falbo, A., Pilone, M.S., 1992. Specificity and kinetics of Rhodotorula gracillisd-amino acid oxidase. Biochimica et Biophysica Acta (BBA) - Protein Structure and Molecular Enzymology 1120, 11–16.
- Pollegioni, L., Piubelli, L., Sacchi, S., Pilone, M.S., Molla, G., 2007. Physiological functions of D-amino acid oxidases: from yeast to humans. Cell Mol Life Sci 64, 1373–1394.
- Pooryasin, A., Fiala, A., 2015. Identified Serotonin-Releasing Neurons Induce Behavioral Quiescence and Suppress Mating in Drosophila. J. Neurosci. 35, 12792–12812.
- Qian, Y., Cao, Y., Deng, B., Yang, G., Li, J., Xu, R., zhang, D., Huang, J., Rao, Y., 2017. Sleep homeostasis regulated by 5HT2b receptor in a small subset of neurons in the dorsal fan-shaped body of drosophila. eLife 6, e26519.
- Quan, A., 2018. Exploring the Drosophila-yeast mutualism in natural contexts. UC Berkeley.

- Raefsky, S.M., Furman, R., Milne, G., Pollock, E., Axelsen, P., Mattson, M.P., Shchepinov, M.S., 2018. Deuterated Polyunsaturated Fatty Acids Reduce Brain Lipid Peroxidation and Hippocampal Amyloid β-Peptide Levels, Without Discernable Behavioral Effects in an APP/PS1 Mutant Transgenic Mouse Model of Alzheimer's Disease. Neurobiol Aging 66, 165–176.
- Raichle, M.E., Gusnard, D.A., 2002. Appraising the brain's energy budget. PNAS 99, 10237–10239.
- Ramanathan, L., Gulyani, S., Nienhuis, R., Siegel, J.M., 2002. Sleep deprivation decreases superoxide dismutase activity in rat hippocampus and brainstem. Neuroreport 13, 1387–1390.
- Rapport, E.W., Stanley-Samuelson, D., Dadd, R.H., 1983. Ten generations of Drosophila melanogaster reared axenically on a fatty acid-free holidic diet. Archives of Insect Biochemistry and Physiology 1, 243–250.
- Rechtschaffen, A., Bergmann, B.M., 2002. Sleep Deprivation in the Rat: An Update of the 1989 Paper. Sleep 25, 18–24.
- Reimund, E., 1994. The free radical flux theory of sleep. Med Hypotheses 43, 231–233.
- Reynolds, B., Laynes, R., Ögmundsdóttir, M.H., Boyd, C.A.R., Goberdhan, D.C.I., 2007. Amino acid transporters and nutrient sensing mechanisms. Biochem Soc Trans 35, 1215–1217.
- Roth, T., 2007. Insomnia: Definition, Prevalence, Etiology, and Consequences. J Clin Sleep Med 3, S7–S10.

- Ryter, S.W., Kim, H.P., Hoetzel, A., Park, J.W., Nakahira, K., Wang, X., Choi, A.M.K., 2007. Mechanisms of cell death in oxidative stress. Antioxid Redox Signal 9, 49–89.
- Schindelin, J., Arganda-Carreras, I., Frise, E., Kaynig, V., Longair, M., Pietzsch, T., Preibisch, S., Rueden, C., Saalfeld, S., Schmid, B., Tinevez, J.-Y., White, D.J., Hartenstein, V., Eliceiri, K., Tomancak, P., Cardona, A., 2012. Fiji: an open-source platform for biological-image analysis. Nat Methods 9, 676–682.
- Sharma, S., Kavuru, M., 2010. Sleep and Metabolism: An Overview. International Journal of Endocrinology 2010, e270832.
- Shaw, P.J., Cirelli, C., Greenspan, R.J., Tononi, G., 2000. Correlates of sleep and waking in Drosophila melanogaster. Science 287, 1834–1837.
- Shaw, P.J., Tononi, G., Greenspan, R.J., Robinson, D.F., 2002. Stress response genes protect against lethal effects of sleep deprivation in Drosophila. Nature 417, 287–291.
- Shchepinov, M.S., 2020. Polyunsaturated Fatty Acid Deuteration against Neurodegeneration. Trends in Pharmacological Sciences 41, 236–248.
- Shen, L.R., Lai, C.Q., Feng, X., Parnell, L.D., Wan, J.B., Wang, J.D., Li, D., Ordovas, J.M., Kang, J.X., 2010. Drosophila lacks C20 and C22 PUFAs. Journal of Lipid Research 51, 2985–2992.
- Shu, X., Lev-Ram, V., Deerinck, T.J., Qi, Y., Ramko, E.B., Davidson, M.W., Jin, Y., Ellisman, M.H., Tsien, R.Y., 2011. A Genetically Encoded Tag for Correlated Light and Electron Microscopy of Intact Cells, Tissues, and Organisms. PLoS Biol 9, e1001041.

- Sitaraman, D., Aso, Y., Rubin, G.M., Nitabach, M.N., 2015. Control of Sleep by Dopaminergic Inputs to the Drosophila Mushroom Body. Front Neural Circuits 9, 73.
- Smolyarova, DD., Podgorny OV., Bilan DS., Belousov VV. 2021. A guide to genetically encoded tools for the study of H_2O_2. The FEBS Journal.
- Steinhorn, B., Sorrentino, A., Badole, S., Bogdanova, Y., Belousov, V., Michel, T., 2018. Chemogenetic generation of hydrogen peroxide in the heart induces severe cardiac dysfunction. Nat Commun 9, 4044.
- Thorpy, M.J., Adler, C.H., 2005. Parkinson's disease and sleep. Neurol Clin 23, 1187–1208.
- Tipparaju, S.M., Barski, O.A., Srivastava, S., Bhatnagar, A., 2008. Catalytic Mechanism and Substrate Specificity of the β-Subunit of the Voltage-Gated Potassium Channel. Biochemistry 47, 8840–8854.
- Toda, H., Williams, J.A., Gulledge, M., Sehgal, A., 2019. A sleep-inducing gene, nemuri, links sleep and immune function in Drosophila. Science 363, 509–515.
- Tomita, J., Ueno, T., Mitsuyoshi, M., Kume, S., Kume, K., 2015. The NMDA Receptor Promotes Sleep in the Fruit Fly, Drosophila melanogaster. PLoS One 10, e0128101.
- Tononi, G., Cirelli, C., 2014. Sleep and the Price of Plasticity: From Synaptic and Cellular Homeostasis to Memory Consolidation and Integration. Neuron 81, 12–34.
- Torda, C., 1967. Effect of brain serotonin depletion on sleep in rats. Brain Res 6, 375–377. h

- Tully, T., Gold, D., 1993. Differential effects of dunce mutations on associative learning and memory in Drosophila. J Neurogenet 9, 55–71.
- Ueno, T., Tomita, J., Tanimoto, H., Endo, K., Ito, K., Kume, S., Kume, K., 2012. Identification of a dopamine pathway that regulates sleep and arousal in Drosophila. Nat Neurosci 15, 1516–1523.
- Vaccaro, A., Dor, Y.K., Nambara, K., Pollina, E.A., Lin, C., Greenberg, M.E., Rogulja, D., 2020. Sleep Loss Can Cause Death through Accumulation of Reactive Oxygen Species in the Gut. Cell 181, 1307-1328.e15.
- van Swinderen, B., Nitz, D.A., Greenspan, R.J., 2004. Uncoupling of brain activity from movement defines arousal States in Drosophila. Curr Biol 14, 81–87.
- Villafuerte, G., Miguel-Puga, A., Murillo Rodríguez, E., Machado, S., Manjarrez, E., Arias-Carrión, O., 2015. Sleep Deprivation and Oxidative Stress in Animal Models: A Systematic Review. Oxidative Medicine and Cellular Longevity 2015, e234952.
- Volkow, N.D., Fowler, J.S., Logan, J., Alexoff, D., Zhu, W., Telang, F., Wang, G.-J., Jayne, M., Hooker, J.M., Wong, C., Hubbard, B., Carter, P., Warner, D., King, P., Shea, C., Xu, Y., Muench, L., Apelskog-Torres, K., 2009. Effects of Modafinil on Dopamine and Dopamine Transporters in the Male Human Brain: Clinical Implications. JAMA 301, 1148–1154.
- Volkow, N.D., Tomasi, D., Wang, G.-J., Telang, F., Fowler, J.S., Logan, J., Benveniste, H., Kim, R., Thanos, P.K., Ferré, S., 2012. Evidence That Sleep Deprivation Downregulates Dopamine D2R in Ventral Striatum in the Human Brain. J Neurosci 32, 6711–6717.

- Vollert, C., Zagaar, M., Hovatta, I., Taneja, M., Vu, A., Dao, A., Levine, A., Alkadhi, K., Salim, S., 2011. Exercise prevents sleep deprivation-associated anxiety-like behavior in rats: potential role of oxidative stress mechanisms. Behav Brain Res 224, 233–240.
- Weitzman, E.D., Rapport, M.M., McGregor, P., Jacoby, J., 1968. Sleep patterns of the monkey and brain serotonin concentration: effect of p-chlorophenylalanine. Science 160, 1361–1363.
- Weng, J., Cao, Y., Moss, N., Zhou, M., 2006. Modulation of voltage-dependent Shaker family potassium channels by an aldo-keto reductase. J Biol Chem 281, 15194–15200.
- White, K.E., Humphrey, D.M., Hirth, F., 2010. The Dopaminergic System in the Aging Brain of Drosophila. Front. Neurosci. 4.
- Whitworth, A., 2011. Drosophila models of Parkinson's disease. Advances in genetics.
- Wisor, J.P., 2013. Modafinil as a Catecholaminergic Agent: Empirical Evidence and Unanswered Questions. Front. Neurol. 4.
- Wisor, J.P., Nishino, S., Sora, I., Uhl, G.H., Mignot, E., Edgar, D.M., 2001. Dopaminergic Role in Stimulant-Induced Wakefulness. J Neurosci 21, 1787–1794.
- Xie, T., Ho, M.C.W., Liu, Q., Horiuchi, W., Lin, C.-C., Task, D., Luan, H., White, B.H., Potter, C.J., Wu, M.N., 2018. A Genetic Toolkit for Dissecting Dopamine Circuit Function in Drosophila. Cell Rep 23, 652–665.
- Yamazaki, M., Tomita, J., Takahama, K., Ueno, T., Mitsuyoshi, M., Sakamoto, E., Kume, S., Kume, K., 2012. High calorie diet augments age-associats sleep

impairment in Drosophila. Biochemical and Biophysical Research Communications 417, 812–816.

- Yap, M.H.W., Grabowska, M.J., Rohrscheib, C., Jeans, R., Troup, M., Paulk, A.C., van Alphen, B., Shaw, P.J., van Swinderen, B., 2017. Oscillatory brain activity in spontaneous and induced sleep stages in flies. Nat Commun 8, 1815.
- Yuan, Q., Joiner, W.J., Sehgal, A., 2006. A sleep-promoting role for the Drosophila serotonin receptor 1A. Curr Biol 16, 1051–1062.
- Zimmerman, J.E., Chan, M.T., Lenz, O.T., Keenan, B.T., Maislin, G., Pack, A.I., 2017. Glutamate Is a Wake-Active Neurotransmitter in Drosophila melanogaster. Sleep 40.